UNIVERSITÀ DEGLI STUDI DI MILANO

PhD COURSE IN PHARMACEUTICAL SCIENCE
XXXVII cycle

DEPARTMENT OF PHARMACEUTICAL SCIENCES

STUDY OF SOLUBLE OR BIODEGRADABLE DEVICES FOR PROLONGED DRUG DELIVERY IN HOLLOW ORGANS

CHIM/09

Micol Cirilli
R13348

SUPERVISOR: Prof. Matteo Cerea

PhD COURSE COORDINATOR: Prof. Giulio Vistoli

Academic Year: 2023-2024

Index

ABSTRACT

The present work was aimed to investigate the possibility to design and produce organ retentive systems for the delivery of drugs used in chronic treatments or in case of specific drug solubility or absorbability requirements. Attention was focused on three hollow organs: the urinary bladder, the stomach and the upper small intestine. Since development of drug delivery systems (DDS) is strictly connected to pharmaceutical technology used for their production, also this research area was deepened with a particular attention to innovative techniques such as 3D or 4D printing.

For what concerns urinary bladder, a prototype of a DDS able to be administered through catheter was produced. Such system was made in a shape of a ring consisting of coated mini-matrices loaded with a drug tracer and connected by an absorbable suture thread. Drug release profile was studied in order to obtain a sustained release that lasted for some days. The purpose of the system was, in fact, to allow for catheter administration, acquire a sufficient special encumbrance to permit its retention in the organ for a few days releasing the drug, and be finally able to disassemble or dissolve once exhausted for leaving the organ physiologically with urination.

Based on the need to treat topically diseases affecting the stomach or the upper small intestine or to improve absorption of drugs having narrow absorption windows in these anatomic districts, a novel Organ-Retentive Osmotically Driven System (ORODS) was studied. With the purpose to obtain a size increasing system that could eventually be retained in the stomach, a novel DDS exhibiting of one or two drug-containing units (HPMC matrices) promoting prolonged drug release, connected with osmotic units used as increasing volume compartments was prepared. The most important aspect that was taken into account while designing such a system, was that the device had to be able to gain encumbrance after administration for avoiding gastric-emptying, but also to disassemble and/or dissolve after a few hours. Preliminary studies were conducted by using

paracetamol as the drug tracer and by assessing the expansion ability and mechanical resistance of osmotic units made of regenerated cellulose (dialysis membranes) containing sodium chloride as the osmotic agent. Based on these results the system was also exploited to deliver metformin, a drug used for type II diabetic patients, which needs frequent administrations of high doses, is characterized by high solubility, and exhibits a narrow absorption window in the upper intestine. The development of this system required granulation of the drug and application of external drug free layers to the matrices in order to obtain the desired drug release rate. Also, expanding osmotic units were better studied by using dialysis membranes having different cut-off (3.5-5 and 12-14 kD) and by filling them with two different osmotic agents (sodium chloride or mannitol) in different amounts.

Considering the upper small intestine, the last organ taken into account, the development of a retentive system was conducted by applying 3D printing, which includes many different technologies from the mostly known fused deposition modeling (FDM) to the more recent stereolithography (SLA). The aim of this part of the work was to develop a retentive system meant to remain *in situ* for a few minutes, allowing for the contact of the drug containing units to the intestinal lumen membranes, eventually enabling a better absorption of the drug. The study was focused on the development of a device consisting in two drug containing units, or supports for a drug loaded dosage form, connected by a spring. Thanks to the design of the mentioned device, the system can have a space saving when the spring is compressed, eventually allowing for an oral administration, and a consequent expanded configuration when the spring is free to expand. The geometry, sizes and cross-section of the springs were evaluated in order to prepare systems able to withstand luminal pressure of small intestine. Triggering devices prepared by coating soluble thread with enteric polymers were studied for maintaining the systems in the compact configuration during oral administration and transit in the stomach, and for enabling a prompt expansion of the system when the upper intestine was reached.

Preface

Patients' compliance is a very serious issue to be taken in consideration when pharmacological therapies are concerned since it can compromise the result of the drug treatment and endanger health of the patients [Maroni et al., 2020]. In particular, when multiple drug administration is required to maintain high drug concentrations in specific organs, the development of systems designed to release the drug for long times in these anatomic sites is an interesting a promising field of research. This approach can be also beneficial for improving bioavailability of drugs having narrow absorption windows in the gastrointestinal tract. For example, in case of molecules mainly absorbed in the stomach or in proximal section of intestine, a sustained local release by gastro-retentive drug delivery systems (GRDDS) can be of great help for increasing bioavailability.

Moreover, since the small intestine is the most important organ for the absorption of orally administered drugs due to its villi and microvilli, in recent years, enteric-retentive systems have been developed and designed for targeting drug delivery in the small intestine and to prolong the transit times in the proximal intestine.

Treatments of urinary bladder pathologies could also benefit from retentive systems to overcome problems related to the need of frequent catheterization for local administration due to small bioavailability and short duration of drug release, which are strictly linked to the difficulties to maintain high drug concentration and short permanence of the drug inside the organ [Zacchè et al., 2015; Stockwell Morris & Schulz, 1992; Vrettos et al., 2021].

In order to achieve retention of the dosage form in hollow organs and a desired drug release kinetic, formulations of the drug and retention mechanisms have to be carefully designed and combined. In detail the retention mechanism need to exert its action in specific physiological conditions, such as pH, ionic strength, volume, composition and hydrodynamics of the medium, presence of enzymes, mucus, etc.[Maroni et al., 2020; Altreuter et al., 2018]. Strategies proposed so far for organ retention involve bioadhesion, buoyancy and size enlargement of the DDS. The latter approach, which requires an initial small size configuration able to reach a special encumbrance large enough to prevent early emptying from the

organ, seems to be the most promising one. [Palugan et al., 2021; Tripathi et al., 2019]. It is necessary, for size enlarging systems, that the bulky configuration is stiff enough to withstand mechanical forces possibly exerted by the organ wall and that undergoes dissolution, biodegradation or disassembling to decrease in size and spontaneously empty from the organ without external intervention when exhausted [Cima et al., 2014; Klausner et al., 2003; Zacchè et al., 2015].

Metformin is one of the most commonly prescribed drugs to treat type 2 diabetes mellitus as an oral glucose-lowering agent [Sanchez-Rangel et al.,2017] and it is also indicated for polycystic ovary syndrome. Metformin is mostly administered orally with an immediate-release profile, which leads to an absorbance of approximately 60-70% of the dose from the small intestine, due to narrow absorption window confined to this anatomic site with negligible absorption in the stomach or large intestine. Efficacy of the drug is dose-dependent with the minimal daily dose being 500 mg and maximal 2000 mg [Sanchez-Range et al., 2017; Garber et al., 1997]. Metformin oral absorption is reported to be saturable and dose-dependent [McCreight et al., 2016; Bonnet et al., 2017] and high doses delivered with immediate dosage forms have shown to frequently cause GI adverse events including diarrhea, nausea, flatulence, indigestion, vomiting, and abdominal discomfort. Metformin induced collateral effects clearly have a bad impact on quality of life and compliance to the therapy [Bonnet et al., 2017]. Side effects appeared to be less severe, and therefore metformin was better tolerated, when patients were administered with sustained drug release compositions [Feher et al., 2007] leading to a higher compliance.

For the mentioned reasons, the delivery of metformin in a sustained-release system capable of remaining in the stomach for a long time are expected to introduce great advantages [Corti et al., 2008; Zhao et al., 2012; Wadher et al., 2011]. To date, three main prolonged release metformin products are available on the market: Glocophage® XR, Fortamet® and Glumetza® [https://www.fda.gov/drugsatfda; Guo et al., 2021; Sun et al., 2023]. In recent years, a variety of drug delivery technologies have been developed for targeted drug delivery to the gastro intestinal tract, including some very creative

approaches in terms of shape, mechanism and technology. With the impressive development of different additive manufacturing technologies, such as 3D printing, new possibilities are now available for the development of novel dosage concepts [Pitzanti et al., 2022]. The ability to design and manufacture systems with specific shapes, configurations and complex geometries that interact with the physiology of the gastrointestinal tract, in a way that can lead to targeted application in a specific area of the gastrointestinal tract, can be made possible through the use of novel technologies such as 3D printing, where the construction of solid objects of any shape is achieved by adding materials layer-by-layer based on a digital model. 3D-printing includes many techniques that differ from each other in the nature of the substrate, mechanism of layer formation/deposition mode, printer used and, of course, characteristics of the final product [Karakurt et al., 2020]. Thanks to the possibility of producing small batches, this technology is also very interesting for personalized and on-demand production, which keeps costs down despite sometimes extremely complex structures [Vaz et al., 2021].

REFERENCES

Altreuter, David H., et al. "Changing the pill: developments toward the promise of an ultralong-acting gastroretentive dosage form." Expert opinion on drug delivery 15.12 (2018): 1189-1198. https://doi.org/10.1080/17425247.2018.1544615

Andreessen, Linda, Mary H. Wilde, and Pam Herendeen. "Preventing catheter-associated urinary tract infections in acute care: the bundle approach." Journal of nursing care quality 27.3 (2012): 209-217. https://doi.org/10.1097/NCQ.0b013e318248b0b1

ASTM. "Annual Book of ASTM Standards, 1990: Subject Index; Alphanumeric List." American Society for Testing & Materials, 1990

Bellinger, Andrew M., et al. "Oral, ultra–long-lasting drug delivery: application toward malaria elimination goals." Science translational medicine 8.365 (2016): 365ra157-365ra157. https://doi.org/10.1126/scitranslmed.aag2374

Bonnet, Fabrice, and André Scheen. "Understanding and overcoming metformin gastrointestinal intolerance." Diabetes, Obesity and Metabolism 19.4 (2017): 473-481. https://doi.org/10.1111/dom.12854

Cima, Michael J., et al. "Single compartment drug delivery." Journal of controlled release 190 (2014): 157-171. https://doi.org/10.1016/j.jconrel.2014.04.049

Corti, Giovanna, et al. "Sustained-release matrix tablets of metformin hydrochloride in combination with triacetyl-β-cyclodextrin." European Journal of Pharmaceutics and Biopharmaceutics 68.2 (2008): 303-309. https://doi.org/10.1016/j.ejpb.2007.06.004

Feher, Michael D., et al. "Tolerability of prolonged-release metformin (Glucophage® SR) in individuals intolerant to standard metformin—results from four UK centres." The British Journal of Diabetes & Vascular Disease 7.5 (2007): 225-228. https://doi.org/10.1177/14746514070070050501

Garber, Alan J., et al. "Efficacy of metformin in type II diabetes: results of a double-blind, placebo-controlled, dose-response trial." The American journal of medicine 103.6 (1997): 491-497. https://doi.org/10.1016/S0002-9343(97)00254-4

Guo, Li-xin, et al. "Comparison of clinical efficacy and safety of metformin sustained-release tablet (II) (Dulening) and metformin tablet (Glucophage) in treatment of type 2 diabetes mellitus." Frontiers in Endocrinology 12 (2021): 712200. https://doi.org/10.3389/fendo.2021.712200

Karakurt, Ilbey, and Liwei Lin. "3D printing technologies: techniques, materials, and postprocessing." Current Opinion in Chemical Engineering 28 (2020): 134-143. https://doi.org/10.1016/j.coche.2020.04.001

Klausner, Eytan A., et al. "Expandable gastroretentive dosage forms." Journal of controlled release 90.2 (2003): 143-162. https://doi.org/10.1016/S0168-3659(03)00203-7

Laulicht, Bryan, et al. "Understanding gastric forces calculated from high-resolution pill tracking." Proceedings of the National Academy of Sciences 107.18 (2010): 8201-8206. https://doi.org/10.1073/pnas.1002292107

Maroni, Alessandra, et al. "Retentive drug delivery systems based on shape memory materials." Journal of Applied Polymer Science 137.25 (2020): 48798. https://doi.org/10.1002/app.48798

McCreight, Laura J., Clifford J. Bailey, and Ewan R. Pearson. "Metformin and the gastrointestinal tract." Diabetologia 59.3 (2016): 426-435. https://doi.org/10.1007/s00125-015-3844-9

Morris, L. Stockwell, and R. M. Schulz. "Patient compliance—an overview." Journal of clinical pharmacy and therapeutics 17.5 (1992): 283-295. https://doi.org/10.1111/j.1365-2710.1992.tb01306.x

Neumann, Marco, et al. "A novel mechanical antrum model for the prediction of the gastroretentive potential of dosage forms." International Journal of Pharmaceutics 530.1-2 (2017): 63-70. https://doi.org/10.1016/j.ijpharm.2017.07.067

Neumann, Marco, et al. "Development of a furosemide-containing expandable system for gastric retention." Journal of Controlled Release 338 (2021): 105-118. https://doi.org/10.1016/j.jconrel.2021.08.026

Palugan, Luca, et al. "Intravesical drug delivery approaches for improved therapy of urinary bladder diseases." International Journal of Pharmaceutics: X 3 (2021): 100100. https://doi.org/10.1016/j.ijpx.2021.100100

Pavan, M. Venkata, K. Balamurugan, and T. P. Latchoumi. "PLA-Cu reinforced composite filament: Preparation and flexural property printed at different machining conditions." Advances in Computational Mathematics 31.1 (2022): 102-117. https://doi.org/10.1080/09243046.2021.1918608

Pitzanti, Giulia, et al. "3D Printing: an appealing technology for the manufacturing of solid oral dosage forms." Journal of Pharmacy and Pharmacology 74.10 (2022): 1427-1449. https://doi.org/10.1093/jpp/rgab136

Sanchez-Rangel, Elizabeth, and Silvio E. Inzucchi. "Metformin: clinical use in type 2 diabetes." Diabetologia 60 (2017): 1586-1593. https://doi.org/10.1007/s00125-017-4336-x

Schneider, Felix, et al. "In vitro simulation of realistic gastric pressure profiles." European Journal of Pharmaceutical Sciences 107 (2017): 71-77. https://doi.org/10.1016/j.ejps.2017.06.037

Schneider, Felix, et al. "Influence of postprandial intragastric pressures on drug release from gastroretentive dosage forms." AAPS PharmSciTech 19 (2018): 2843-2850. https://doi.org/10.1208/s12249-018-1022-3

Sun, Hong-Yan, and Xiao-Yan Lin. "Analysis of the management and therapeutic performance of diabetes mellitus employing special target." World Journal of Diabetes 14.12 (2023): 1721. https://doi.org/10.4239/wjd.v14.i12.1721

Tripathi, Julu, et al. "Current state and future perspectives on gastroretentive drug delivery systems." Pharmaceutics 11.4 (2019): 193. https://doi.org/10.3390/pharmaceutics11040193

Vaz, Vanessa Marcia, and Lalit Kumar. "3D printing as a promising tool in personalized medicine." Aaps Pharmscitech 22 (2021): 1-20. https://doi.org/10.1208/s12249-020-01905-8

Vrettos, Napoleon-Nikolaos, Clive J. Roberts, and Zheying Zhu. "Gastroretentive technologies in tandem with controlled-release strategies: A potent answer to oral drug bioavailability and patient compliance implications." Pharmaceutics 13.10 (2021): 1591. https://doi.org/10.3390/pharmaceutics13101591

Wadher, Kamlesh J., Rajendra B. Kakde, and Milind J. Umekar. "Study on sustained-release metformin hydrochloride from matrix tablet: Influence of

hydrophilic polymers and in vitro evaluation." International journal of pharmaceutical investigation 1.3 (2011): 157. https://doi.org/10.4103/2230-973X.85966

Zacchè, Martino Maria, Sushma Srikrishna, and Linda Cardozo. "Novel targeted bladder drugdelivery systems: a review." Research and reports in urology (2015): 169-178. https://doi.org/10.2147/RRU.S56168

Zhao, Ling, et al. "Preparation and in vitro drug release evaluation of once-daily metformin hydrochloride sustained-release tablets." Pharmacology & Pharmacy 3.04 (2012): 468. http://dx.doi.org/10.4236/pp.2012.34064

https://www.fda.gov/drugsatfda

Chapter 1

Intravesical drug delivery approaches for improved therapy of urinary bladder diseases

Published as:

Luca Palugan, Matteo Cerea*, Micol Cirilli, Saliha Moutaharrik, Alessandra Maroni, Lucia Zema, Alice Melocchi, Marco Uboldi, Ilaria Filippin, Anastasia Foppoli, Andrea Gazzaniga, International Journal of Pharmaceutics: X, 100100 (2021).

https://doi.org/10.1016/j.ijpx.2021.100100

* Corresponding author

§ The contribution given by Micol Cirilli to the work associated with published article was validation, investigation, visualization.

ABSTRACT

Diseases of the urinary bladder have high incidence rates and burden healthcare costs. Their pharmacological treatment involves systemic and local drug administration. The latter is generally accomplished through instillation of liquid formulations and requires repeated or long-term catheterization that is associated with discomfort, inflammation and bacterial infections. Consequently, compliance issues and dropouts are frequently reported. Moreover, instilled drugs are progressively diluted as the urine volume increases and rapidly excreted. When penetration of drugs into the bladder wall is needed, the poor permeability of the urothelium has also to be accounted for. Therefore, much research effort is spent to overcome these hurdles, thereby improving the efficacy of available therapies. Particularly, indwelling delivery systems suited for i) insertion into the bladder through the urethra, ii) intra-organ retention and prolonged release for the desired time lapse, iii) final elimination, either spontaneous or by manual removal, have been proposed to reduce the number of catheterization procedures and reach higher drug levels at the target site. Vesical retention of such devices is allowed by the relevant expansion that can either be triggered from the outside or achieved exploiting elastic and purposely 4D printed shape memory materials. In this article, the main rationales and strategies for improved intravesical delivery are reviewed.

KEYWORDS

Bladder

Intravesical delivery

Expandable systems

3D and 4D printing

Controlled release

1. INTRODUCTION

Diseases of the urinary tract, such as incontinence, overactive bladder, interstitial cystitis, bladder cancer and bacterial infections, are widespread in individuals of different ages and gender. However, their incidence increases in elderly people, who represent the population segment of developed countries in continuous growth and whose therapeutic treatments consequently have great impact on healthcare expenses. Particularly, bladder cancer is one of the most diagnosed tumors in the male population worldwide, and is the one with the highest cost from diagnosis to death as well as the fifth most expensive for overall treatment (Leal et al., 2016). The therapy of the above-mentioned pathologies has mainly involved the systemic administration of drugs by the oral route in some cases coupled with the instillation of liquid formulations directly into the bladder through catheters. Because systemic treatments fail to effectively target the affected tissues, they generally require higher drug doses in order to reach therapeutic concentrations in situ. This may lead to overwork of the organs responsible for elimination, which, in the case of elderly people most likely receiving multiple chronic therapies, may increase the risk for complications and onset of side effects. On the other hand, the catheterization procedure used for the local administration of drugs into the bladder is particularly invasive, poorly tolerated and may require to be carried out by specialized personnel often involving repeated hospitalization periods. Furthermore, it has a major impact on the patient quality of life, from a social and relational point of view, causing psychological discomfort, depression, personal disesteem and a sense of loss of control over the bladder function. From an occupational point of view, an increase in the number of absences, not only for therapy administration but also as a consequence of the discomforts arising, is often recorded. As a common side effect, the repeated insertion of catheters for intra-bladder in instillation of drugs causes inflammatory phenomena and infections. 10 to 30% of subjects undergoing short-term catheterization develops bacteriuria, often asymptomatic, and after longer-term catheterizations bacteria are found in urine samples from almost all treated subjects. Infections associated with

the use of the short-term catheters have been shown to prolong the average hospitalization time from 2.4 up to 4.5 days and have also been correlated with an increase in hospital mortality. Thanks to early detection procedures, in about 75% of patients, bladder cancer is found limited to the mucosa/submucosa area, and this percentage increases when patients under 40 are considered (Babjuk et al., 2019). To reduce mortality and prevent recurrence, the treatment of bladder cancer involves surgical resection and, after surgery, chemotherapy with repeated instillation of anticancer drugs into the bladder. The effectiveness of the current chemotherapy is limited not only by the high risk of dropout of patients due to the problems mentioned above, but also by the difficulties in keeping the active molecules inside the bladder for a sufficiently long period of time and promoting their penetration into the wall. Such difficulties are worsened by the urgency to urinate immediately after installation and by the progressive dilution of the bladder content over time. The strong therapeutic, social and economic interests related to the vast population affected by diseases of the urinary apparatus have given a decisive boost in recent years towards the identification of drug delivery strategies able to overcome all the issues previously discussed. The present review aims at presenting a brief excursus through the evolution of intravesical administration of drugs focusing on the development of delivery systems capable of maintaining effective concentrations of bioactive molecules within the bladder for strategic periods of time. Indeed, special emphasis was placed on indwelling solid dosage forms for prolonged release, also covering 3D and 4D printed devices.

2. ANATOMY AND PHYSIOLOGY OF URINARY BLADDER

The urinary bladder is a hollow organ, placed in the anterior part of the pelvic cavity, responsible for the collection and short-term storage of waste substances from the systemic circulation, coming from the kidneys, and their elimination as urinary fluids (Standring, 2005). Its shape, relative position and dimensions vary according to the gender, filling state and condition of the

adjacent organs. When empty, the bladder is similar to a tetrahedron, while in the state of maximum filling, under normal conditions around 400–600 mL, tends to assume a pseudospheric shape (Fig. 1). The fundus, also called body of the bladder, is the portion that constitutes the deposit of urine, where the two ureters coming from the kidneys define a triangular-shaped area together with the internal urethral orifice. The bladder neck, having a length of about 2–3 cm, is connected by the urethra to the external urinary meatus that in females also corresponds to the urine exit point, while in males continues into the anterior urethra that runs along the penis. The bladder wall is made of muscular and epithelial tissues. The mucosa at the interface with the urinary space consists of the uroepithelium, or urothelium, resting on a lamina propria. It is a transitional epithelial tissue composed of at least three layers: a basal cell layer attached to a basement membrane, an intermediate layer, and a superficial layer composed of large hexagonal cells (diameters of 25–250 μm) known as "umbrella cells". The urothelium plays a critical role as a permeability barrier to urine (Khandelwal et al., 2009). Epithelial integrity is maintained through complex processes of migration and proliferation, to restore cell number, and of differentiation to restore function. Basal epithelial cells, which have been suggested to have stemcell-like properties, typically exhibit very slow (3–6 month) proliferative rates. When the bladder is empty, the urothelium takes on a wrinkled appearance, while it stretches and appears smoother as the amount of urine collected increases. This change is made possible by the ability of the umbrella cells to modify their shape and of the intermediate cells to slide over one another, varying the thickness of the intermediate layer in relation to the state of filling of the organ, without loss of the urothelial barrier function. The bladder muscular layer, which overall constitutes the detrusor muscle, consists in a series of interconnected smooth muscle fibers arranged in different directions: while the fibers belonging to the inner and the external layer mostly show a longitudinal direction, those located in the middle area are characterized by a circular orientation. These three layers converge into the bladder neck and, together with the spiraliform smooth muscle fibers of the urethral sphincter, provide the sphincteric

mechanism responsible for urination. Such a process is ruled by a cortical autonomous stimulus, which is triggered by the stretching of bladder and urethra walls and causes both the contraction of the muscle tissue here located and the relaxation of the internal urethral sphincter. However, urine release is also under voluntary control, as a voluntary cortical stimulus is needed to allow the relaxation of the external urethral sphincter. The presence of approximately 150–200 mL of urine in the bladder initially stimulates urination, which is controlled by myovesical plexus sending signals for voiding to detrusor muscle. The latter controls the extent and frequency of bladder emptying.

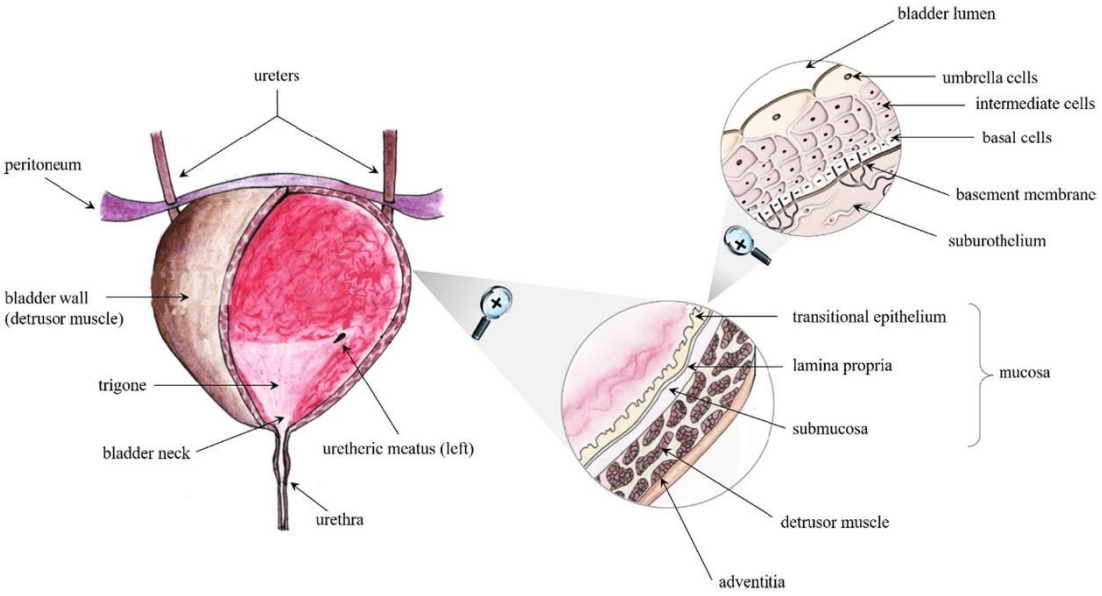

Fig. 1. Schematic of urinary bladder. Adapted from (Hamza, 2020).

3. PATHOLOGY OF URINARY BLADDER

Considering the bladder role in the homeostasis of the human body, it is evident how any change in its functionality would necessarily be associated with inconveniences of different severity (Guha Sarkar and Banerjee, 2010; Kolawole et al., 2017; Zacchè et al., 2015). These could be caused either by the natural aging process or by the activation of an inflammatory response, and also be brought about by the onset of various diseases (e.g. infections and cancer). Particularly, some chronic vesical pathologies, such as atonic and

hyperactive bladder, interstitial cystitis and cancer, are characterized by high current incidence, major discomfort for the patient and limited efficacy as well as tolerability of available treatments. Moreover, such diseases are often followed by opportunistic infections, which can in turn become recurrent. Atonic and hyperactive bladder, as well as urinary incontinence, relate to an alteration in the control of the muscular activity of bladder wall and sphincters responsible for urination (Chen and Kuo, 2019; Li and Liao, 2016). More in detail, while in the atonic bladder syndrome the contractility of the detrusor muscle is limited and associated with difficulties in performing the emptying process, in the hyperactive bladder disease there is an increased contractility of the organ, thus causing urgency and increased frequency in urination and nycturia. In urinary incontinence, the sphincter control is seriously reduced or lost, with difficulties in, or impossibility of, controlling the urine flow. These diseases are pretty common, showing huge diffusion, and their incidence increases with aging, being slightly higher in men. The treatment generally requires a pharmacological therapy acting on the cholinergic system, chiefly responsible for the modulation of the detrusor muscle tone, on the one hand, and the use of invasive mechanical methods, such as the application of catheters for the correct draining of urine, on the other. Interstitial cystitis is a painful chronic syndrome with higher incidence in women, mainly associated with a damage in the glycosaminoglycans (GAGs) layer with a loss of vesical epithelium functionality (McLennan, 2014). Symptoms include pelvic pain, urinary frequency, urgency and nycturia. Etiology is linked to alteration of urothelium GAGs, with activation of mast cell, autoimmune reaction and central sensitization. Unfortunately, the therapy is based on empirical studies and suffers from low efficacy. It is limited to the use of a combination of painkillers to be administered systemically and anesthetics instilled in situ. Finally, bladder cancer is one of the most common neoplastic pathologies, the etiology of which lies in the abnormal growth and proliferation of bladder wall cells. Although it generally affects the inner bladder surface (i.e. superficial tumors), a small percentage of cases in which tumor cells may infiltrate the muscular layer of the bladder is also described (i.e. muscle-invasive cancer).

The onset of cancer impacts the normal activity of the bladder, causing hematuria, frequency and urgency in urination together with dysuria. First-line treatment of non-muscle-invasive bladder cancer envisages surgical resection of the tumor followed by local instillations, repeated over time, of different chemotherapeutic agents (e.g. epirubicin, mitomycin, Bacillus Calmette-Guérin) to prevent recurrence and progress into muscle-invasive bladder cancer (Babjuk et al., 2019; Yoon et al., 2020).

4. ADMINISTRATION OF DRUGS INTO THE BLADDER AND RELEVANT OPEN ISSUES

Local treatment of bladder diseases, despite being a poorly acceptable choice for the patient, exhibits the advantage of reducing the side effects of specific drugs. Indeed, substances that would not be considered safe when administered via other routes, such as dimethyl sulfoxide and botulinum toxin, have been approved for intravesical infusion. Moreover, compared to the oral route, partial elimination due to the first-pass effect can be avoided, thus allowing possibly lower drug strengths to be used. Local administration is made by instilling liquid formulations containing one or more drugs into the bladder cavity, through a catheter inserted directly into the urethra of the patient; such liquids can be left in situ for a pre-determined time lapse before being excreted or withdrawn. The use of catheters is a widespread practice, not only exploited to support the treatment of urinary system diseases, but also for diagnostic purposes. However, catheterization causes inconvenience and discomfort to the patient, which is generally treated by local application of ointments or gels containing anesthetic drugs having short-lasting efficacy (usually limited to minutes). Indwelling urethral catheters (IUCs), also named Foley catheters, are designed to remain in place for many days or weeks and to be held in position by an inflated balloon in the bladder. They are typically used to enable urinary bladder emptying in the case of pathologies impairing natural urination or to drain urine when the patient is bedridden. The tube of the catheter has two separated lumens, or channels, running down its length. One lumen, open at both ends, drains urine into a collecting bag; the other has

a valve on the outer end and connects to the balloon at the inside tip. The balloon is inserted through the urethra and positioned deflated inside the bladder. Then it is inflated with a prefixed volume of sterile water to maintain the position and avoid accidental slipping out. For removal, the balloon is deflated, and the catheter is simply pulled out. Prolonged release of an anesthetic for reducing the pain induced by IUC has been recently proposed by Kim and co-authors, who designed a drug-loaded polymer strand releasing lidocaine up to 7 days (Kim et al., 2021). The thin poly(lactic-co-glycolic acid) (PLGA) strand was wrapped around the external tube of the urinary catheter and released the drug from the surface thus alleviating the discomfort associated with the presence of the device (Fig. 2). When urinary catheters are placed in the bladder through the urethra for days or weeks, long-term residence often entails other complications such as the onset of infections. These are generally caused by bacteria found in the external area close to the urinary orifice, such as Escherichia coli, Enteroccoccus fecalis, Proteus mirabilis and Pseudomonas aeruginosa, which could reach the bladder either during catheter insertion or by moving upstream through the catheter cavity from the drainage bag where they can proliferate. Once in the bladder, such microorganisms form complex structures called biofilms that make penetration of drugs, and thus the relevant action, even more difficult. In any case, the elimination of pathogens is fundamental to avoid worsening of infections and further problems, and it generally requires systemic and local administration of antibiotics. Several papers reported on the coating of urinary catheters with drug-containing formulations in order to reduce such a risk. For instance, salicylic acid-releasing polyurethane acrylate polymers, silver nanoparticles, antibacterial polycationic nanospheres and chlorhexidine-loaded poly(ethylene glycol)-block-poly(ε-caprolactone) micelles were investigated (Francesko et al., 2016; Gefter et al., 2018; Nowatzki et al., 2012; Srisang and Nasongkla, 2019; Thomas et al., 2015). A further issue involved in therapies based on intravesical administration of drugs, particularly those for bladder cancer, is given by the poor permeability of urothelium, which may represent a tough barrier to be crossed especially by molecules with high

molecular weight (Yoon et al., 2020). In addition to the problems associated with the poor urothelium permeability, it should be considered that the maximum residence time of drugs instilled into the urinary bladder is approximately of 2 h and their concentration is constantly diluted by excreted liquids drained by ureters, with consequent need for frequent instillations to maintain the desired therapeutic properties. Even though drug elimination after the instillation treatment can be deferred by restricting the liquid intake, which reduces the production of urinary fluid, and urinating before intravesical infusion, compliance issues may arise especially when elderly patients are involved, for whom holding the urge to urinate and complete bladder emptying are often problematic. Moreover, the large variability in the residence of drugs in situ makes it difficult to define personalized therapeutic regimens for individual patients, thus implying the application of rigid therapeutic protocols. For all of these reasons, the distress caused by catheterization and discomfort of frequent treatment regimens are connected with high dropout rates, with severe consequences especially in the case of bladder cancer.

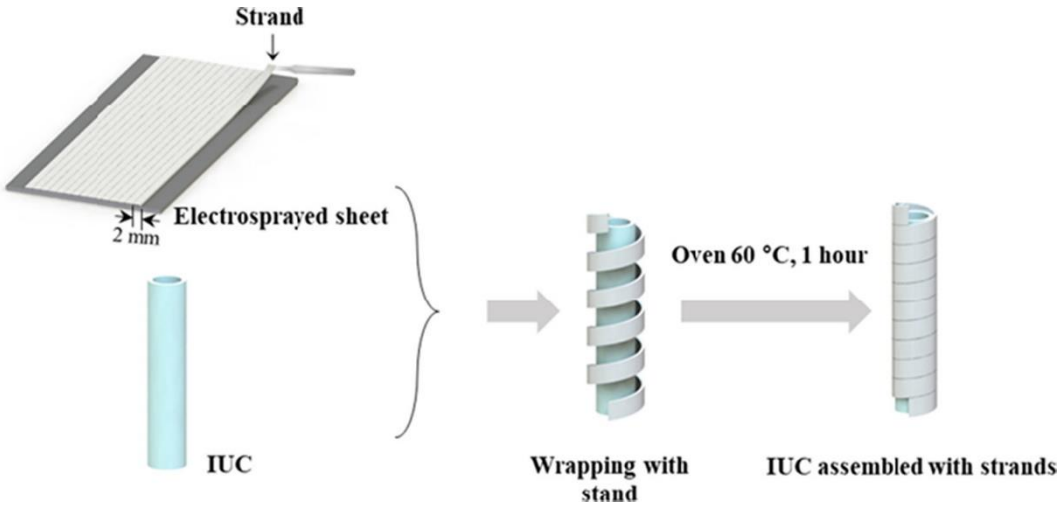

Fig. 2. Schematic of the fabrication procedure of strand-wrapped indwelling urethral catheters for lidocaine release. Reprinted with permission from (Kim et al., 2021).

5. STRATEGIES TO IMPROVE THE PHARMACOLOGICAL THERAPY OF URINARY BLADDER DISEASES

Based on the above considerations, it is clear that the local therapy of urinary bladder diseases is a challenging goal. The success of such treatments necessarily depends on proper exposure of the organ to the drug (Wang et al., 2021). Therefore, strategies to improve the outcome of intravesical pharmacological treatments have been aimed at maintaining effective drug levels in situ through the use of delivery systems able to be retained and release the drug into the organ for a prolonged period of time and/or enhancing permeation of locally administered drugs throughout the bladder wall.

1.1. Enhancement of urothelium permeation

Enhancement of permeation of the urothelium has been obtained through intravesical device-assisted therapies. Radiofrequency-induced thermos-chemotherapeutic effect (RITE), conductive hyperthermic chemotherapy, and electromotive drug administration (EMDA) have shown promising results (Tan and Kelly, 2018). In particular, EMDA is based on the application of electric impulses through a catheter equipped with an inner electrode (Fig. 3). Its use for the treatment of non-muscle-invasive bladder cancer demonstrated enhanced transmembraneous transport of mitomycin-C into all bladder wall layers compared to passive diffusion following standard instillation (Di Stasi and Riedl, 2009). Nanocarrier drug delivery systems, formulated from lipids, polymers, proteins and metals, have also been leveraged to increase the penetration across the bladder mucosa (Zacchè et al., 2015). In particular, liposomes are based on concentric bilayers with nanometric sizes and composition mimicking the human cell membrane. Liposomes for intravesical administration of lipophilic or hydrophilic drugs have been described as well as solid lipid nanoparticles, nanoparticles with specific ligands for cell targeting, silver, gold or magnetic nanoparticles, and branched polymeric dendrimers (Fraser et al., 2003; Guha Sarkar and Banerjee, 2010; Sansare et al., 2021; Tyagi et al., 2016; Yu et al., 2020). Peptide molecules having less than 40 amino acids showed an intrinsic capacity

of transduction across biological membranes and have been exploited to transport various substrates inside cells. Drug conjugates with arginine-rich peptides have been described to enhance intracellular uptake of the active molecule (Nakase et al., 2017). Specific peptides have also been used in liposome, nanoparticle and microparticle formulations showing effectiveness in promoting drug permeation in vitro and in vivo (Hsieh et al., 2011). Chemical agents, such as polymers, dimethyl sulfoxide and protamine sulphate, have been also proposed as enhancers (Chen et al., 2003). However, both EMDA and substances employed to promote permeation may induce irreversible alteration of urothelial cells, interfering with the relevant barrier function and causing unwanted side effects.

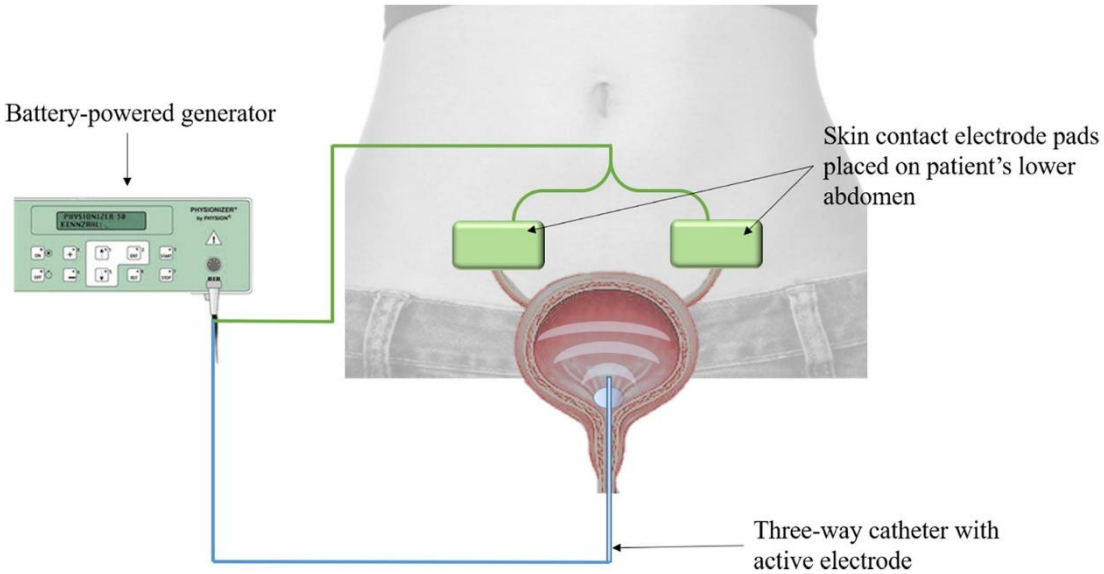

Fig. 3. Schematic of intravesical device-assisted therapy for non-muscle-invasive bladder cancer electromotive drug administration.

1.2. Prolongation of vesical residence time

A common strategy to extend the contact time of intravesical formulations with the luminal surface of the bladder is based on increased adhesivity or viscosity of solutions or suspensions instilled by catheterization (Kolawole et al., 2017). Mucoadhesive systems are based on polymers able to interact with the urothelial GAGs (Chatta et al., 2015). As viscosity enhancers, thermo-sensitive polymers, which present low viscosity at low temperature (refrigeration temperature) and undergo rapid gelation at higher temperature (e.g. TCGel®), are used (GuhaSarkar

et al., 2017; Qiu et al., 2020). Solutions/suspensions containing such polymers can easily be instilled into the bladder where the body temperature activates the formation of a gel depot, having adhesive properties, from which the drug could be slowly released via diffusion/ erosion mechanisms. Viscosity of liquid formulations can also be increased by polymers sensitive to ionic concentration changes. This may be relied on to have originally syringeable formulations thickened in the bladder environment due to the presence of ions in the urine triggering the relevant gelation (Vigani et al., 2020). Even though in situ gel formation is a good option for prolonging intravesical residence time, the risk of urethra obstruction due to the increased viscosity of urine might be quite problematic. Moreover, adhesion of gels to the luminal surface of the bladder can affect the urothelium structure inducing inflammatory reaction. To prolong residence time in the bladder, floating systems have also been proposed (Kolawole et al., 2017; Lin et al., 2014a, 2014b; Zhu et al., 2016). These exploit buoyancy of low-density dosage forms in urine, thus resisting excretion through the urethra. The approach is based on the use of excipients generating CO2 when in contact with aqueous fluids as occurs with effervescent formulations. Besides NaHCO3 or NH4HCO3, perfluoropentane (PFP) has been used as a solid material that converts to gas when subjected to temperatures above 29.2 ◦C (Zhu et al., 2016). Despite the promising approach, floating systems have been poorly investigated, and the risk of occlusion of the urethra should be accounted for when the urine volume in the bladder is low. Excessive gas production could also induce expansion of the organ wall with consequent need for urination.

1.2.1. Expandable devices for prolonged drug delivery

Indwelling drug delivery devices are physical systems administered by transurethral catheterization aimed at prolonged release of active pharmaceutical ingredients in the urinary bladder. Upon insertion into the bladder, they undergo an increase in spatial encumbrance when the bladder neck is passed, which enables intra-organ retention. As with other intravesical delivery systems previously discussed, it is important that physiological urination is not hampered by the device. Indwelling systems can be water-soluble or biodegradable and

therefore designed to be excreted spontaneously by urination: at the end of the drug release process, they may dissolve or release fragments able to pass the urethral sphincter freely. These portions should be small enough to avoid urinary tract obstruction. On the other hand, insoluble and/or non-degradable intravesical devices require removal procedures after depletion. Potentially, indwelling vesical systems may extend intra-organ residence and related drug delivery over time periods in the order of few to several days. The mechanism allowing for increase in spatial encumbrance may rely on external triggering of expansion, elastic relaxation or shape memory effect. In Table 1, an overview of the main expandable devices reported in the literature is presented. 5.2.1.1. Devices based on externally-triggered expansion. An intravesical system resembling indwelling urethral catheters is the UROS oxybutynin infusion pump by Situs Corporation (Oxybutynin Intravesical — Situs, 2002). This includes a reservoir that can be easily inserted empty into the bladder and filled from the outside with the desired drug formulation (Matsuura et al., 2001). The reservoir, made of poly(dimethylsiloxane), is large enough not to be drained out even when voided but not so large as to cause bladder irritation or occlusion (dimensions before filling: 100 mm in length and 6 mm in diameter). After the device is filled, it is allowed to float freely or alternatively is tied to the bladder wall. The two ends are connected with an inextensible material (polyester ribbon), which allows annular shaping. In order to deliver the drug at a controlled rate, the device is equipped with a pressure-responsive valve. The flow resistance of the latter is sensitive to the pressure at which the drug is stored inside the chamber. The UROS system is proposed for delivery of drugs for approximately 30 days, after which it is removed by urethral cystoscopy (Fraser et al., 2002; Cima et al., 2014). Tested in vivo in healthy volunteers, it provided clinical benefits in terms of reduced frequency and urgency of urination (Situs Co, 2000). Nevertheless, it failed to go beyond Phase II. Yachia and Hirszowicz patented an invention for intravesical drug delivery with the aim of treating urinary incontinence, chronic urinary infections, cancer or of monitoring the bladder activity (Innoventions Ltd, 2000; Yachia and Hirszowicz, 2001). The system is based on an expandable balloon which can be inserted into the urinary bladder and filled afterwards, or

filled and compressed prior to insertion. A magnetic element located at the inner surface of the balloon or embedded in its wall can help the relevant positioning for sealing the bladder or directing to specific regions of the urothelium. In addition, the device has a self-sealing valve in the wall of the balloon, which prevents the fluid from leaking out after the needle used for filling is withdrawn. The device may float or sink into the urinary fluid depending on the type of filling. Another system for intravesical drug delivery has been proposed by Hopmann and co-authors for the treatment of overactive bladder syndrome (OAB) (Hopmann et al., 2015). The device is composed of multiple spherical units having a diameter of 2.4 or 4 mm connected by a flexible and resorbable suture thread. The spherical units consist of foamed matrices of poly-D, L-lactide-co-glycolide-co-polyethylene glycol diblock copolymer (PLGA-PEG) embedding microspheres of poly (dimethylsiloxane) loaded with trospium chloride, an anticholinergic drug. The device is arranged in a way that it can be expanded in the bladder after insertion through the urethra via a catheter. The retention mechanism is activated externally by pulling the threads, and the change in shape allows the system to safely be maintained inside the bladder. After degradation of the PLGA-PEG matrix, the microspheres are eliminated in the urine. The approach relies on continuous release of the drug from the microspheres and complete elimination of device residues after less than 4 weeks, to avoid the onset of potential side effects such as the appearance of scale due to the deposit of salts on the microparticles.

Table 1 Expandable devices for prolonged drug delivery.

Schematic of the device	**Expansion mode**	**References**
UROS infusor 	Drug reservoir with a pressure responsive-valve. Expansion is achieved after filling with the drug solution	(Situs Co, 2000) (Matsuura et al., 2001)

Intravesical balloon 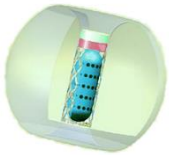	Intravesical balloon inflated with drug formulations and positioned within the bladder via magnetic control	(Innoventions Ltd, 2000) (Yachia and Hirszowicz, 2001 (Yachia and Hirszowicz, 2002) (Yachia and Hirszowicz, 2006a, 2006b)
Multiple spherical units device 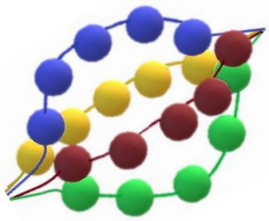	Drug-containing polydimethylsiloxane microspheres embedded in biodegradable matrix units that are connected by flexible resorbable suture threads. The retentive configuration is achieved by pulling the threads	(Hopmann et al., 2015)
S-shaped 3D printed hollow device 	Drug reservoir fabricated by SLA 3D printing based on an elastomer. The retentive configuration is achieved after catheter removal	(Xu et al., 2021)
LiRIS™ and GemRIS™ 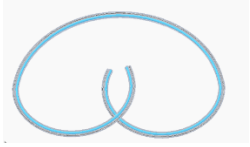	Silicon tube prefilled with the drug formulation. The retentive pretzel-like configuration is achieved thanks to the superelastic properties of a nitinol wire that regains its starting shape after catheter removal	(Lee et al., 2007) (Nickel et al., 2012) (Giesing et al., 2015) (Lee and Daniel, 2015) (Cima and Lee, 2020)

Osmotic device based on elastomeric materials 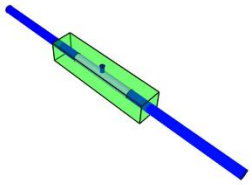	Biodegradable elastomer-based device having osmotic release mechanism	(Tobias et al., 2010)
PVA-based 4D printed intravesical device 	U- and helix-shaped PVA matrices, fabricated by HME and 4D printing via FDM and deformed to an elongated temporary shape for insertion into the bladder via catheter. Retentive configurations achieved thanks to shape memory effect induced by exposure to urine at body temperature.	(Melocchi et al., 2019a)

5.2.1.2. Systems based on elastic materials.

Elastic materials are able to regain their shape following the removal of an external force (i.e. compression, bending, stretching). Polymers presenting these features are named elastomers. They express weak interchain forces, low Young's moduli and are characterized by high values of failure strains. Mechanical properties of elastomers are particularly advantageous for numerous pharmaceutical applications and are ideal for devices that need to acquire different shapes for insertion and retention in hollow organs (Lendlein and Langer, 2002). However, one of the major drawbacks of intravesical devices based on elastic materials is the need for a transurethral removal procedure, which unavoidably reduces the patient compliance. Recently, an elastomer-based system for intravesical delivery was prepared by 3D printing using stereolithography (SLA) (Fig. 4) (Xu et al., 2021). SLA consists in the polymerization of liquid monomers by light irradiation for obtaining precise and complex 3D geometries, smooth finish and high resolution (approximately 25 μm). The device composition includes a thermosetting resin that is polymerized

by 405 nm laser light. Lidocaine hydrochloride has been added to the liquid resin prior to printing, thus being uniformly distributed in the printed item, or filled in after printing of hollow shells. Different shapes (solid and hollow) and drug loadings have been evaluated for mechanical properties that should allow the device to fast regain its starting shape after deformation by stretching. The systems offer satisfactory mechanical characteristics and the desired tuneable release behavior. A reservoir ciprofloxacin hydrochloride system prepared from a biodegradable elastomer has been proposed for urinary bladder and, more in general, local urological therapies (Tobias et al., 2010). The device is composed of poly(glycerol-co-sebacic acid) casted in a tubular geometry and filled with drug powder (Fig. 5). A laser-drilled orifice allowed the release of the drug induced by osmotically-driven water permeation. In vitro experiments have demonstrated that the elastomer is susceptible to hydrolytic degradation indicating the possibility of producing a completely resorbable drug delivery device. In addition, modulation of the release rate is achieved by varying the orifice size. TARIS Biomedical is a pharmaceutical company with extensive experience in intravesical drug delivery. Among various devices proposed over the years, GemRIS™ (gemcitabine-releasing intravesical system) and LiRIS™ (lidocaine-releasing intravesical system) have been developed taking advantage of the superelastic characteristics of nitinol (Cima and Lee, 2020; Daneshmand et al., 2017; Grimberg et al., 2020). This material, an almost equiatomic metal alloy of nickel and titanium, exhibits not only superelasticity (good combination of high strength and low elastic module) but also high corrosion resistance, non-ferromagnetic behavior, biocompatibility and, importantly, shape memory, unique properties that are largely exploited in the area of medical devices (Fig. 6). GemRIS™ and LiRIS™ show a common design but differ for the drug conveyed. Both are conceived as an osmotic pump, leading to a prolonged release for approximately 2 weeks. The final goal is to reduce as much as possible the overall dimensions of the system with respect to those already available (e.g. UROS) in order to limit patient discomfort. The reduction in size without decreasing the payload has been attained because the drug is present in the solid state rather than as a solution. The devices include a water-permeable silicone

tube with different inner cavities. While the larger cavity is filled with mini-tablets containing either lidocaine hydrochloride or gemcitabine, the smaller one contains a nitinol wire. The pretzel-like shape of the systems prevents emptying from the bladder. To enable intravesical administration, the wire is mechanically forced into an elongated shape. This way, it is possible to insert the system into a catheter, which acts as an external constraint. When the catheter reaches the bladder and the DDS is positioned into the cavity, nitinol regains the initial pretzel-like shape thanks to its superelastic behavior, thus promoting retention in the target area. In a phase 1 study, the systems have been well tolerated while retained in the bladder in both volunteers and interstitial cystitis/ bladder pain syndrome patients, even when administered to healthy subjects in a placebo form (Nickel et al., 2012). In the case of LiRIS™, this rules out any possible misleading effects on tolerability caused by the conveyed anesthetic drug. Pain relief and reduction in voiding urgency and frequency have been reported after a two-week treatment together with signs of bladder healing. Two phase 2 studies have also been carried out, in which no significant treatment effect was assessed with lidocaine hydrochloride 400 mg LiRIS™ as compared with placebo (Evans et al., 2021). However, one of the major drawbacks of the described devices based on elastic materials is the need for a transurethral removal procedure, which unavoidably reduces the patient compliance.

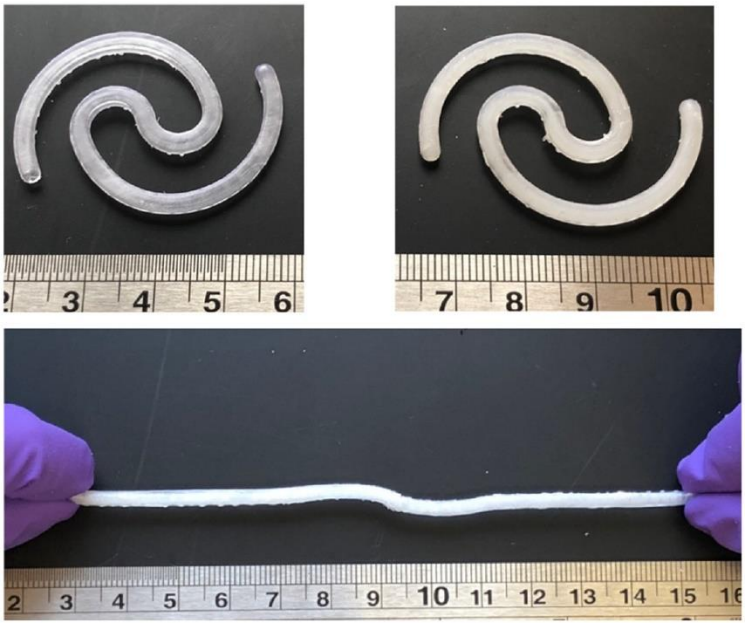

Fig. 4. Photograph of the SLA 3D printed hollow device before (top left) and after (top right) filling, and under stretching (bottom). Scale in cm. Reprinted with permission from (Xu et al., 2021).

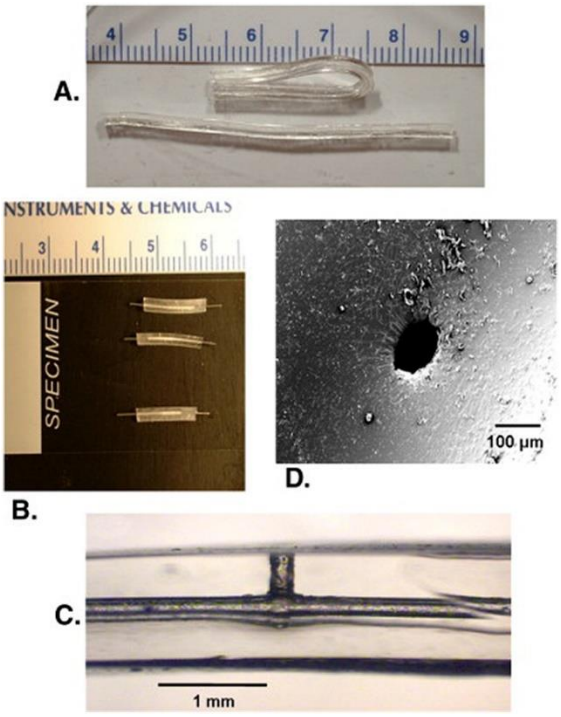

Fig. 5. Photographs of the reservoir system based on a biodegradable elastomeric polymer. A) tubes demonstrating flexibility of material. B) modules loaded with drug and plugged with steel wires. C) zoomed-in view of module having 150 µm diameter laser-drilled orifice channel leading into 300 µm diameter core. D) SEM image of 100 µm diameter laser-drilled orifice viewed from the orifice surface. Reprinted with permission from (Tobias et al., 2010)

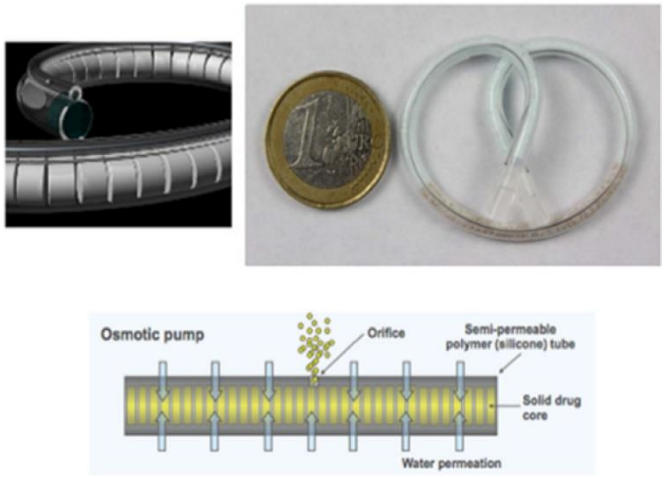

Fig. 6. Images of GemRIS™ (top) and schematic of the device in operation (bottom). Reprinted with permission from (Grimberg et al., 2020).

5.2.1.3. Devices based on shape-memory materials.

Shape memory polymers (SMPs) are able to undergo major shape modifications under the application of a range of triggering stimuli, such as changes in temperature, light, magnetic field and electrical currents, which could even be applied remotely (Lendlein and Langer, 2002; Melocchi et al., 2021c; Shin et al., 2017; Zhang et al., 2019). The rising interest towards these polymers could be considered a consequence of the spread of shape memory alloys (SMAs), which dates back to the end of the 90s. In this respect, among SMAs, nitinol still represents the material of choice in the biomedical field for its above-mentioned peculiar characteristics. More recently, SMPs have started to be considered as an interesting alternative. Indeed, as compared with SMAs, they are lightweight, compliant with many cost-effective manufacturing processes, can be combined with specific adjuvants to attain products with innovative properties and their shape recovery may be triggered by different external stimuli. The so-called multifunctional materials have aroused particular interest in that they show many attractive properties, such as biocompatibility, mechanical characteristics matching those of soft biological tissues, sterilizability and solubility and/or biodegradability, the latter being especially useful in case of products intended for temporary applications. Overall, the simple processability combined with the possibility of fine-tuning the mechanical properties and the actuation stimulus (e.g. activation temperature) have further boosted the interest in SMPs. The activation of the shape memory effect through heating, either direct or indirect, may lead to an

undesired increase of temperature in the target area, potentially causing thermal damage of the surrounding tissues. In this respect, water-induced shape memory response could be highly advantageous. Indeed, water is always present in physiological environments - such as the bloodstream and the urinary bladder - and, acting as a plasticizer, may reduce the temperature required to trigger the targeted shape modifications. This is achieved when interaction with water causes an increase in the mobility of selected macromolecular chains, typically when dealing with polymers having hydrophobic and hydrophilic domains. Several SMP-based systems intended for implantation have been described in the scientific literature, mainly for surgical and cardiovascular applications. This is the case with micrometric drug delivery carriers, self-tightening sutures, catheters, endovascular stents and clot removal systems. As a further step forward and with the aim of circumventing invasive removal of exhausted devices, the use of water-soluble SMPs has been proposed for the development of indwelling systems for intra-organ release of drugs (Maroni et al., 2020; Melocchi et al., 2019a, 2019b). Particularly, poly(vinyl alcohol) (PVA) of pharmaceutical grade has been investigated based on preliminary data on its water-induced shape memory effect. Moreover, it is a thermoplastic polymer suitable for hot melt extrusion (HME) and fused deposition modeling (FDM) 3D printing, which allows for great versatility in terms of achievable shapes and sizes (Melocchi et al., 2018, 2020a, 2021a). Interestingly, the potential of FDM for the fabrication of personalized drug products has drawn special attention, and 3D printing coupled with the use of SMPs has been translated into 4D printing, the time frame during which the shape modifications takes place being the 4th dimension (Melocchi et al., 2020b, 2021b). Prototypes for intravesical delivery having rather simple original shapes (i.e. I-, U- and helix shapes) have been obtained by both the above-mentioned hot-processing techniques and manually deformed into differing temporary shapes (i.e. U- and I- shapes) (Fig. 7) (Melocchi et al., 2019a). Upon immersion in simulated urine fluid at body temperature, the samples show controlled release of the loaded drug tracer and the expected shape recovery effect. Feasibility of the proposed approach relying on 4D printing for the fabrication of retentive DDSs has therefore been demonstrated. However, there are still open challenges, mainly involving the duration of release and mechanical properties of the system upon interaction with aqueous fluids.

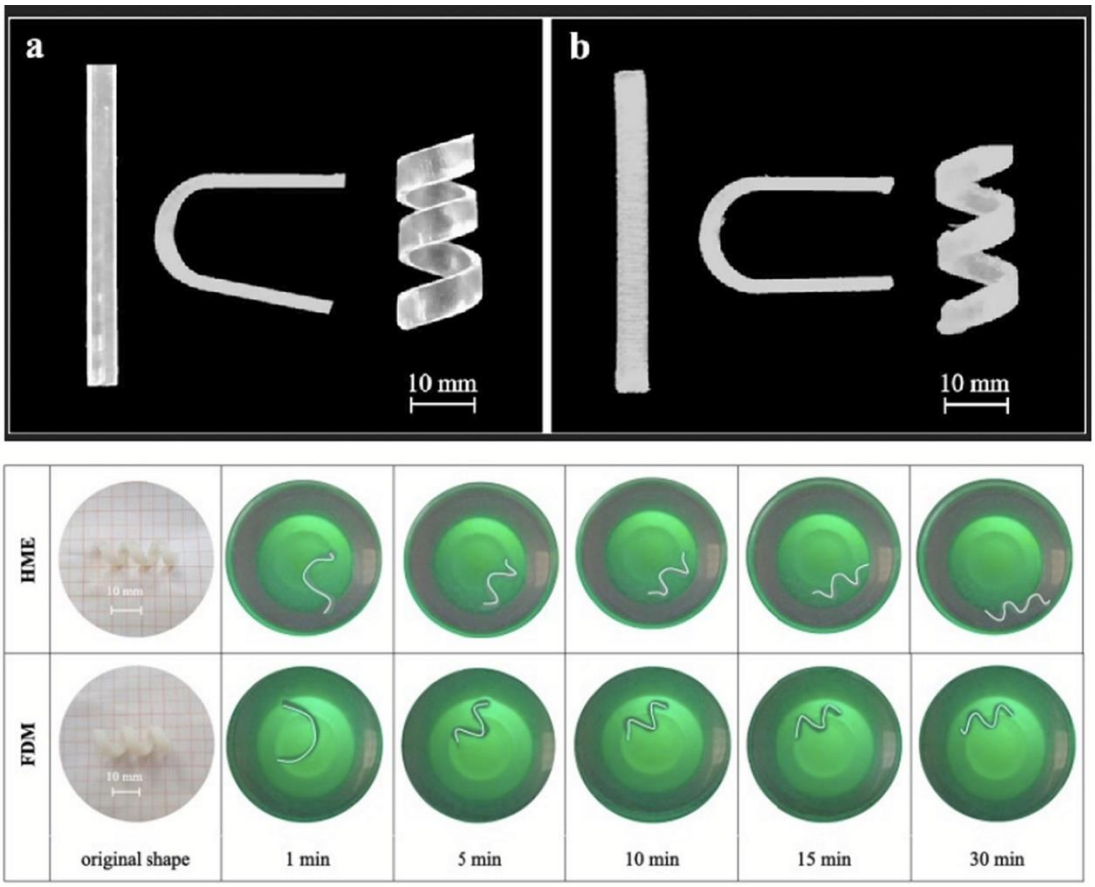

Fig. 7. Photographs of originally I-, U- and helix-shaped intravesical specimens based on PVA obtained by (a) HME or (b) FDM and acquired on specimens having original helix shape, programmed to take on a temporary I-shape, during shape recovery experiments (bottom). Reprinted with permission from (Melocchi et al., 2019a).

6. CONCLUSIONS

Considering the current medical treatments of urinary bladder diseases and their prevalence in the population, development of advanced delivery systems conveying reduced though effective drug doses directly to the site of interest appears a priority in the pharmaceutical area. Direct and indirect savings as well as social benefits arising from use of intravesical delivery systems would especially be provided by devices that, once inserted into the bladder, may be retained within the organ and yield sustained release of the drug for the desired time frame, at least hours, requiring no other specific intervention. Indeed, this could limit the need for catheterization, reduce involvement of trained healthcare personnel and enhance the perceived quality of life for the patients. Furthermore, the decreased number of catheterizations could remarkably lower the incidence of secondary infections. Given the growing interest in precision

medicine, the possibility of personalizing the pharmacological therapy in terms of type as well as dose of drugs and release performance is also of utmost interest. Among the various formulation strategies described for bladder retention and delivery, systems based on externally-triggered expansion, elastic or smart materials have mainly been proposed, fabricated by different techniques. Particularly, the use of 3D and 4D printing, when dealing with shape-memory polymers, has been proved specially suited for fabrication of customizable therapeutic systems. Allowing patients to lead a regular daily life in spite of the disease conditions they have to face and, at the same time, receive a less invasive and more effective therapy, could result in an increase in the well-being of the treated subjects and in a greater adherence to the treatment, with further improvement of life expectancy.

REFERENCES

Babjuk, M., Burger, M., Comp´erat, E., Gontero, P., Mostafid, A.H., Palou, J., Van Rhijn, B.W.G., Roupr^et, M., Shariat, S.F., Sylvester, R., Zigeuner, R., 2019. Non-muscleinvasive (TaT1, CIS) Bladder cancer. Eur. Assoc. Urol. 1, 9–27.

Chatta, D., Cottrell, L., Burnett, B., Laverty, G., McConville, C., 2015. The use of watersoluble mucoadhesive gels for the intravesical delivery of epirubicin to the bladder for the treatment of non-muscle-invasive bladder cancer. J. Pharm. Pharmacol. 67, 1355–1362. https://doi.org/10.1111/JPHP.12441.

Chen, L.-C., Kuo, H.-C., 2019. Pathophysiology of refractory overactive bladder. Low. Urin. Tract Symptoms 11, 177–181. https://doi.org/10.1111/LUTS.12262.

Chen, D., Song, D., Wientjes, M.G., Au, J.L.-S., 2003. Effect of dimethyl sulfoxide on bladder tissue penetration of intravesical paclitaxel. Clin. Cancer Res. 9, 363 LP – 369.

Cima, M.J., Lee, H., 2020. Intravesical Drug Delivery Methods and Devices. US 10,646,691 B2.

Cima, M.J., Lee, H., Daniel, K., Tanenbaum, L.M., Mantzavinou, A., Spencer, K.C., Ong, Q., Sy, J.C., Santini, J., Schoellhammer, C.M., Blankschtein, D., Langer, R.S.,

2014. Single compartment drug delivery. J. Control. Release 190, 157–171. https:// doi.org/10.1016/j.jconrel.2014.04.049.

Daneshmand, S., Pohar, K.S., Steinberg, G.D., Aron, M., Cutie, C., 2017. Effect of GemRIS (gemcitabine-releasing intravesical system, TAR-200) on antitumor activity in muscle-invasive bladder cancer (MIBC). J. Clin. Oncol. 35, e16000. https://doi.org/10.1200/JCO.2017.35.15_suppl.e16000.

Di Stasi, S.M., Riedl, C., 2009. Updates in intravesical electromotive drug administration® of mitomycin-C for non-muscle invasive bladder cancer. World J. Urol. 27, 325–330. https://doi.org/10.1007/s00345-009-0389-x.

Evans, R., Kohan, A., Moldwin, R., Radecki, D., Geib, T., Peters, K.M., 2021. Safety, tolerability, and efficacy of LiRIS 400mg in women with interstitial cystitis/bladder pain syndrome with or without Hunner lesions. Neurourol. Urodyn. 40, 1730–1739. https://doi.org/10.1002/NAU.24702.

Francesko, A., Fernandes, M.M., Ivanova, K., Amorim, S., Reis, R.L., Pashkuleva, I., Mendoza, E., Pfeifer, A., Heinze, T., Tzanov, T., 2016. Bacteria-responsive multilayer coatings comprising polycationic nanospheres for bacteria biofilm prevention on urinary catheters. Acta Biomater. 33, 203–212. https://doi.org/10.1016/j.actbio.2016.01.020.

Fraser, M.O., Lavelle, J.P., Sacks, M.S., Chancellor, M.B., 2002. The future of bladder control-intravesical drug delivery, a pinch of pepper, and gene therapy. Rev. Urol. 4, 1–11.

Fraser, M.O., Chuang, Y.-C., Tyagi, P., Yokoyama, T., Yoshimura, N., Huang, L., De Groat, W.C., Chancellor, M.B., 2003. Intravesical liposome administration—a novel treatment for hyperactive bladder in the rat. Urology 61, 656–663. https://doi.org/ 10.1016/S0090-4295(02)02281-1.

Gefter, J., Zaks, B., Kirmayer, D., Lavy, E., Steinberg, D., Friedman, M., 2018. Chlorhexidine sustained-release varnishes for catheter coating – dissolution

kinetics and antibiofilm properties. Eur. J. Pharm. Sci. 112, 1–7. https://doi.org/10.1016/j.ejps.2017.10.041.

Giesing, D., Lee, H., Daniel, K.D., 2015. Drug Delivery Systems and Methods for Treatment of Bladder Cancer with Gemcitabine. US 2015/0250717 A1.

Grimberg, D.C., Shah, A., Inman, B.A., 2020. Overview of taris GemRIS, a novel drug delivery system for bladder cancer. Eur. Urol. Focus 6, 620–622. https://doi.org/ 10.1016/j.euf.2019.09.006.

GuhaSarkar, S., Banerjee, R., 2010. Intravesical drug delivery: challenges, current status, opportunities and novel strategies. J. Control. Release 148, 147–159. https://doi. org/10.1016/j.jconrel.2010.08.031.

GuhaSarkar, S., More, P., Banerjee, R., 2017. Urothelium-adherent, ion-triggered liposome-in-gel system as a platform for intravesical drug delivery. J. Control. Release 245, 147–156. https://doi.org/10.1016/j.jconrel.2016.11.031.

Hamza, 2020. What Is Urinary Bladder? Function and Embryonic Development of Urinary Bladder along with Diseases Related to Urinary Bladder. Medlepius. URL. http://www.medlepius.com/2020/01/what-is-urinary-bladder-function-and.html.

Hopmann, C., Kaltbeitzel, D., Kauth, T., Dittrich, B., Grosse, J., Huppertz, N., Schwantes, U., Neumeister, C., von Walter, M., 2015. Degradation of microcellular PLGA-PEG copolymer for use in a drug delivery system for the urinary bladder. Plast. Eng. 71, 60–64.

Hsieh, J.-T., Zhou, J., Gore, C., Zimmern, P., 2011. R11, a novel cell-permeable peptide, as an intravesical delivery vehicle. BJU Int. 108, 1666–1671. https://doi.org/ 10.1111/J.1464-410X.2011.10185.X.

Innoventions Ltd, 2000. PharmaSphere Intravesical Drug Delivery. URL. https://www. innoventions-med.com/pharmasphere (accessed 8.4.21).

Khandelwal, P., Abraham, S.N., Apodaca, G., 2009. Cell biology and physiology of the uroepithelium. Am. J. Physiol. Ren. Physiol. 297 https://doi.org/10.1152/ajprenal.00327.2009.

Kim, C.R., Jang, E.B., Hong, S.H., Yoon, Y.E., Huh, B.K., Kim, S.N., Kim, M.J., Moon, H.S., Choy, Y. Bin, 2021. Indwelling urinary catheter assembled with lidocaine-loaded polymeric strand for local sustained alleviation of bladder discomfort. Bioeng. Transl. Med. 6, 1–12. https://doi.org/10.1002/btm2.10218.

Kolawole, O.M., Lau, W.M., Mostafid, H., Khutoryanskiy, V.V., 2017. Advances in intravesical drug delivery systems to treat bladder cancer. Int. J. Pharm. 532, 105–117. https://doi.org/10.1016/j.ijpharm.2017.08.120.

Leal, J., Luengo-Fernandez, R., Sullivan, R., Witjes, J.A., 2016. Economic burden of bladder cancer across the European Union. Eur. Urol. 69, 438–447. https://doi.org/10.1016/j.eururo.2015.10.024.

Lee, H., Daniel, K.D., 2015. Intravesical Drug Delivery Devices and Methods Including Elastic Polymer-drug Matrix Systems. WO 2015/200752 Al.

Lee, H., Daniel, K., Duc, Ho, Hong, L., Cima, Michael, J., Castillo-Ortiz, M., Froelich, S., Dimitrakov, J., 2007. Intravesical Drug Delivery Device and Method. WO 2007/021964 A3.

Lendlein, A., Langer, R., 2002. Biodegradable, elastic shape-memory polymers for potential biomedical applications. Science 296, 1673–1676. https://doi.org/10.1126/SCIENCE.1066102.

Li, X., Liao, L., 2016. Updates of underactive bladder: a review of the recent literature. Int. Urol. Nephrol. 48, 919–930. https://doi.org/10.1007/S11255-016-1251-X.

Lin, T., Wu, J., Zhao, X., Lian, H., Yuan, A., Tang, X., Zhao, S., Guo, H., Hu, Y., 2014a. In situ floating hydrogel for intravesical delivery of adriamycin without

blocking urinary tract. J. Pharm. Sci. 103, 927–936. https://doi.org/10.1002/jps.23854.

Lin, T., Zhang, Y., Wu, J., Zhao, X., Lian, H., Wang, W., Guo, H., Hu, Y., 2014b. A floating hydrogel system capable of generating Co2 bubbles to diminish urinary obstruction after intravesical instillation. Pharm. Res. 31, 2655–2663. https://doi.org/10.1007/ S11095-014-1362-Y.

Maroni, A., Melocchi, A., Zema, L., Foppoli, A.A., Gazzaniga, A., 2020. Retentive drug delivery systems based on shape memory materials. J. Appl. Polym. Sci. 137, 1–9. https://doi.org/10.1002/app.48798.

Matsuura, D.G., Gillespie, W.D., Greelis, J.P., Parsons, L., Mikxay, S., Zupkas, P.F., 2001. Intravescical Infuser. US 6,171,298 B1.

McLennan, M.T., 2014. Interstitial cystitis: epidemiology, pathophysiology, and clinical presentation. Obstet. Gynecol. Clin. N. Am. 41, 385–395. https://doi.org/10.1016/j. ogc.2014.05.004.

Melocchi, A., Parietti, F., Maccagnan, S., Ortenzi, M.A., Antenucci, S., Briatico Vangosa, F., Maroni, A., Gazzaniga, A., Zema, L., 2018. Industrial development of a 3D-printed nutraceutical delivery platform in the form of a multicompartment HPC capsule. AAPS PharmSciTech 19, 3343–3354. https://doi.org/10.1208/s12249-018-1029-9.

Melocchi, A., Inverardi, N., Uboldi, M., Baldi, F., Maroni, A., Pandini, S., Briatico Vangosa, F., Zema, L., Gazzaniga, A., 2019a. Retentive device for intravesical drug delivery based on water-induced shape memory response of poly(vinyl alcohol): design concept and 4D printing feasibility. Int. J. Pharm. 559, 299–311. https://doi. org/10.1016/j.ijpharm.2019.01.045.

Melocchi, A., Uboldi, M., Inverardi, N., Briatico-Vangosa, F., Baldi, F., Pandini, S., Scalet, G., Auricchio, F., Cerea, M., Foppoli, A., Maroni, A., Zema, L., Gazzaniga, A., 2019b. Expandable drug delivery system for gastric retention based on shape

memory polymers: Development via 4D printing and extrusion. Int. J. Pharm. 571, 118700. https://doi.org/10.1016/j.ijpharm.2019.118700.

Melocchi, A., Uboldi, M., Cerea, M., Foppoli, A., Maroni, A., Moutaharrik, S., Palugan, L., Zema, L., Gazzaniga, A., 2020a. A graphical review on the escalation of fused deposition modeling (FDM) 3D printing in the pharmaceutical field. J. Pharm. Sci. 109, 2943–2957. https://doi.org/10.1016/j.xphs.2020.07.011.

Melocchi, A., Uboldi, M., Parietti, F., Cerea, M., Foppoli, A.A., Palugan, L., Gazzaniga, A., Maroni, A., Zema, L., 2020b. Lego-inspired capsular devices for the development of personalized dietary supplements : proof of concept with multimodal release of caffeine. J. Pharm. Sci. 109, 1990–1999. https://doi.org/10.1016/j. xphs.2020.02.013.

Melocchi, A., Briatico-Vangosa, F., Uboldi, M., Parietti, F., Turchi, M., von Zeppelin, D., Maroni, A., Zema, L., Gazzaniga, A., Zidan, A., 2021a. Quality considerations on the pharmaceutical applications of fused deposition modeling 3D printing. Int. J. Pharm. 592, 119901. https://doi.org/10.1016/J.IJPHARM.2020.119901.

Melocchi, A., Uboldi, M., Briatico-Vangosa, F., Moutaharrik, S., Cerea, M., Foppoli, A., Maroni, A., Palugan, L., Zema, L., Gazzaniga, A., 2021b. The ChronotopicTM system for pulsatile and colonic delivery of active molecules in the era of precision medicine: feasibility by 3D printing via fused deposition modeling (FDM). Pharmaceutics 13, 759. https://doi.org/10.3390/pharmaceutics13050759.

Melocchi, A., Uboldi, M., Cerea, M., Foppoli, A., Maroni, A., Moutaharrik, S., Palugan, L., Zema, L., Gazzaniga, A., 2021c. Shape memory materials and 4D printing in pharmaceutics. Adv. Drug Deliv. Rev. 173, 216–237. https://doi.org/10.1016/J. ADDR.2021.03.013.

Nakase, I., Noguchi, K., Aoki, A., Takatani-Nakase, T., Fujii, I., Futaki, S., 2017. Arginine‐rich cell-penetrating peptide-modified extracellular vesicles for active

macropinocytosis induction and efficient intracellular delivery. Sci. Rep. 7, 1991. https://doi.org/10.1038/s41598-017-02014-6.

Nickel, J.C., Jain, P., Shore, N., Anderson, J., Giesing, D., Lee, H., Kim, G., Daniel, K., White, S., Larrivee-Elkins, C., Lekstrom-Himes, J., Cima, M., 2012. Continuous intravesical lidocaine treatment for interstitial cystitis/bladder pain syndrome: safety and efficacy of a new drug delivery device. Sci. Transl. Med. 4 https://doi.org/ 10.1126/scitranslmed.3003804.

Nowatzki, P.J., Koepsel, R.R., Stoodley, P., Min, K., Harper, A., Murata, H., Donfack, J., Hortelano, E.R., Ehrlich, G.D., Russell, A.J., 2012. Salicylic acid-releasing polyurethane acrylate polymers as anti-biofilm urological catheter coatings. Acta Biomater. 8, 1869–1880. https://doi.org/10.1016/j.actbio.2012.01.032.

Oxybutynin Intravesical — Situs, 2002. Drugs R D 3, pp. 82–83. https://doi.org/ 10.2165/00126839-200203020-00002. Qiu, H., Guo, H., Li, D., Hou, Y., Kuang, T., Ding, J., 2020. Intravesical hydrogels as drug reservoirs. Trends Biotechnol. 38, 579–583. https://doi.org/10.1016/J. TIBTECH.2019.12.012.

Sansare, V., Gupta, M.K., Shrivastava, B., 2021. Nanocarrier mediated urinary bladder targeted drug delivery. In: Sharma, Shaweta (Ed.), Recent Research in Pharmaceutical. Weser Books, p. 57.

Shin, D.G., Kim, T.H., Kim, D.E., 2017. Review of 4D printing materials and their properties. Int. J. Precis. Eng. Manuf. Green Technol. 4, 349–357. https://doi.org/ 10.1007/s40684-017-0040-z.

Situs Co, 2000. Findings Presented on Successful Clinical Results Involving Incontinence Therapy Using Situs Corporation's Novel Drug Delivery System. URL.https://www.globenewswire.com/en/news-release/2000/04/30/278397/178/en/Findings-Presented-on-Successful-Clinical-Results-Involving-Incontinence-Therapy-Using-Situs-Corporation-s-Novel-Drug-Delivery-System.html.

Srisang, S., Nasongkla, N., 2019. Layer-by-layer dip coating of Foley urinary catheters by chlorhexidine-loaded micelles. J. Drug Deliv. Sci. Technol. 49, 235–242. https://doi. org/10.1016/j.jddst.2018.11.019.

Standring, S., 2005. Gray's Anatomy, The Anatomical Basis of Clinical Practice, 39th ed. London (UK). Tan, W.S., Kelly, J.D., 2018. Intravesical device-assisted therapies for non-muscle-invasive bladder cancer. Nat. Rev. Urol. 15, 667–685. https://doi.org/10.1038/s41585-018-0092-z.

Thomas, R., Soumya, K.R., Mathew, J., Radhakrishnan, E.K., 2015. Inhibitory effect of silver nanoparticle fabricated urinary catheter on colonization efficiency of Coagulase negative Staphylococci. J. Photochem. Photobiol. B Biol. 149, 68–77. https://doi.org/10.1016/j.jphotobiol.2015.04.034.

Tobias, I.S., Lee, H., Engelmayr, G.C., Macaya, D., Bettinger, C.J., Cima, M.J., 2010. Zero-order controlled release of ciprofloxacin-HCl from a reservoir-based, bioresorbable and elastomeric device. J. Control. Release 146, 356–362. https://doi.org/10.1016/ j.jconrel.2010.05.036.

Tyagi, P., Kashyap, M., Hensley, H., Yoshimura, N., 2016. Advances in intravesical therapy for urinary tract disorders. Expert Opin. Drug Deliv. 13, 71–84. https://doi. org/10.1517/17425247.2016.1100166.

Vigani, B., Rossi, S., Sandri, G., Bonferoni, M.C., Caramella, C.M., Ferrari, F., 2020. Recent advances in the development of in situ gelling drug delivery systems for non-parenteral administration routes. Pharmaceutics 12, 1–29. https://doi.org/10.3390/ pharmaceutics12090859.

Wang, S., Jin, S., Shu, Q., Wu, S., 2021. Strategies to get drugs across bladder penetrating barriers for improving bladder cancer therapy. Pharmaceutics 13, 1–14. https://doi. org/10.3390/pharmaceutics13020166.

Xu, X., Goyanes, A., Trenfield, S.J., Diaz-Gomez, L., Alvarez-Lorenzo, C., Gaisford, S., Basit, A.W., 2021. Stereolithography (SLA) 3D printing of a bladder

device for intravesical drug delivery. Mater. Sci. Eng. C 120, 111773. https://doi.org/10.1016/ j.msec.2020.111773.

Yachia, D., Hirszowicz, E., 2001. Intravesicular Baloon. US 6,293,923 B1.

Yachia, D., Hirszowicz, E., 2002. Intravesicular Device. US 2002/0165427 A1.

Yachia, D., Hirszowicz, E., 2006a. Implantable Mecidal Device for Controlled Release of Substance. US 2006/0100479 A1.

Yachia, D., Hirszowicz, E., 2006b. Implantable Device Which is Freely Movable in a Body Cavity. US 2006/0155163 A1.

Yoon, H.Y., Yoshimura, N., Kim, C.H., Goo, Y.T., Kang, M.J., Lee, S., Choi, Y.W., 2020. Current status of the development of intravesical drug delivery systems for the treatment of bladder cancer. Expert Opin. Drug Deliv. 17, 1555–1572. https://doi. org/10.1080/17425247.2020.1810016.

Yu, K., Liu, M., Dai, H., Huang, X., 2020. Targeted drug delivery systems for bladder cancer therapy. J. Drug Deliv. Sci. Technol. https://doi.org/10.1016/j. jddst.2020.101535.

Zacchè, M.M., Srikrishna, S., Cardozo, L., 2015. Novel targeted bladder drug-delivery systems: a review. Res. Rep. Urol. 7, 169–178. https://doi.org/10.2147/RRU. S56168.

Zhang, Z., Demir, K.G., Gu, G.X., 2019. Developments in 4D-printing: a review on current smart materials, technologies, and applications. Int. J. Smart Nano Mater. 10, 205–224. https://doi.org/10.1080/19475411.2019.1591541.

Zhu, G., Zhang, Y., Wang, K., Zhao, X., Lian, H., Wang, W., Wang, H., Wu, J., Hu, Y., Guo, H., 2016. Visualized intravesical floating hydrogel encapsulating vaporized perfluoropentane for controlled drug release. Drug Deliv. 23, 2820–2826. https:// doi.org/10.3109/10717544.2015.1101791.

Chapter 2

Towards 4D printing in pharmaceutics

Published as:

Andrea Gazzaniga, Anastasia Foppoli*, Matteo Cerea, Luca Palugan, Micol Cirilli, Saliha Moutaharrik, Alice Melocchi, Alessandra Maroni, International Journal of Pharmaceutics: X 100171 (2023)

https://doi.org/10.1016/j.ijpx.2023.100171

* Corresponding author

§ The contribution given by Micol Cirilli to the work associated with published article was validation, investigation, visualization.

ABSTRACT

Four-dimensional printing (4DP) is emerging as an innovative research topic. It involves the use of smart materials for three-dimensional printing (3DP) of items that change their shape after production, in a programmed way over time, when exposed to appropriate external non-mechanical *stimuli* (moisture, electric or magnetic fields, UV, temperature, pH or ion composition). In the performance of 4D printed devices, time is involved as the 4th dimension. 4D smart structures have been known for many years in the scientific literature, well before the advent of 3D printing, and the concepts of shape evolution as well as self-assembly have been applied to drug delivery at the nano-, micro- and macro-scale levels. The neologism "4DP" was coined by Tibbits, Massachusetts Institute of Technology, in 2013, who also showed the earliest examples of 4D printed objects. Since then, smart materials have often been combined with additive manufacturing, which makes production of complex shapes easy to achieve: going beyond 3DP, 4D printed items are no static objects. Two main categories of raw materials have been employed for 4DP: shape memory polymers (SMPs) and shape morphing hydrogels (SMHs). In principle, all types of 3D printers could be used for 4DP. In this article, examples of systems for use in the biomedical field, such as stents and scaffolds, and in drug delivery are reviewed, with special emphasis on indwelling devices for retention in the urinary bladder and in the stomach.

KEYWORDS

4D printing

3D printing

Smart materials

Shape memory polymers

Hydrogels

Drug release

Delivery systems

1. INTRODUCTION

Research in the field of drug delivery always strives to meet new challenges and hard-to-reach therapeutic objectives, for instance through improvement of pharmacokinetic profiles, enhanced patient compliance and possible adaption to the needs of a specific subject. This approach entails the identification of new therapeutic agents, including biological compounds, novel formulation strategies and, recently, has been broadened to manufacturing approaches unusual for the pharmaceutical area. Such a scenario laid the basis for scientists to start investigating the application potential of new fabrication techniques. The growing interest in 3D printing (3DP) would be one of the main examples in this respect.

4D printing (4DP) is also emerging as an innovative and challenging research topic. As an advancement of 3D printing, it involves the use of special raw materials, often referred to as smart or intelligent, to print items that can change their shape after production when exposed to an appropriate external non-mechanical *stimulus*. This peculiar behavior could be attained because smart materials are characterized by one or more properties that undergo major modifications in response to environmental variations, such as changes in moisture, electric and magnetic fields, light, temperature, pH or ion composition. Items made of smart materials and fabricated through 3DP processes are often considered as smart devices, since they can change their morphology in a programmed way over time. This is the reason why they are categorized as 4D printed systems, being time - the 4th dimension- involved in their definition.

2. WHEN “4DP” WAS COINED?

The neologism “4DP” was born on stage during a Technology, Entertainment, Design (TED) Talk, which was held in February 2013. TED Talks are public debates, which are posted online for free distribution under the slogan “ideas worth spreading” by an homonymous US-based media organization. In that occasion, the founder and director of the Self-Assembly Lab (SAL) at the Massachusetts Institute of Technology (MIT), Skylar Tibbits, showed what can be defined as the earliest examples of 4D printed objects capable of self-

transformation over time (Tibbits, 2013). These structures were printed as a single strand and were composed of a sequence of rigid parts and flexible hinges. The latter were made of smart materials that, when immersed in water, underwent asymmetric swelling, thus resulting into folding of the strands to take on the desired shape (e.g. MIT and the SAL acronyms and a closed polygon) (Fig. 1).

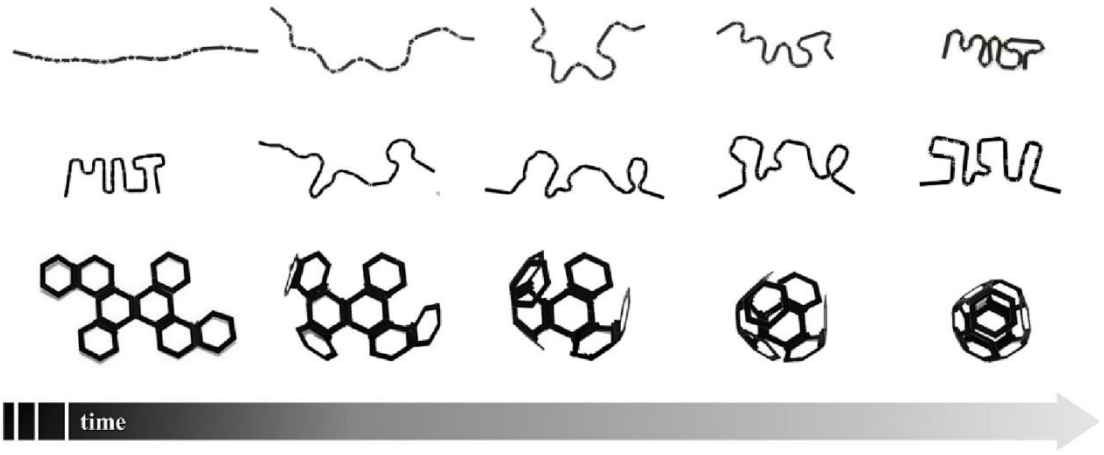

Fig. 1. Sequential images of the printed structures developed in the Self-Assembly Lab at MIT, showing self-modification of shape over time. Adapted from (Raviv et al., 2014).

Almost at the same time, other research groups came up with 4DP self-moving systems. By way of example, Ge and colleagues designed and printed devices including hinges made of an "active" composite material and "inactive" plates based on rigid plastics (Ge et al., 2013). The resulting devices were then thermo-mechanically programmed to take on complex 3D configurations, and shape modifications were triggered in response to change in temperature (Fig. 2). Subsequently, 3DP self-folding origami started to be described in the scientific literature. In this respect, most applications were aimed at the fabrication of innovative actuators to be used in robots (De Marco et al., 2019; Hann et al., 2020; Shiblee et al., 2019). Opportunities in the biomedical field were also explored. This is the case with Jamal and coworkers, who proposed printed scaffolds composed of differently cured hydrogel bilayers able to transform into curved micrometer-scale geometries encapsulating insulin-secreting cells (Jamal et al., 2013).

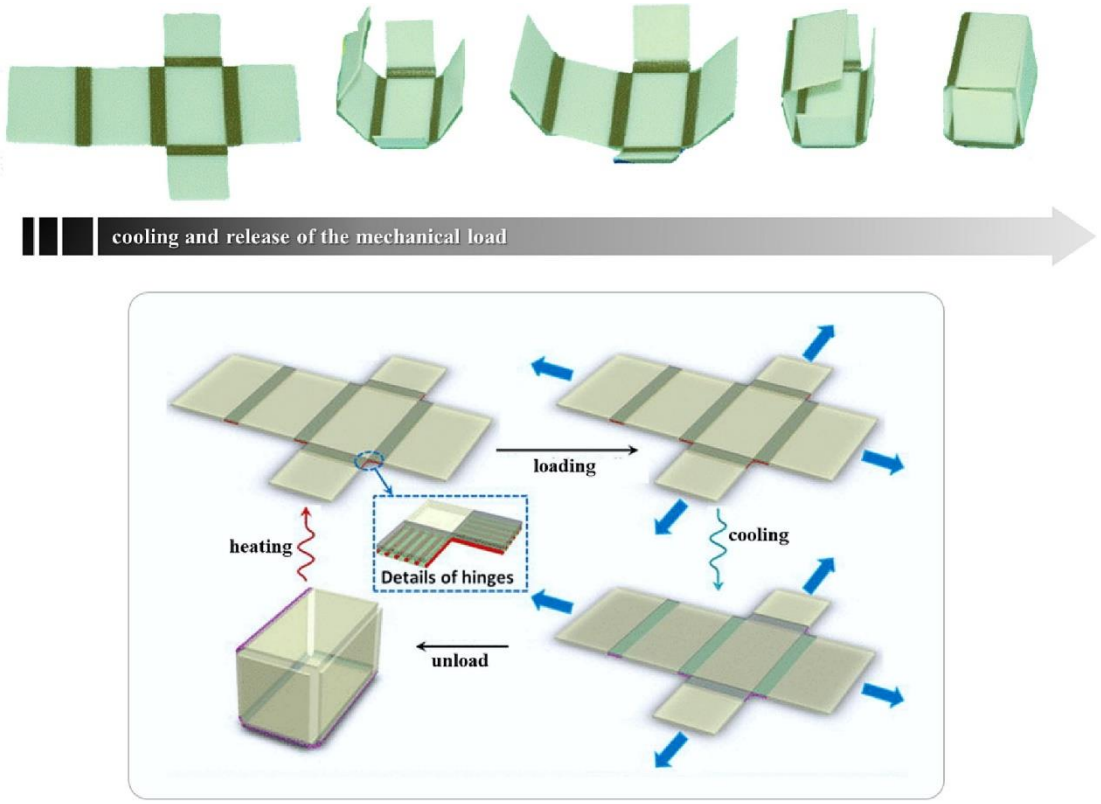

Fig. 2. Photographs of the self-folding printed structure developed by Ge and colleagues (top image) and outline of the thermomechanical protocol followed to attain the desired shape modifications (bottom image). Adapted from (Ge et al., 2013).

3. WHERE DOES 4DP FIND ITS ROOTS?

So-called smart devices have been known in the biomedical and pharmaceutical fields for many years. 4D smart structures, intended as items capable to transform over time and adapt to the surrounding environment, have been fabricated taking advantage of a range of manufacturing processes and may be found in the scientific literature well before the advent of 3D printers. Actually, the concepts of shape evolution and self-assembly have been applied to drug delivery systems at the nano-, micro- and macro (*i.e.* human)-scale levels. Self-assembly of molecules of different chemical nature (*e.g.* lipidic, peptidic, polymeric) resulting in supramolecular structures such as micelles, liposomes and nanoparticles are known for their ability to encapsulate active compounds, thus being examples of shape modifications at the nano-level (Jing et al., 2022). Microstructures based on self-folding/unfolding thin films are also described. In this respect, self-folding units were developed by

Stoychev and colleagues for controlled capture and release of yeast cells in response to a temperature signal (Stoychev et al., 2011). The systems comprised two layers, one of which was made of a thermoresponsive hydrogel able to swell and shrink upon temperature variation. The other one was composed of a biodegradable hydrophobic polymer responsible for contrasting the change in volume of the hydrogel layer in one direction. This peculiar composition resulted in a programmed change in geometry of the entire structure, as highlighted in Fig. 3.

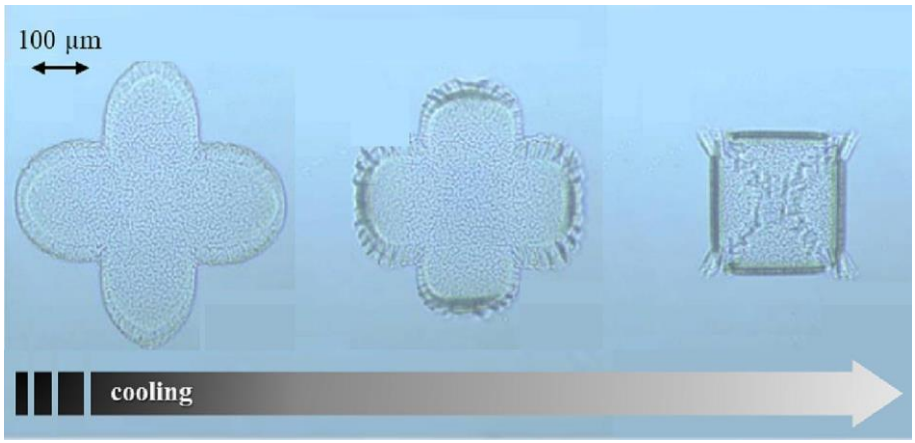

Fig. 3. Optical microscope photographs of the self-folding device developed by Stoychev et al. displaying shape modifications triggered by cooling. Adapted from (Stoychev et al., 2011).

Moving to smart structures performing at the macro/human-scale, a noteworthy application of the self-folding concept is represented by the device designed by He and colleagues to be retained in the intestine (He et al., 2006). In this case, a drug-containing mucoadhesive layer was coupled with bilayer laminates made of soft smart "active" materials and inert "passive" ones, respectively (Fig. 4). In more detail, a layer based on a pH-sensitive hydrophilic polymer, able to swell at pH 6.5, was superimposed on a film composed of a hydrophobic material. Once in the intestinal environment, the drug-containing layer allowed mucoadhesion and, due to the different swelling capabilities of the layers the self-folding laminate was composed of, the overall structure tended to curl into the mucus, thus resulting in a prolonged residence at porcine small intestinal wall.

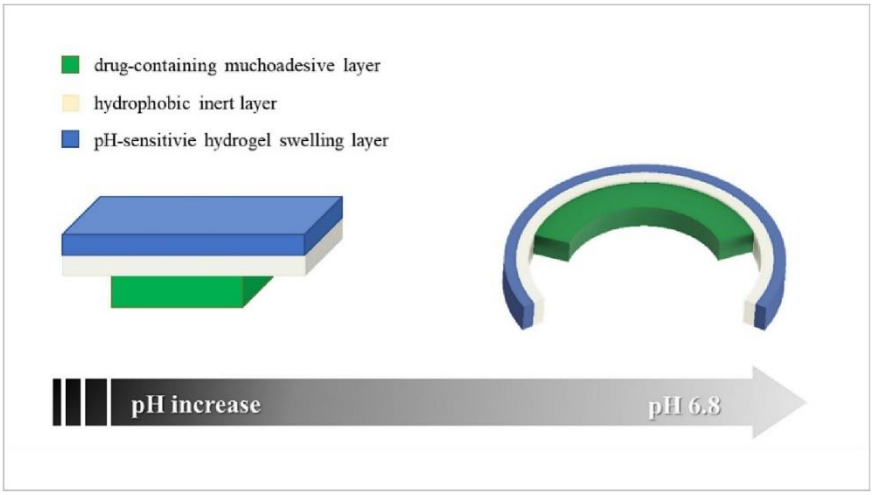

Fig. 4. Outline of the self-folding device developed by He et al. displaying shape modifications triggered by the pH of the intestinal environment. Adapted from (He et al., 2006).

4. 3DP MAKES ITS WAY IN THE LANDSCAPE OF SMART MATERIALS

The development of 3DP over the last decades has led to a huge number of applications of additive manufacturing (AM) in many fields, including the biomedical and, more recently, the pharmaceutical ones. In this respect, among all the 3D printing techniques available, binder jetting, fused deposition modeling, stereolithography and selective laser sintering were those having the greatest application potential for the fabrication of DDS, at least at the research level (Melocchi et al., 2020, Melocchi et al., 2021a).

Since 4DP was first mentioned in 2013, many attempts to combine smart materials and AM have been described. The main advantage for resorting to 3DP is represented by the possibility of easily obtaining complex shapes that would not be feasible with other methods in a single step. In this respect, 4DP would involve printing of single- and/or multi-material objects capable of changing their configuration over time, thus going beyond the concept of 3DP, 4D printed items being no longer static objects.

As several research groups have been working on this topic, the significance of 4DP has expanded: items showing self-transformation ability after production, in response to a desired *stimulus,* have been fabricated *via* different 3DP techniques

using smart materials as feedstocks (Fig. 5). Although modifications would mostly occur in the size and shape of the object, these may reflect in improvement of its performance thus possibly adding new functionalities. Notably, when dealing with applications relevant to the biomedical/pharmaceutical field, shape changes are mainly intended to take place after application/administration into the human body. This behavior can even be more advantageous when a physiological condition (*e.g.* body temperature, biological fluids and their pH or ion composition in a specific body district) would trigger the above-mentioned evolution of the system.

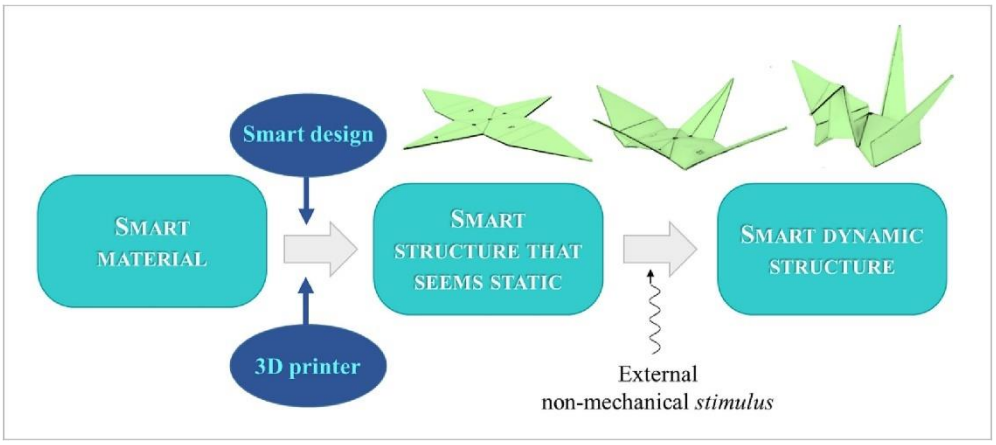

Fig. 5. Schematic of the 4DP concept.

The overall shape shifting process of 3D printed items would necessarily involve *i)* use of smart materials, as such and/or in combination, *ii)* fine-tuning of the item design and *iii)* appropriate setup of the printing process (*e.g.* printing orientation and composition of layers). Accordingly, 4DP also takes into account how x, y and z coordinates change after the production process and during transformation of the product. Due to the complexity of such a fabrication approach, the conceptualization step is often referred to as smart design phase. In such a phase, various aspects have to be carefully considered: *i)* the peculiar initial and transformed shapes the object would present, *ii)* the transformations to shift from one to another and *iii)* the relevant mechanisms. The basic principle of 4DP is to create precisely localized stress within a printed item that, upon release of this stress, would undergo further 3D shape changes in a predictable manner. This can be attained by exploiting shape memory effect or deformation mismatch.

In the former case, materials capable of recovering the original shape in which they were fabricated are involved, after being fixed in a temporary shape and following a specific non-mechanical triggering *stimulus*. The mechanism based on deformation mismatch, which is typically used in multi-material printing, relies on material differences in terms of physical properties, such as thermal expansion coefficient and swelling ratio. In this case, 4D printed items either involve rigid structures coupled with soft ones or materials having different degrees of crosslinking. By using materials with different chemical structures and physical properties, endless combinations can therefore be imagined and created.

5. SHAPE MEMORY POLYMERS AND SHAPE MORPHING HYDROGELS: CORNERSTONE OF 4DP APPLICATIONS

In the last two decades, much effort has been devoted to smart materials or to identifying smart properties of those already available for use in 4DP. The previous knowledge of self-transforming drug delivery structures along with the diffusion of 3DP has certainly given a strong boost to 4DP. This, in turn, has further prompted the research to develop novel smart materials, often designed for specific 3DP applications - especially in stereolithography and gel extrusion - as well as to in depth characterize the existing ones. Based on the mechanisms discussed above for 4D printing, shape memory polymers (SMPs) and shape morphing hydrogels (SMHs) are the two main categories of raw materials employed, demonstrating potential for addressing special needs related to 4DP in terms of both processability and functionality (Champeau et al., 2020; Melocchi et al., 2021b; Zhang et al., 2019). Feedstocks of both categories are mostly synthesized on an *ad hoc* basis and would reasonably have the regulatory status of new chemical entities. In Table 1, a selection of printable materials of potential interest for biomedical and/or pharmaceutical 4DP applications, being already employed in the fields or of proven biocompatibility, is presented.

Table 1. Selection of printable materials of potential interest for biomedical and/or pharmaceutical 4DP applications.

Stimulus-responsive materials	**Printing technique and post-printing treatment**	**Printed object**	**Stimulus-induced change**	**Application**	**Reference**
gelatin/EC	direct ink writing (gel extrusion)	casted gelatin films with printed EC patterns	swelling mismatch upon hydration	edible composites	(Pulatsu et al., 2022)
AA	digital light processing	items of different shape	pH-responsive swelling	modulated drug release	(Larush et al., 2017)
PLA/PCL	direct ink writing + temporary shape programming by heating/cooling	tubular scaffolds	temperature-induced shape recovery	tracheal scaffold	(Pandey et al., 2022)
PVA	FDM 3DP + temporary shape programming by heating/cooling	items of different shape	temperature- and water-induced shape recovery	gastro-retentive and intravesical drug delivery systems	(Melocchi et al., 2019b, Melocchi et al., 2019a) (Inverardi et al., 2021)
PNIPAM	gel extrusion and UV cross-linking	cylindrical hydrogel shell	temperature-induced modification of pore size	modulated drug release	(Zu et al., 2022)
PDA	gel extrusion of hydrogel core + coating with PDA and PCL by soaking in $CHCl_3$ solution	core/shell fiber scaffolds: core (alginate + gelatine), shell (PCL and PDA)	NIR irradiation triggered drug release	localized cancer therapy and tissue regeneration	(Liu et al., 2021)

s-PCL-MA	direct ink printing + UV photocuring with polythiol as initiator	vascular stent	temperature-induced shape recovery	drug-releasing deployable devices	(He et al., 2022)
βCD-g-PCL	direct ink printing + UV photocuring	vascular stent	temperature-induced shape recovery	stent for 1-month drug release	(Zhou et al., 2021)
crosslinked alginate and F127DA hydrogels	direct ink printing + subsequent UV light photocuring + temporary shape programming (immersion in $CaCl_2$ solution)	hydrogel with an internal mesh structure	unfolding by Ca^{2+} removal upon immersion in Na_2CO_3 solution	actuators, tissue engineering, drug delivery	(Wang et al., 2018)

AA Acrylic Acid; βCD-g-PCL star polymer having βCD core and 21 PCL arms with acrylate end group; EC ethylcellulose F127DA Pluronic F127 diacrylate macromer; PCL poly-ε-caprolactone; PDA polydopamine; PLA poly-l-lactide; PNIPAM poly(N-isopropylacrylamide); PVA polyvinyl alcohol; s-PCL-MA star poly-caprolactone with methacrylated end-group.

In the molecular network of a typical SMP, permanent netpoints, involved in memorizing the original shape, coexist interconnected with chain segments responsible for the material deformability. Such netpoints can result from either chemical bonding or physical interactions, and are not affected in the programming step. The most common type of chemical netpoint is crosslinking, which can be introduced directly during the synthesis of the SMP or in a post-processing/printing step (*e.g.* UV curing) (Liang et al., 2018; Song et al., 2020).

Physical netpoints are typical of semicrystalline polymers, where domains with different transition temperatures can be found. Specifically, domains that are responsible for shape retainment are generally named as permanent and characterized by the highest thermal transition temperature (T_{perm}). Conversely, chain segments having lower thermal transition temperature (T_{trans}) behave as switching domains and are essential for programming the temporary shape.

Focusing on the mechanisms triggering the shape change, thermo- and chemo-responsive SMPs are those mainly described. In thermo-responsive SMPs, the temporary shape is generally programmed by heating the printed item at a temperature above T_{trans} (but below T_{perm}) while applying an external stress. The temporary shape is then set by cooling the item below T_{trans}. Subsequently, the recovery of the original shape occurs when the temperature is raised above T_{trans}. In this respect, Fig. 6 shows the behavior, upon heating, of 4D printed objects fabricated by Zarek et al. starting from temperature-sensitive SMPs.

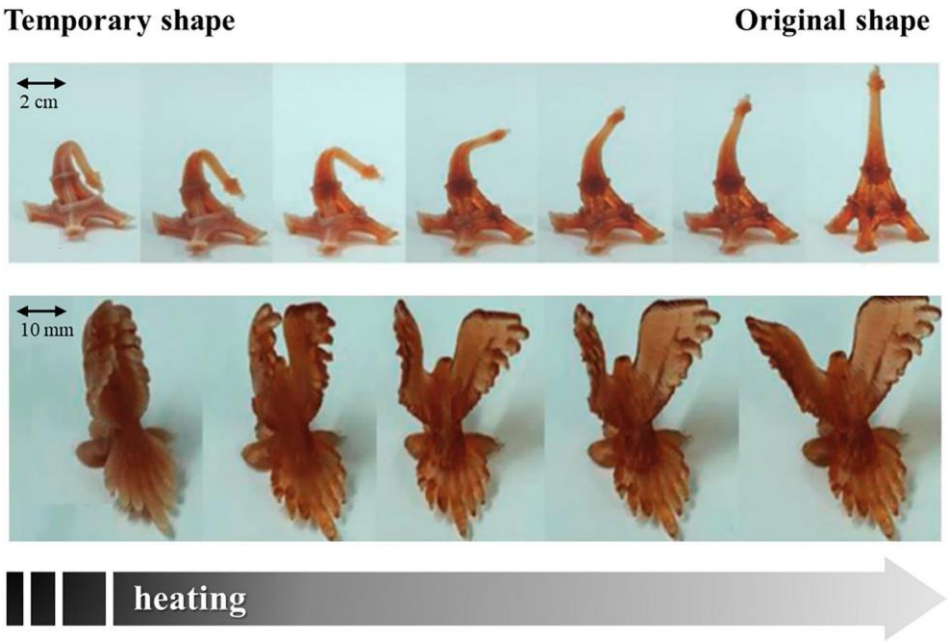

Fig. 6. Photographs of 4D printed objects fabricated by stereolithography during relevant shape recovery triggered by heating. Adapted from (Zarek et al., 2016).

In the case of chemo-responsive SMPs, the programming step is similar although the shape recovery process is activated by a chemical triggering *stimulus* able to alter the polymer mobility through softening, swelling or dissolution. In particular, in softening-induced shape memory effect, solvent molecules absorbed by the polymer would act as a plasticizer, thus promoting the mobility of its chains. The switching temperature is thus reduced, allowing the recovery of the original shape to take place even at body or room temperature. This represents the basis for the water-induced shape memory effect, which has started to be tested in the medical field. As regards the swelling-induced shape memory behavior, the polymer

network, upon immersion into the appropriate medium, progressively hydrates and swells, thus resulting in the formation of a gel. The latter is able to undergo a relatively large deformation, which can be translated in a volume expansion until an equilibrium state for a given environment is reached. At the same time, a reduction in the transition temperature of the polymer could be attained activating the shape recovery process.

Hydrogels are three-dimensional networks of hydrophilic, cross-linked polymers that can adsorb a large amount of water without dissolving. Shape and/or functionality change of hydrogel-based items could occur, as already observed for SMPs, in response to a range of triggering *stimuli*, such as changes in temperature, pH, ion concentration or upon the application of electric as well as magnetic fields (Champeau et al., 2020; Dong et al., 2020; Larush et al., 2017). More commonly, shape modifications can be obtained by making use of materials that respond to simple solvent absorption/desorption phenomena, thus leading to the so-called shape morphing or smart hydrogels. Indeed, diffusion of water into the network would cause controlled swelling to a different extent, depending on the specific characteristics of the area directly involved. In any case, to manage the modifications of the object in shape and size, a swelling mismatch needs to be induced in the structure, for instance by defining the material composition and its spatial arrangement during printing. To this aim, hydrogels having diverse hydration ability can be combined into multi-material structures. Alternatively, a single hydrogel type capable of different swelling degree along its structure (anisotropic swelling), can be developed. This can be pursued by incorporating anisotropic particles to the hydrogel or by creating regions with a different degree of crosslinking and density in the material (Huang et al., 2017; Jamal et al., 2011; Mulakkal et al., 2018; Zhao et al., 2017).

Notably, for some hydrogels shape programming of the 3D printed object is also possible so that they can be referred to as shape memory hydrogels, being included into the SMP category (Korde and Kandasubramanian, 2020; Wang et al., 2018).

6. INSIGHTS ON 4DP IN THE BIOMEDICAL FIELD

In the last few decades, the exploration of smart materials for application in the medical field has been strongly prompted by the progress of 3DP techniques and the continuous improvement in the understanding of biological systems. The benefits associated with 4DP have been recognized in many different areas, such as tissue regeneration, soft robotics, medical devices, diagnosis and delivery of biologics (Javaid and Haleem, 2019; Moroni et al., 2022; Zhou et al., 2021). In case of tissue regeneration, for example, functional scaffolds purposely engineered to assist in remodeling and replacing diseased or injured areas represent an ongoing topic of research. In this respect, new materials showing bio-mimicking features and bio-responsiveness can greatly help the development of such technologies (Free, 2021; Naniza et al., 2022; Senatov et al., 2016; Tamay et al., 2019; Zhang et al., 2018).

Personalized medical devices, provided with a dynamic behavior in a desired timescale and designed around the needs of a specific patient, may represent an advantageous alternative to otherwise static implants. By way of example, they can be positioned in the body in a minimally invasive way or can adapt themselves to physiological growth conditions. The use of printing processes in this specific context can be considered particularly suitable for obtaining the desired complex geometries, and potentially applicable to the fabrication of customized products in a rapid and cost-efficient manner. Multiple studies have reported proof-of-concept 4DP applications for thermally induced SMP-based devices, such as catheters, microgrippers, vascular stents, aneurysmal foams, orthodontic wires and surgical sutures (Delaey et al., 2020; Javaid and Haleem, 2019; Yakacki and Gall, 2010; Zhao et al., 2019). Nevertheless, despite the strong academic interest generated, engineering into clinically useful devices has demonstrated to be rather challenging.

The most advanced examples in this respect are represented by stents to be used in cardiovascular applications. They are conceived to have a small size to enable minimally invasive insertion, and to expand once positioned into the body.

Having as a reference the traditionally used shape memory alloys (*e.g.* nitinol), researchers started to test photo-curable methacrylate copolymers when dealing with 3DP. Through high resolution projection microstereolithography (μSLA), polymeric stents were successfully printed in the desired original shape and, afterwards, were thermally programmed in the temporary - generally shrunk - shape, which eased insertion into the blood vessel. Restoration to the larger original 3D-printed shape was generally triggered when the temperature of the stent reached that of the body (Fig. 7). A paclitaxel-loaded vascular stent was also successfully prepared making use of a purposely designed photocurable star polymer composed of a β-cyclodextrin core and polycaprolactone arms with acrylate end groups (Zhou et al., 2021). The stent showed biocompatibility and shape memory effect, along with suitable mechanical properties and the ability to provide sustained release of the loaded drug.

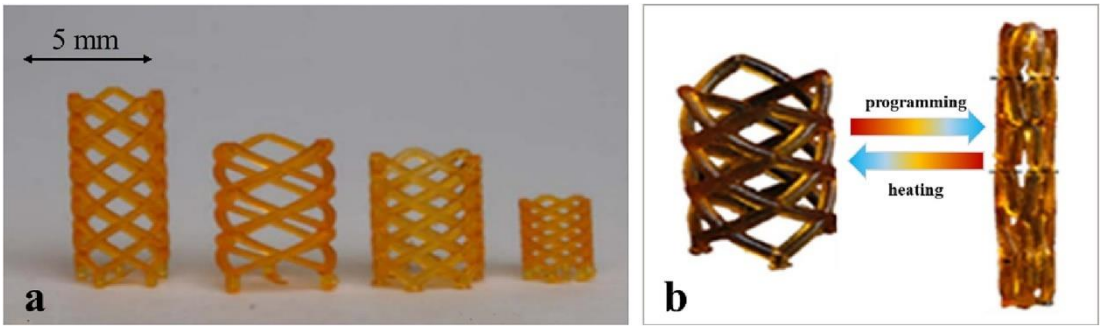

Fig. 7. Photographs of 3D printed stents with different geometric parameters (height, diameter, number of joints, diameter of ligaments and angle between ligaments) (a); 3D printed stent programmed into the temporary shape with a smaller diameter for minimally invasive surgery: after heating, the stent recovers the original shape with a larger diameter (b). Adapted from (Ge et al., 2016).

Such a peculiar behavior was also exploited in non-cardiovascular applications. By way of example, pediatric bronchial growing stents, conceived to adapt themselves to child's growth over time, have been proposed (Freitag et al., 2017). In this case, a different 4DP approach was followed, entailing the combination of degradable and stable elastic polymers. Hybrid stents were printed by means of a self-developed 3D multimode-multimaterial printer using polyurethane for the

elastic tubular structure of the stent and polylactic acid to create a biodegradable restricting element. *In vivo* degradation of the latter polymer enabled slow expansion of the device over an adequate time frame.

4DP was also proposed to address the need for personalized endoluminal stents intended to maintain the respiratory tract patency in a variety of disorders affecting the trachea. In this case, engineering fully conformable devices, able to ensure a precise fit and anchor-in-place of the stent represents a potential approach to prevent stent migration and related complications. Zarek et al. printed by SLA a prototype of tracheal stent based on semicrystalline methacrylated polycaprolactone, having peculiar C-shaped protuberances of the trachea (Zarek et al., 2017). Personalization of the printed object based on anatomical dimensions was pursued by obtaining a digital model of the trachea from an online repository of human anatomy, which was acquired by whole body MRI. The printed constructs, obtained after a proper selection of molecular weight fractions of the polycaprolactone precursor, displayed mechanical properties suitable to prevent obstruction of the trachea by counteracting external compression, while allowing a certain degree of bending freedom. When shape memory recovery was thermally triggered the airway stent proved able to promptly restore its original expanded shape, from the temporary programmed abridged one, thus matching the target anatomy (Fig. 8).

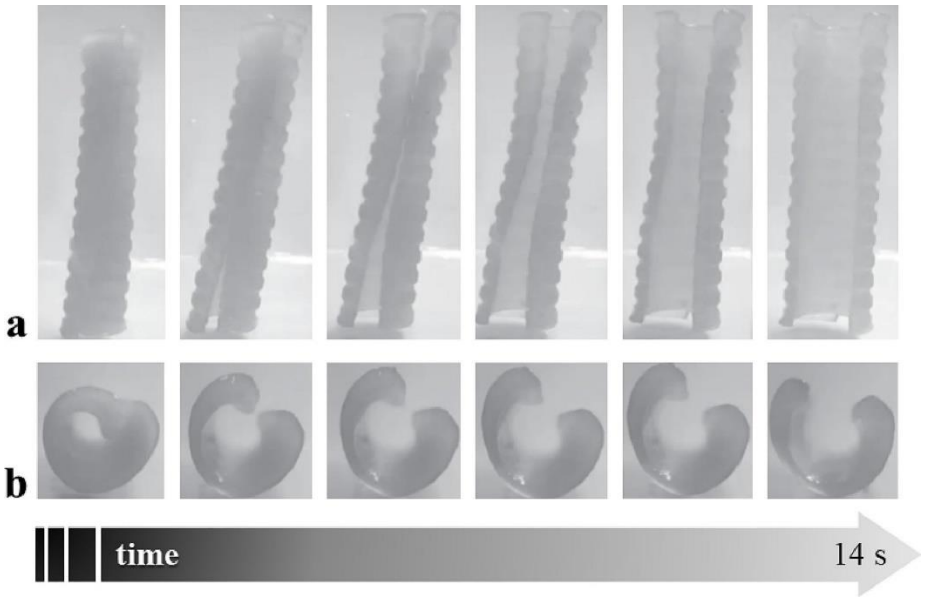

Fig. 8. Series of photographs of a 3D printed airway tracheal stent, showing the transition between the temporary open configuration state (for deployment) to the permanent shape (for performance): dorsal view (a) on-end view of the stent (b). Reprinted with permission from (Zarek et al., 2017).

7. 4DP IN DRUG DELIVERY

Despite the huge interest in the application of 4DP, few projects have been pursued so far in the pharmaceutical field, and a limited number of papers have been published on this topic. Indeed, although many articles have been published on 4D printing since 2013 (Fig. 9A), only a relatively small number involved drug, pharmaceutical or medical applications (Fig. 9B).This is also highlighted in recent reviews on 3DP, which also covered the specific domain of 4DP (Firth et al., 2018; Trenfield et al., 2019). Within the specific area of drug delivery, efforts have mainly been directed towards the development of novel responsive materials, suitable for being used in the design of DDSs with desired kinetics and/or providing localized release of drugs (Ahmed, 2018; Larush et al., 2017; Li et al., 2016; Wang et al., 2021).

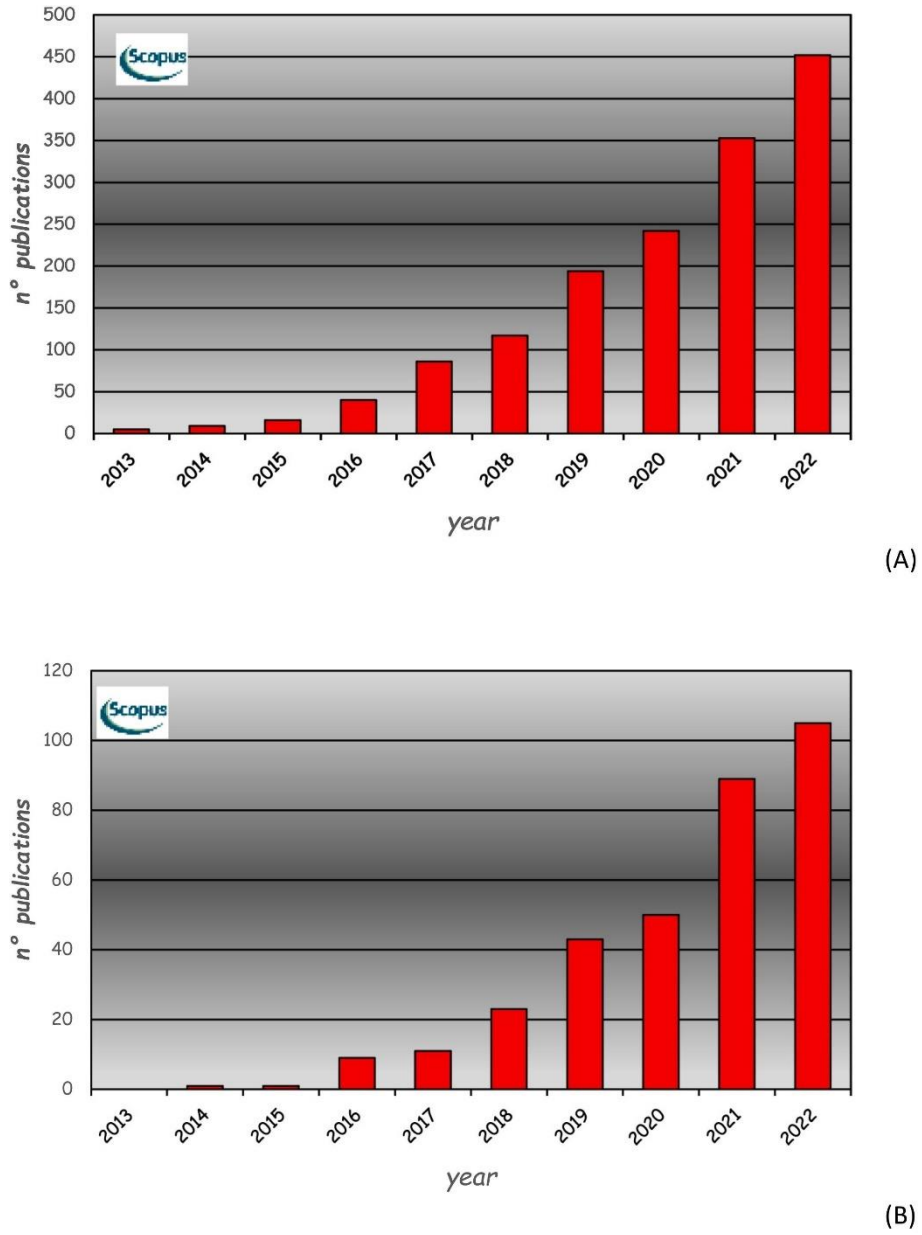

Fig. 9. Articles published in the last decade in the scientific literature on 4D printing (A), and specifically involving drug, pharmaceutical or medical applications (B) (source: Scopus).

From reactive materials to reactive devices, the inventive step has been relatively short, with the advent of new ideas to conceive more acceptable ways to deliver drugs to the patient. In some cases, inspiration for new proposals originated from the observation of elements present in nature. This was for example the case with the microneedles proposed by Li et al. for painless administration of drugs through the skin, which have a hierarchical, limpet tooth-inspired architectures (Li et al., 2021). The proposed devices are reinforced composite structures obtained by magnetic field-assisted 3D printing able to reach high mechanical

strength upon shape change, thus potentially being more suitable for harmless penetration into the skin. Moreover, a certain number of preliminary 4D printed products were proposed as drug-loaded scaffolds or implantable devices. They would take advantage of the *in vivo* changes occurring in their shape and size to enable minimal surgical intervention for insertion into the body (Vehse et al., 2014; Wang et al., 2018). These systems could be considered at the intersection of medical devices, scaffolds and actual DDSs, because they were generally proposed in response to the strong clinical trend towards minimally invasive surgery without identifying a specific administration site or therapeutic goal.

With a similar intent of reducing the discomfort associated with medication, and more specifically to enhance the patient adherence to a complex therapy, DDSs designed to enable a less frequent regimen of administration certainly play a prominent role. In this respect, 4DP has been proposed to prepare different organ-retentive devices intended to be held within hollow organs and to release drugs meanwhile in a controlled manner. Theragrippes for example are gastrointestinal-resident mini- or microdevices, generally consisting of multilayer structures provided with sharp microtips, which can latch (self-close) onto the mucosal tissue following different kind of *stimuli* (Ghosh et al., 2020; Malachowski et al., 2014). These systems were proved able to remain within the GI tract of live animals for 24 h after rectal administration.

More recently, 4DP has been applied to other administration routes for the development of novel DDSs designed to be retained in the target organ following a shape change and to release drug in a controlled manner. The urinary bladder and stomach were particularly appealing for such 4DP devices because of the number of still pending issues associated with the delivery of drugs to these anatomical sites (Maroni et al., 2020; Melocchi et al., 2019a, Melocchi et al., 2019b; Palugan et al., 2021; Uboldi et al., 2022). As already observed with stents, key points in the design and formulation of such systems are that sizes differing from one another would be required for safe entry into and effective retention within the hollow organs, respectively. On the one hand, a sufficiently small-sized conformation would be needed for administration and positioning of the drug-

loaded device inside the body cavity. On the other hand, a larger spatial encumbrance would be mandatory for preventing untimely emptying of the system. Evolution from a smaller to a larger size can effectively arise from unfolding processes triggered by *stimuli,* such as the uptake of physiological fluids and/or the achievement of body temperature. In these cases, SMPs are necessarily involved.

Basic requirements need to be fulfilled in the development of these DDSs, namely *i)* prompt achievement of the retentive configuration after dosing, *ii)* its maintenance over the desired time, also in spite of the mechanical stresses associated to smooth muscle contraction undergone by the device during its residence in the organ, *iii)* release of the drug in a rate-controlled way and *iv)* spontaneous removal from the retaining organ after exhaustion.

Polyvinyl alcohol of pharmaceutical grade having diverse molecular weight was selected as the main polymeric component to fabricate both bladder and stomach-retentive devices by fused deposition modeling 3DP, by virtue of its swelling/erosion properties, good hot-processability and shape memory ability. PVA-based items were either printed or extruded in the desired original shape and then programmed into a temporary one by heating up the prototypes and shaping them manually or with the aid of templates. The temporary shape was then fixed by cooling the samples in the deformed shape at low temperatures.

In more detail, the retentive system for intravesical drug delivery was designed to be administered into the bladder in a temporary rod-like form, suitable for insertion by urethral catheterization, and to be retained after recovery of the original bent or curled shape not compatible with physiological bladder emptying (Fig. 10). Elimination of the device would therefore be possible only after its dissolution/erosion. Prototypes were successfully obtained and characterized by differential scanning calorimetry and dynamic-mechanical thermal analysis as well as in terms of fluid uptake, mass loss, shape recovery and release behavior. The samples exhibited the desired ability to recover the original shape, consistent in kinetics with the relevant thermo-mechanical properties, and concomitant

prolonged release of a drug tracer. Although preliminary in scope, this study pointed out the viability of the proposed approach to the design of retentive intravesical DDSs.

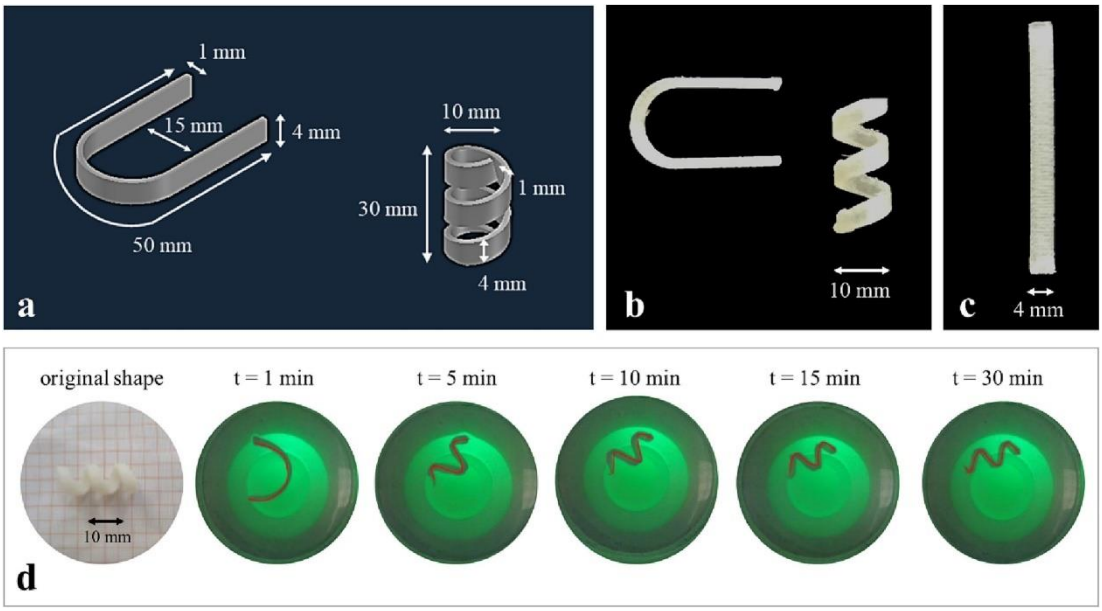

Fig. 10. 4DP vesical-retentive DDS: virtual model of U and helix-shaped devices (a), photographs of printed prototypes in their original (b) and programmed temporary rod shape (c), photographs acquired during shape recovery experiments (37 °C) of prototypes having original helix shape and programmed to take on a temporary I-shape (d). Adapted from (Melocchi et al., 2019a).

The gastroretentive system, based on the same approach described for the vesical one, was devised as a step forward with respect to expandable devices already described in the scientific literature, which generally relied on a mechanically-driven working mechanism. The shape was selected to enable retention in the stomach during the interdigestive phase. For this reason, it showed 2 dimensions ≥15 mm, which represent a commonly reported size of open pylorus. On the other hand, the system temporary shape was conceived to be in principle compatible with swallowing, *i.e.* suitable to be inserted into commercially available hard-gelatin capsules. Once in the stomach, following dissolution of the capsule, the device was expected to recover its original cumbersome configuration upon contact with gastric fluids at body temperature. Allopurinol-containing cylindrical helices were manufactured by FDM and then manually fixed into supercoiled configurations (Fig. 11b-c). When immersed in 0.1 N HCl

solution at 37 °C, the prototypes showed the expected behavior, reaching the desired spatial encumbrance within few minutes (Fig. 11d-e) and releasing the tracer in a controlled manner. Additionally, the application of mixed Eudragit® RS/RL or of Eudragit® NE polymeric films by means of a purposely assembled small-scale coating equipment, turned out to be a suitable strategy to control the release rate of the delivery systems without affecting their smart performance (Uboldi et al., 2021). Furthermore, by means of an engineering approach, relying on the comparison between computational and experimental mechanical and thermo-mechanical characterization data, a validated model was developed to investigate - and potentially predict - the shape changes undergone by a specific PVA-based geometry, allowing to choose an optimized shape without the need for fabricating a range of different prototypes (Inverardi et al., 2021).

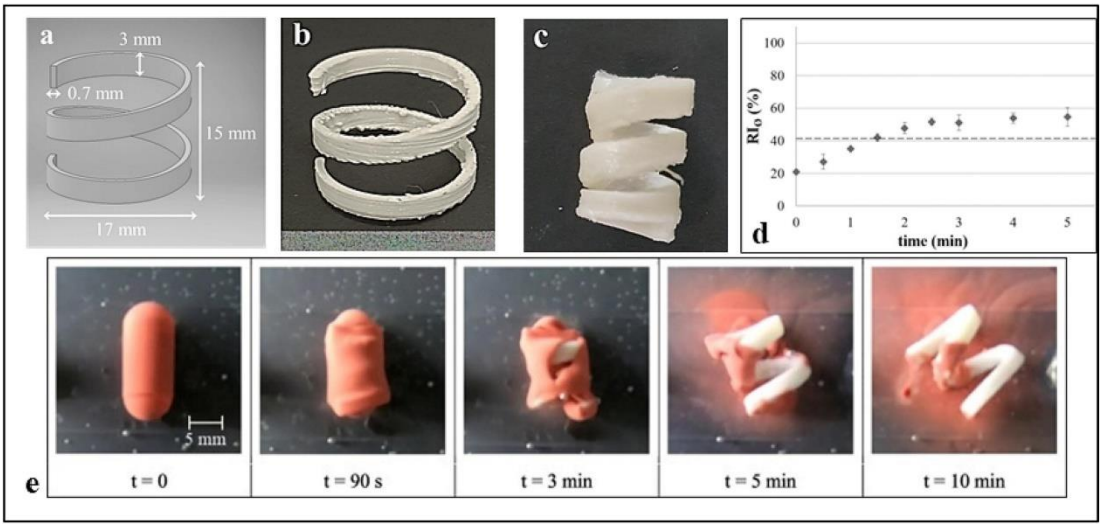

Fig. 11. 4DP gastroretentive helix-shaped device: virtual model of the device (a), photographs of a printed prototype in its original (b) and programmed temporary shape (c), shape recovery profile (d), photographic sequence acquired during shape recovery of the device (e). Adapted from (Melocchi et al., 2019b).

8. CONCLUSION

4D printing is an emerging technology and represents an evolution of 3DP, encompassing the use of smart materials to design structures with the ability to transform over time, in a predictable manner, in response to external *stimuli* of non-mechanical nature.

Since its introduction in 2013, this new concept has been attracting more and more interest in different areas of research. This prompted major advances in material science, to make printable ones available, and researchers to develop increasingly complex mathematical models to boost the shift from proof of concept to real-life 4DP applications. This would also require the identification of processes that could be suitable for mass production, enabling the scaling up of 4D printing.

As far as the pharmaceutical field is concerned, the opportunity to attain complex, purposely designed structures starting from materials either newly synthesized or already in use and showing a potential for shape memory, is deemed of particular interest. The implementation of 4D printing in drug delivery would allow to address unmet needs, for instance to develop less invasive and more compliant ways to administer medications and attain therapeutic objectives that are currently unfeasible. In this respect, a few original ideas have already been put forward, mainly relating to the fabrication of scaffolds/implants and systems intended for retention into hollow muscular organs, able to transform themselves upon administration and to release the drug conveyed according to the desired kinetics. Although the exploitation of 4DP concept to pharmaceutics is still in its infancy, its application potential seems huge, allowing the researchers to focus on very innovative devices and purse delivery approaches that have not yet been explored. In such a sense, significant progress will be possible taking advantage of creativity and especially if the horizons of research will be widened towards new targets in terms of temporal and spatial control of release.

REFERENCES

Ahmed, J., 2018. Recent advances of novel materials for 3D/4D printing in biomedical applications. In: Maniruzzaman, Mohammed (Ed.), 3D and 4D Printing in Biomedical Applications: Process Engineering and Additive Manufacturing. WileyVCH Verlag GmbH & Co, KGaA, pp. 239–271. https://doi.org/10.1002/ 9783527813704.ch10.

Champeau, M., Heinze, D.A., Viana, T.N., de Souza, E.R., Chinellato, A.C., Titotto, S., 2020. 4D printing of hydrogels: a review. Adv. Funct. Mater. 30, 1–22. https://doi. org/10.1002/adfm.201910606.

De Marco, C., Alcˆ antara, C.C.J., Kim, S., Briatico, F., Kadioglu, A., de Bernardis, G., Chen, X., Marano, C., Nelson, B.J., Pan´e, S., 2019. Indirect 3D and 4D printing of soft robotic microstructures. Adv. Mater. Technol. 4, 1900332. https://doi.org/10.1002/ admt.201900332.

Delaey, J., Dubruel, P., Van Vlierberghe, S., 2020. Shape-memory polymers for biomedical applications. Adv. Funct. Mater. 30, 1909047. https://doi.org/10.1002/ adfm.201909047.

Dong, Y., Wang, S., Ke, Y., Ding, L., Zeng, X., Magdassi, S., Long, Y., 2020. 4D printed hydrogels: fabrication, materials, and applications. Adv. Mater. Technol. 5, 1–19. https://doi.org/10.1002/admt.202000034.

Firth, J., Gaisford, S., Basit, A.W., 2018. A new dimension: 4D printing opportunities in pharmaceutics. In: Basit, A.W., Gaisford, S. (Eds.), 3D Printing of Pharmaceuticals. Springer International Publishing, Cham, pp. 153–162. https://doi.org/10.1007/ 978-3-319-90755-0_8.

Free, T., 2021. Stay smart: It's all about the materials for 4D printing in biomedicine. Biotechniques 70, 191–194. https://doi.org/10.2144/BTN-2021-0016.

Freitag, L., Gordes, ¨ M., Zarogoulidis, P., Darwiche, K., Franzen, D., Funke, F., Hohenforst-Schmidt, W., Dutau, H., 2017. Towards individualized tracheobronchial stents: technical, practical and legal considerations. Respiration 94, 442–456. https://doi.org/10.1159/000479164.

Ge, Q., Qi, H.J., Dunn, M.L., 2013. Active materials by four-dimension printing. Appl. Phys. Lett. 103, 1–5. https://doi.org/10.1063/1.4819837.

Ge, Q., Sakhaei, A.H., Lee, H., Dunn, C.K., Fang, N.X., Dunn, M.L., 2016. Multimaterial 4D printing with tailorable shape memory polymers. Sci. Rep. 6, 1–11. https://doi. org/10.1038/srep31110.

Ghosh, A., Li, L., Xu, L., Dash, R.P., Gupta, N., Lam, J., Jin, Q., Akshintala, V., Pahapale, G., Liu, W., Sarkar, A., Rais, R., Gracias, D.H., Selaru, F.M., 2020. Gastrointestinal-resident, shape-changing microdevices extend drug release in vivo. Sci. Adv. 6 https://doi.org/10.1126/sciadv.abb4133.

Hann, S.Y., Cui, H., Nowicki, M., Zhang, L.G., 2020. 4D printing soft robotics for biomedical applications. Addit. Manuf. 36, 101567 https://doi.org/10.1016/j. addma.2020.101567.

He, H., Guan, J., Lee, J.L., 2006. An oral delivery device based on self-folding hydrogels. J. Control. Release 110, 339–346. https://doi.org/10.1016/j.jconrel.2005.10.017.

He, W., Zhou, D., Gu, H., Qu, R., Cui, C., Zhou, Y., Wang, Y., Zhang, X., Wang, Q., Wang, T., Zhang, Y., 2022. A biocompatible 4D printing shape memory polymer as emerging strategy for fabrication of deployable medical devices. Macromol. Rapid Commun. 2200553, 1–12. https://doi.org/10.1002/marc.202200553.

Huang, L., Jiang, R., Wu, J., Song, J., Bai, H., Li, B., Zhao, Q., Xie, T., 2017. Ultrafast digital printing toward 4D shape changing materials. Adv. Mater. 29, 1605390. https://doi.org/10.1002/adma.201605390.

Inverardi, N., Scalet, G., Melocchi, A., Uboldi, M., Maroni, A., Zema, L., Gazzaniga, A., Auricchio, F., Briatico-Vangosa, F., Baldi, F., Pandini, S., 2021. Experimental and computational analysis of a pharmaceutical-grade shape memory polymer applied to the development of gastroretentive drug delivery systems. J. Mech. Behav. Biomed. Mater. 124, 104814 https://doi.org/10.1016/j.jmbbm.2021.104814.

Jamal, M., Zarafshar, A.M., Gracias, D.H., 2011. Differentially photo-crosslinked polymers enable self-assembling microfluidics. Nat. Commun. 2 https://doi.org/ 10.1038/ncomms1531.

Jamal, M., Kadam, S.S., Xiao, R., Jivan, F., Onn, T.M., Fernandes, R., Nguyen, T.D., Gracias, D.H., 2013. Bio-origami hydrogel scaffolds composed of photocrosslinked PEG bilayers. Adv. Healthc. Mater. 2, 1142–1150. https://doi.org/10.1002/ adhm.201200458.

Javaid, M., Haleem, A., 2019. 4D printing applications in medical field: a brief review. Clin. Epidemiol. Glob. Heal. 7, 317–321. https://doi.org/10.1016/j. cegh.2018.09.007.

Jing, Z., Ma, Y., Zhu, J., 2022. Application of a novel electrostatic dry powder coating technology on capsules for enteric release. J. Drug Deliv. Sci. Technol. 68, 103058 https://doi.org/10.1016/j.jddst.2021.103058.

Korde, J.M., Kandasubramanian, B., 2020. Naturally biomimicked smart shape memory hydrogels for biomedical functions. Chem. Eng. J. 379, 122430 https://doi.org/ 10.1016/j.cej.2019.122430.

Larush, L., Kaner, I., Fluksman, A., Tamsut, A., Pawar, A.A., Lesnovski, P., Benny, O., Magdassi, S., 2017. 3D printing of responsive hydrogels for drug-delivery systems. J. 3D Print. Med. 1, 219–229. https://doi.org/10.2217/3dp-2017-0009.

Li, H., Go, G., Ko, S.Y., Park, J.O., Park, S., 2016. Magnetic actuated pH-responsive hydrogel-based soft micro-robot for targeted drug delivery. Smart Mater. Struct. 25 https://doi.org/10.1088/0964-1726/25/2/027001.

Li, X., Shan, W., Yang, Y., Joralmon, D., Zhu, Y., Chen, Yiyu, Yuan, Y., Xu, H., Rong, J., Dai, R., Nian, Q., Chai, Y., Chen, Yong, 2021. Limpet tooth-inspired painless microneedles fabricated by magnetic field-assisted 3D printing. Adv. Funct. Mater. 31 https://doi.org/10.1002/adfm.202003725.

Liang, Z., Liu, Y., Zhang, F., Ai, Y., Liang, Q., 2018. Dehydration-triggered shape morphing based on asymmetric bubble hydrogel microfibers. Soft Matter 14, 6623–6626. https://doi.org/10.1039/c8sm00984h.

Liu, C., Wang, Z., Wei, X., Chen, B., Luo, Y., 2021. 3D printed hydrogel/PCL core/shell fiber scaffolds with NIR-triggered drug release for cancer therapy and wound healing. Acta Biomater. 131, 314–325. https://doi.org/10.1016/j. actbio.2021.07.011.

Malachowski, K., Breger, J., Kwag, H.R., Wang, M.O., Fisher, J.P., Selaru, F.M., Gracias, D.H., 2014. Stimuli-responsive theragrippers for chemomechanical controlled release. Angew. Chem. Int. Ed. 53, 8045–8049. https://doi.org/10.1002/ anie.201311047.

Maroni, A., Melocchi, A., Zema, L., Foppoli, A.A., Gazzaniga, A., 2020. Retentive drug delivery systems based on shape memory materials. J. Appl. Polym. Sci. 137, 1–10. https://doi.org/10.1002/app.48798.

Melocchi, A., Inverardi, N., Uboldi, M., Baldi, F., Maroni, A., Pandini, S., Briatico-Vangosa, F., Zema, L., Gazzaniga, A., 2019a. Retentive device for intravesical drug delivery based on water-induced shape memory response of poly(vinyl alcohol): design concept and 4D printing feasibility. Int. J. Pharm. 559, 299–311. https://doi. org/10.1016/j.ijpharm.2019.01.045.

Melocchi, A., Uboldi, M., Inverardi, N., Briatico-Vangosa, F., Baldi, F., Pandini, S., Scalet, G., Auricchio, F., Cerea, M., Foppoli, A., Maroni, A., Zema, L., Gazzaniga, A., 2019b. Expandable drug delivery system for gastric retention based on shape memory polymers: development via 4D printing and extrusion. Int. J. Pharm. 571, 118700 https://doi.org/10.1016/j.ijpharm.2019.118700.

Melocchi, A., Uboldi, M., Cerea, M., Foppoli, A., Maroni, A., Moutaharrik, S., Palugan, L., Zema, L., Gazzaniga, A., 2020. A graphical review on the escalation of fused deposition modeling (FDM) 3D printing in the pharmaceutical field. J. Pharm. Sci. 109, 2943–2957. https://doi.org/10.1016/j.xphs.2020.07.011.

Melocchi, A., Briatico-Vangosa, F., Uboldi, M., Parietti, F., Turchi, M., von Zeppelin, D., Maroni, A., Zema, L., Gazzaniga, A., Zidan, A., 2021a. Quality considerations on the pharmaceutical applications of fused deposition modeling 3D printing. Int. J. Pharm. 592, 119901 https://doi.org/10.1016/J.IJPHARM.2020.119901.

Melocchi, A., Uboldi, M., Cerea, M., Foppoli, A., Maroni, A., Moutaharrik, S., Palugan, L., Zema, L., Gazzaniga, A., 2021b. Shape memory materials and 4D printing in pharmaceutics. Adv. Drug Deliv. Rev. 173, 216–237. https://doi.org/10.1016/J. ADDR.2021.03.013.

Moroni, S., Casettari, L., Lamprou, D.A., 2022. 3D and 4D printing in the fight against breast cancer. Biosensors 12. https://doi.org/10.3390/bios12080568.

Mulakkal, M.C., Trask, R.S., Ting, V.P., Seddon, A.M., 2018. Responsive cellulose hydrogel composite ink for 4D printing. Mater. Des. 160, 108–118. https://doi.org/ 10.1016/j.matdes.2018.09.009.

Naniza, M.A., Askarib, M., Zolfaghariand, A., Nanize, M.A., Bodaghi, M., 2022. 4D printing: a cutting-edge platform for biomedical applications. ACS Appl. Mater. Interfaces 10, 22408–22418. https://doi.org/10.1088/1748-605X/ac8e42.

Palugan, L., Cerea, M., Cirilli, M., Moutaharrik, S., Maroni, A., Zema, L., Melocchi, A., Uboldi, M., Filippin, I., Foppoli, A., Gazzaniga, A., 2021. Intravesical drug delivery approaches for improved therapy of urinary bladder diseases. Int. J. Pharm. X 3, 100100. https://doi.org/10.1016/j.ijpx.2021.100100.

Pandey, H., Mohol, S.S., Kandi, R., 2022. 4D printing of tracheal scaffold using shapememory polymer composite. Mater. Lett. 329, 133238 https://doi.org/10.1016/j. matlet.2022.133238.

Pulatsu, E., Su, J.W., Lin, J., Lin, M., 2022. Utilization of ethyl cellulose in the osmotically-driven and anisotropically-actuated 4D printing concept of edible food composites. Carbohydr. Polym. Technol. Appl. 3, 100183 https://doi.org/10.1016/j. carpta.2022.100183.

Raviv, D., Zhao, W., McKnelly, C., Papadopoulou, A., Kadambi, A., Shi, B., Hirsch, S., Dikovsky, D., Zyracki, M., Olguin, C., Raskar, R., Tibbits, S., 2014. Active printed materials for complex self-evolving deformations. Sci. Rep. 4, 1–9. https://doi.org/ 10.1038/srep07422.

Senatov, F.S., Niaza, K.V., Zadorozhnyy, M.Y., Maksimkin, A.V., Kaloshkin, S.D., Estrin, Y.Z., 2016. Mechanical properties and shape memory effect of 3D-printed PLA-based porous scaffolds. J. Mech. Behav. Biomed. Mater. 57, 139–148. https:// doi.org/10.1016/j.jmbbm.2015.11.036.

Shiblee, M.D.N.I., Ahmed, K., Kawakami, M., Furukawa, H., 2019. 4D printing of shapememory hydrogels for soft-robotic functions. Adv. Mater. Technol. 4, 1900071. https://doi.org/10.1002/admt.201900071.

Song, Z., Ren, Luquan, Zhao, C., Liu, H., Yu, Z., Liu, Q., Ren, Lei, 2020. Biomimetic nonuniform, dual-stimuli self-morphing enabled by gradient four-dimensional printing. ACS Appl. Mater. Interfaces 12, 6351–6361. https://doi.org/10.1021/ acsami.9b17577.

Stoychev, G., Puretskiy, N., Ionov, L., 2011. Self-folding all-polymer thermoresponsive microcapsules. Soft Matter 7, 3277–3279. https://doi.org/10.1039/c1sm05109a.

Tamay, D.G., Usal, T.D., Alagoz, A.S., Yucel, D., Hasirci, N., Hasirci, V., 2019. 3D and 4D printing of polymers for tissue engineering applications. Front. Bioeng. Biotechnol. https://doi.org/10.3389/fbioe.2019.00164.

Tibbits, S., 2013. The Emergence of “4D printing” [WWW Document]. URL. https://www .ted.com/talks/skylar_tibbits_the_emergence_of_4d_printing.

Trenfield, S.J., Awad, A., Madla, C.M., Hatton, G.B., Firth, J., Goyanes, A., Gaisford, S., Basit, A.W., 2019. Shaping the future: recent advances of 3D printing in drug delivery and healthcare. Expert Opin. Drug Deliv. 16, 1081–1094. https://doi.org/ 10.1080/17425247.2019.1660318.

Uboldi, M., Melocchi, A., Moutaharrik, S., Cerea, M., Gazzaniga, A., Zema, L., 2021. Dataset on a small-scale film-coating process developed for self-expanding 4D printed drug delivery devices. Coatings. https://doi.org/10.3390/ coatings11101252.

Uboldi, M., Melocchi, A., Moutaharrik, S., Palugan, L., Cerea, M., Foppoli, A., Maroni, A., Gazzaniga, A., Zema, L., 2022. Administration strategies and smart devices for drug release in specific sites of the upper GI tract. J. Control. Release 348, 537–552. https://doi.org/10.1016/j.jconrel.2022.06.005.

Vehse, M., Petersen, S., Sternberg, K., Schmitz, K.P., Seitz, H., 2014. Drug delivery from poly(ethylene glycol) diacrylate scaffolds produced by DLC based microstereolithography. Macromol. Symp. 346, 43–47. https://doi.org/10.1002/ masy.201400060.

Wang, Y., Miao, Y., Zhang, J., Wu, J.P., Kirk, T.B., Xu, J., Ma, D., Xue, W., 2018. Threedimensional printing of shape memory hydrogels with internal structure for drug delivery. Mater. Sci. Eng. C 84, 44–51. https://doi.org/10.1016/j. msec.2017.11.025.

Wang, J., Zhang, Y., Aghda, N.H., Pillai, A.R., Thakkar, R., Nokhodchi, A., Maniruzzaman, M., 2021. Emerging 3D printing technologies for drug delivery devices: current status and future perspective. Adv. Drug Deliv. Rev. 174, 294–316. https://doi.org/10.1016/j.addr.2021.04.019.

Yakacki, C.M., Gall, K., 2010. In: Lendlein, A. (Ed.), Shape-Memory Polymers for Biomedical Applications BT - Shape-Memory Polymers. Springer, Berlin Heidelberg, Berlin, Heidelberg, pp. 147–175. https://doi.org/10.1007/12_2009_23.

Zarek, M., Layani, M., Cooperstein, I., Sachyani, E., Cohn, D., Magdassi, S., 2016. 3D printing of shape memory polymers for flexible electronic devices. Adv. Mater. 28, 4449–4454. https://doi.org/10.1002/adma.201503132.

Zarek, M., Mansour, N., Shapira, S., Cohn, D., 2017. 4D printing of shape memory-based personalized endoluminal medical devices. Macromol. Rapid Commun. 38, 1–6. https://doi.org/10.1002/marc.201600628.

Zhang, K., Wang, S., Zhou, C., Cheng, L., Gao, X., Xie, X., Sun, J., Wang, H., Weir, M.D., Reynolds, M.A., Zhang, N., Bai, Y., Xu, H.H.K., 2018. Advanced smart biomaterials and constructs for hard tissue engineering and regeneration. Bone Res. 6, 31. https://doi.org/10.1038/s41413-018-0032-9.

Zhang, Z., Demir, K.G., Gu, G.X., 2019. Developments in 4D-printing: a review on current smart materials, technologies, and applications. Int. J. Smart Nano Mater. 10, 205–224. https://doi.org/10.1080/19475411.2019.1591541.

Zhao, Z., Wu, J., Mu, X., Chen, H., Qi, H.J., Fang, D., 2017. Desolvation induced origami of photocurable polymers by digit light processing. Macromol. Rapid Commun. 38, 1–6. https://doi.org/10.1002/marc.201600625.

Zhao, W., Liu, L., Zhang, F., Leng, J., Liu, Y., 2019. Shape memory polymers and their composites in biomedical applications. Mater. Sci. Eng. C 97, 864–883. https://doi. org/10.1016/j.msec.2018.12.054.

Zhou, Y., Zhou, D., Cao, P., Zhang, X., Wang, Q., Wang, T., Li, Z., He, W., Ju, J., Zhang, Y., 2021. 4D printing of shape memory vascular stent based on βCD-gpolycaprolactone. Macromol. Rapid Commun. 2100176, 1–9. https://doi.org/ 10.1002/marc.202100176.

Zu, S., Zhang, Z., Liu, Q., Wang, Z., Song, Z., Guo, Y., Xin, Y., Zhang, S., 2022. 4D printing of core–shell hydrogel capsules for smart controlled drug release. Bio-Design Manuf. 5, 294–304. https://doi.org/10.1007/s42242-021-00175-y.

Chapter 3

Development of a novel retentive system for intravesical drug delivery based on size enlargement approach

To be submitted for publication

§ The contribution given by Micol Cirilli to the work associated with published article was conceptualization, methodology, formal analysis, validation, investigation, writing – original draft, visualization.

ABSTRACT

Urinary bladder diseases are commonly treated by means of systemic administration or, in some cases, through bladder instillations. The latter approach, compared to systemic one, has advantages in terms of required dose and side effects but, being the urinary bladder a frequently drained organ, intensive instillations are required. To overcome discomforts connected to frequent catheterization, urinary bladder retentive systems can be an option and, in the present work, a prototype of such a system has been proposed. Hydrophilic matrices were prepared by tableting, perforated, coated with an insoluble film based on ethylcellulose or Eudragit RL/RS and connected by an absorbable suture thread to prepare a ring-shaped urinary bladder retentive system. The purpose of the novel system was to consent its administration through catheterization and be retained in the organ for a few days releasing the drug. Once exhausted, the ring-shaped system should disassemble, dissolve and leave the organ with urination. The ring-shaped system was designed, prepared and studied for drug release *in vitro* demonstrating to to release the drug tracer with a prolonged release mode for approximately 1 week. At the end of the study the matrices were emptied, only an inconsistent residue remained composed of the insoluble films and the biodegradable suture thread, demonstrating the possibility of the device to be eliminated physiologically from the urinary bladder.

KEYWORDS

Bladder

Intravesical delivery

Retentive drug delivery system

Prolonged release

Hydrophilic matrices

1. INTRODUCTION

For the treatment of clinical conditions of urinary bladder, such as cancer or interstitial cystitis, bladder instillation is the preferred route of administration [Liu et al., 2021; Colaco et al., 2013], as it is more efficient maintaining higher local concentrations of the drug compared to what can be reached following systemic administration. [Dmochowski et al., 2002] Bladder instillation refers to the administration directly into the bladder of a drug solution, suspension or emulsion, and it avoids systemic first-pass metabolism or undesired side effects, thus allowing the use of lower drug dosages. [Krause et al., 2013] However, direct administration into the urinary bladder presents also disadvantages such as the periodic emptying of urine that eliminates the liquids instilled, the progressive dilution of the drug formulation due to the physiological filling of urine [Krhut at al., 2016], and the very low permeability of the urothelium, thus significantly reducing the time the drug remains in the site of interest and requiring frequent instillations to reach adequate topical concentrations. [Tyagi et al., 2006] Another problem associated with *in situ* therapies in urinary bladder concerns the invasive catheterization process, as process causes great discomfort for patients, both physically and psychologically. [Jang et al., 2020] Although early elimination of the drug can be reduced by forcing the patient to urinate before treatment and by limiting fluid intake, compliance problems are still considerable, especially when elderly patients are involved. In addition, when urinary catheters are maintained in the bladder for days or weeks they can often lead to the onset of infections, with further complications. [Nicolle, 2012; Crouzet et al., 2007]

Based on these considerations, new strategies have been studied to improve both the maintenance *in situ* of the drug within levels considered effective and/or to enhance the permeability of the organ. In order to maintain effective drug concentrations in urinary bladder, it may be advantageous to increase the residence time of the formulation, slow down the release rate of the formulation and improve its contact with the internal surface, resulting in augmented drug uptake. [Yoon et al., 2020; Zacchè et al., 2015] In these regards, liposomes and polymeric gels are considered valid tools for improving drug permanence and

absorption in the urinary bladder. Liposomes are lipid vesicles composed of a phospholipid bilayer surrounding an aqueous core, they allow the transport of hydrophilic or hydrophobic drugs and protecting them from degradation. [Guhasarkar and Banerjee 2010] Polymeric hydrogel systems are made up of three-dimensional hydrophilic or amphiphilic polymer networks formed through a chemical or physical cross-linking process of polymers. The gelation process is regulated by different physiological stimuli, including pH, enzymes or temperature. In recent years, temperature has become the most studied stimulus for such formulations and the sol-gel transition occurs at body temperature (Kolawole et al. 2017). Liposomes and polymeric gels are systems capable of forming a protective lipid film on the surface of the urothelium and at the same time ensuring the control of the release of encapsulated drugs. [Guhasarkar and Banerjee 2010)] Although *in situ* gel formation is a good option to prolong intravesical residence time, the risk of urethral obstruction due to increased urine viscosity is quite high. [Vigani et al., 2020] Approaches already exploited for promoting gastric retention, can also be exploited to prolong time of permanence in the urinary bladder. [Kolawole et al., 2017] Among these, floating systems, which use the low density of pharmaceutical forms to allow floating on urine, could help resist excretion through the urethra. [Lin et al., 2014] This approach may seem particularly promising, however, floating systems have not been studied in depth because the risk of urethral occlusion increases significantly when the volume of urine in the bladder is reduced. One of the most recently proposed approaches to significantly increase the residence time of the active in the bladder is represented by expandable retention systems. These devices are designed to be administered via catheter, and removed again through catheterization, or preferably by non-invasive processes of solubilization, erosion or degradation, with the formation of fragments that can be easily eliminated with urination. [Maroni et al., 2020; Palugan et al., 2021] It is possible to increase the residence time of the drug in the bladder by increasing the size of the system or by controlling variation of its geometry, once positioned in the organ. In all cases, it is of fundamental importance that physiological urination is not hindered by the device. These systems have been classified on the basis of the mechanism that

causes the increase in encumbrance and which involve expansion induced by an external mechanical stimulus, elastic relaxation or shape memory behavior induced by a specific component of the system (shape memory materials).

The aim of this work was to develop a novel intravesical drug delivery system consisting of subunits connected by a biodegradable thread that could be administered through urethral catheter and that could expand in volume once reached the urinary bladder. The duration of the retention time should be strictly linked to time required for the drug release and afterward, the system should leave the organ with urination, avoiding the need for an invasive procedure for its removal. For this purpose, prolonged release hydrophilic matrices were prepared by tableting and units were linked with a biodegradable suture thread in order to form a ring-shaped device. Paracetamol was loaded in the tablets as the drug tracer and release performance was evaluated *in vitro*.

2. EXPERIMENTAL

2.1 Materials

Paracetamol Ph Eur Fine Powder (Mallinckrodt, IE); Hydroxypropyl methylcellulose (HPMC, Methocel™ K100LV, Colorcon®, UK); Hydroxypropyl methylcellulose (HPMC, Methocel™ K100M, Colorcon, UK); Calcium phosphate dibasic ($CaHPO_4$, Sigma, USA); Colloidal silica (SiO_2, A.C.E.F., I); Glycerol dibehenate (GlyBeh, Compritol® 888ATO); ethyl cellulose in aqueous dispersion type B NF (Surelease®, Colorcon®); Low viscosity hypromellose (Methocel™ E5 Premium LV, Colorcon®); Ammonium methacrylate copolymer type A (Eudragit RL PO, Evonik); Ammonium methacrylate copolymer type B (Eudragit RS PO, Evonik); Ethanol 96% (VWR Chemicals); Polyglactin 910 (Ethicon®, Vicryl Rapide™).

2.2 Methods

2.2.1 Tablets preparation

To prepare the tablets, a mixture of powders was prepared according to the composition reported in Table 1. More specifically, four types of mixtures were

prepared, each with a weight of 200 g, using HPMC as the swelling hydrophilic polymer, having low-viscosity and high viscosity grades, Methocel™ K100LV and Methocel™ K100M, respectively. Mixing was performed in a mortar operating for approximately five minutes. Tablets were prepared by direct compression using a rotary tablet press (AM-8S, Officine Ronchi, IT) equipped with curved punches (curvature radius and diameter of 3 mm). The machine was set at compression force Fa = 9 kN to obtain tablets with a nominal weight of 38 mg with crushing forces between 60 and 70 N.

Table 1 Hydrophilic matrices composition

Paracetamol (%)	HPMC (%)	$CaHPO_4$ (%)	SiO_2 (%)	GlyBeh (%)	Drilled tablet	Composition code
30	45	19	1	5	Yes	LV45-P
30	45	19	1	5	No	LV45-NP
30	30	34	1	5	Yes	LV30-P
30	30	34	1	6	No	LV30-NP
30	45	19	1	5	Yes	M45-P
30	45	19	1	5	No	M45-NP
30	30	34	1	5	Yes	M30-P
30	30	34	1	5	No	M30-NP

2.2..2 Characterization of tablets

The tablets were characterized according to Ph. Eur. tests: uniformity of mass (analytical balance: Crystal 500, Gibertini, IT), friability test (friabilometer: TA3, Erweka, DE), resistance to breaking (crush tester, Erweka, DE) and the dimensions were measured by caliper (Absolute Digimatic CD-15CP, Mitutoyo, UK). For uniformity of mass, 10 tablets were weighed with the analytical balance (Crystal 500, Gibertini, IT) and then the mean and standard deviation were calculated. A sample of 10 tablets was then characterized by measuring height and diameter using a caliper (Mod. CD-15CP, Mitutoyo, UK). The mean and

standard deviation were then calculated. The coating thickness (s) was calculated using the eq 1.

$s = [(d_1 - d_0)/2]*1000$ Eq.1

where d_0 is the initial and d_1 the final mean diameter of the units before and after coating.

The percentage weight gain (w.g. %) was calculated with eq. 2.

$w.g.\% = (m_1 - m_o) \times 100$ eq.2

where m_0 is the initial mass of the starting tablets while m_1 is the final mass of the coated systems.

The tablets were subjected to the *in vitro* release test to evaluate the paracetamol release profile. The *in vitro* release test was conducted using the dissolving apparatus (Sotax AT7, Sotax, CH) equipped with a paddle stirrer whose speed was set to 50 rpm. 900 mL of distilled water at 37.0 ± 0.5 °C was used as the medium to perform the test. The concentration of paracetamol was automatically measured at predetermined time intervals (15 min) spectrophotometrically (PerkinElmer UV/VIS Spectrometer Lambda 35, US-MA) using cuvettes with an optical path of 1 mm and setting a wavelength of 243 nm.

2.2.3 Fluidized bed coating

The coating of the tablets was performed using the Mini-Glatt (Glatt GmbH, Binzen, De) apparatus equipped with a bottom-spray insert. Different film-forming mixtures were prepared as showed in table 2:

Table 2: tablet coating formulations

Formulation	Ethyl cellulose dispersion (Surelease®)	HPMC (Methocel™ E5)	Low permeable polymethacrylate (Eudragit® RS)	High permeable polymethacrylate (Eudragit® RL)	Triethyl Citrate	Distilled H_2O	EtOH	Code
A	60% w/w	/	/	/	/	40% w/w	/	EC
B	59% w/w	1.6% w/w	/	/	/	39.4% w/w	/	EC-H
C	/	/	7.41% w/w	3.18% w/w	0.32% w/w	4,76% w/w	84.33% w/w	PM

The coating processes were performed on a mass total mass of 50 g of cores.

Coating parameters were set as showed in table 3 for tablets' coating with formulation A, for coating with formulation B and for formulation C.

Table 3: coating process parameters for all of the three formulations (A, B and C)

Parameter	A	B	C
Fluidizing air volume (m^3/ h)	13	21-22	22-23
Fluidizing air temperature (°C)	70	70	30
Product temperature (°C)	37-40	37-42	26-27
Nebulization pressure (bar)	0.8	0.8	0.8
Nozzle (mm)	0.5	0.5	0.5

The quantity of film-forming dispersion to be sprayed was determined based on the percentage of weight increase that was desired: 10% for the two film-forming mixtures based on Surelease® and 12% for the formulation based on Eudragit. At the end of the coating, drying was continued for about four minutes.

Table 4. Codes of coated matrices with the different formulations and being perforated (F) or non-perforated (NF)

Tablet core code	Tablet perforation code	Coating code	Final tablet code
LV45	p	EC	LV45-NP-EC
LV45	np	EC	LV45-P-EC
LV30	p	EC	LV30-P-EC
LV30	np	EC	LV30 -NP-EC
M45	p	EC	M45-P-EC
M45	np	EC	M45--NP-EC
M30	p	EC	M30-P-EC
M30	np	EC	M30-NP-EC
LV45	p	EC-H	LV45-NP-EC-H
LV45	np	EC-H	LV45-P-EC-H
LV30	p	EC-H	LV30-P-EC-H
LV30	np	EC-H	LV30-NP-EC-H
M45	p	EC-H	M45-P-EC-H
M45	np	EC-H	M45-NP-EC-H
M30	p	EC-H	M30-P-EC-H
M30	np	EC-H	M30-NP-EC-H
LV45	p	PM	LV45-NP-PM
LV45	np	PM	LV45-P-PM
LV30	p	PM	LV30-P-PM
LV30	np	PM	LV30-NP-PM
M45	p	PM	M45-P-PM
M45	np	PM	M45-NP-PM
M30	p	PM	M30-P-PM
M30	np	PM	M30-NP-PM

2.2.4 Scanning electron microscope (SEM) analysis

Morphology of coated samples were analyzed by scanning electron microscope (Zeiss, Sigma), after being coated with platinum in a plasma evaporator under Argon flow (Leica EM ACE600, voltage 35 mA; platinum film thickness 5.46 nm, time 11 min). Photomicrographs were acquired at 80x and 250x magnifications.

2.2.5 Suture thread dissolution test

Suture thread (Ethicon®, Vicryl Rapide™) was placed in deionized water at room temperature (25±2 °C) for 30 days. Degradation/dissolution of the wire was visually checked every day.

2.2.6 Preparation of bladder-retentive systems

In this work, expandable bladder-retentive and gastro-retentive systems were studied, they are composed of 20 perforated tablets joined by a biodegradable suture thread (Ethicon®, Vicryl Rapide™) closed in a ring with a double knot.

3. RESULTS AND DISCUSSION

With the aim of developing a pharmaceutical dosage form capable of prolonging the release of the drug and being retained in the urinary bladder, a ring-shaped system prepared by linking hydrophilic matrices was designed. The system needed to have a compact initial configuration sufficiently small to be inserted in a urinary catheter for administration, and to be able to expand right after reaching the urinary bladder for preventing excretion. After being depleted from the drug, the device should disassemble and release the matrices that could leave the urinary bladder with urination.

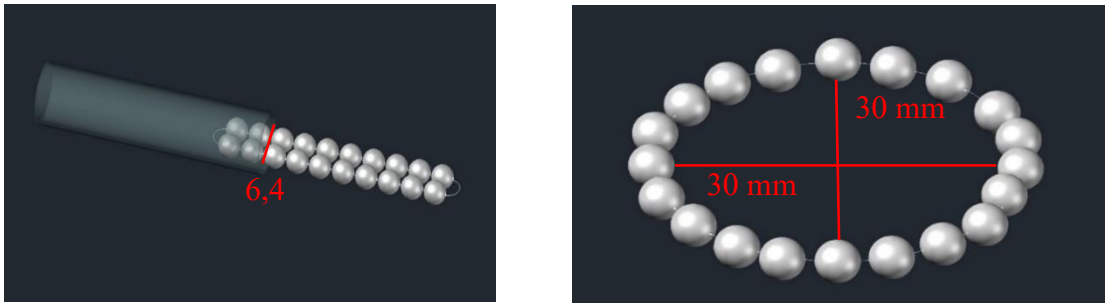

Fig. 1. Schematic diagram of ring-shaped urinary bladder device for prolonged release. (a) device inserted in the urinary bladder catheter tube; (b) device in the expanded configuration

Perforated tablets connected with a biodegradable suture thread to create a ring-shape configuration were prepared. Tablets having a relatively small diameter (3 mm) were selected for the preparation of the matrices. A 0.5 mm diameter hole was obtained by a precision drill, paying particular attention to drilling in the vertical direction of the tablet and not to alter the radius of curvature of upper and lower faces of the tablets.

3.1 *In vitro* release of non-coated tablets

The non-perforated and perforated tablets were characterized according to the compendial tests. Approximately, the perforated tablets lost 5 mg during the drilling procedure. The mass uniformity test was considered satisfied and the friability of the tablets resulted lower than 1% for both types of tablets. Table 5 shows tablets characteristics. It is worth to underline that the crushing strength values resulted in line with the expected values and sufficiently resistant to withstand coating process.

Table 5 shows non coated tablets' characterization results

	Mass (mg ± sd)	Height (mm ± sd)	Diameter (mm ± sd)	Crushing strength (N ± sd)
LV45-P	34.74 ± 0.83	4.56 ± 0.04	3.04 ± 0.02	63.60 ± 6.73
LV30-P	34.58 ± 0.63	4.28 ± 0.07	3.02 ± 0.01	65.80 ± 6.98
M45-P	34.33 ± 0.47	4.49 ± 0.08	3.02 ± 0.01	59.20 ± 8.40
M30-P	34.18 ± 0.71	4.09 ± 0.05	3.03 ± 0.01	64.80 ± 8.23

In Fig. 2 release profiles typical of hydrophilic matrices are reported: in the initial phase, a "burst effect" with greater slope of the curve can be observed due to the drug particles present on the surface, which immediately dissolved before the swelling of the polymer; a progressive decrease of the drug release rate can be seen in the final part of the profile. It is possible to observe how the matrix tablets prepared with the low and high viscosity HPMC polymer presented very similar release profiles and that the drilling process did not significantly modify the release profile. The totality of the active ingredient was released in all cases in about 3 h, a time not long enough to consider these matrices for the preparation of organ-retentive systems, intended to prolong the release of the active ingredient over a period of 24-48 h.

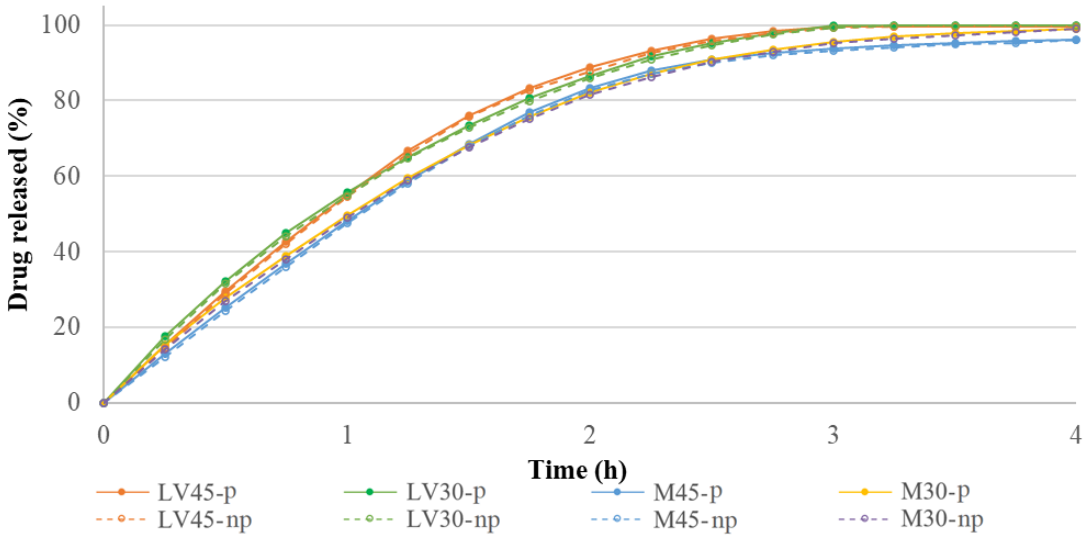

Fig. 2. Average in vitro release profiles of paracetamol from uncoated tablets perforated (P) and non-perforated (NP).

In order to extend the duration of the drug release, insoluble film coating was applied to the tableted matrices. Ethylcellulose (Surelease®) or methacrylic polymers (Eudragit® RL/RS) were considered as the coating materials. Table 3 shows the process parameters used for each coating system. Coating process was performed in fluid bed equipment using a top-spray configuration applying processing parameters suggested by the literature (Surelease® (colorcon.com); EUDRAGIT® Functional Polymers for Oral Solid Dosage Forms - Evonik Industries) and to obtain a good fluidization of the tablets without having problems of sticking. Systems having final 10% weight increase were obtained by interrupting the process at predetermined times and checking the weight of the samples.

3.2 In vitro release test of coated tablets

The non-perforated and perforated coated tablets were subjected to the *in vitro* release test to evaluate the release performance of the systems. The release profiles were observed by comparing formulations having different percentages of HPMC at the same degree of viscosity for both the perforated and non-perforated tablets for all the three coating formulations (Table 2) are shown in Fig. 4, 5 and 6.

To evaluate the impact of perforation procedure on the coating film applied on the tablets, the drilling procedure was performed before and after coating process with ethylcellulose-based formulation A. The drilling process of the coated tablets caused the partial breakage of the film at the exit point, leading to the loss of tablet material and damaging the continuity of the film coating. It was hypothesized that the film tended to adhere to the rotating tip during piercing and may expand the size of the entry hole. Coated tablets sectioned horizontally when analyzed by scanning electron microscope (SEM) exhibited uniform external coating, while the film was totally absent from the internal surface of the hole. The coating thickness resulted approximately 100 μm, in agreement with measurements based on sizes of coated tablets. From the SEM photographs of the vertically-sectioned tablets it is evident that the geometry of the hole is much more regular when the tablets were perforated before the coating process than for those perforated after.

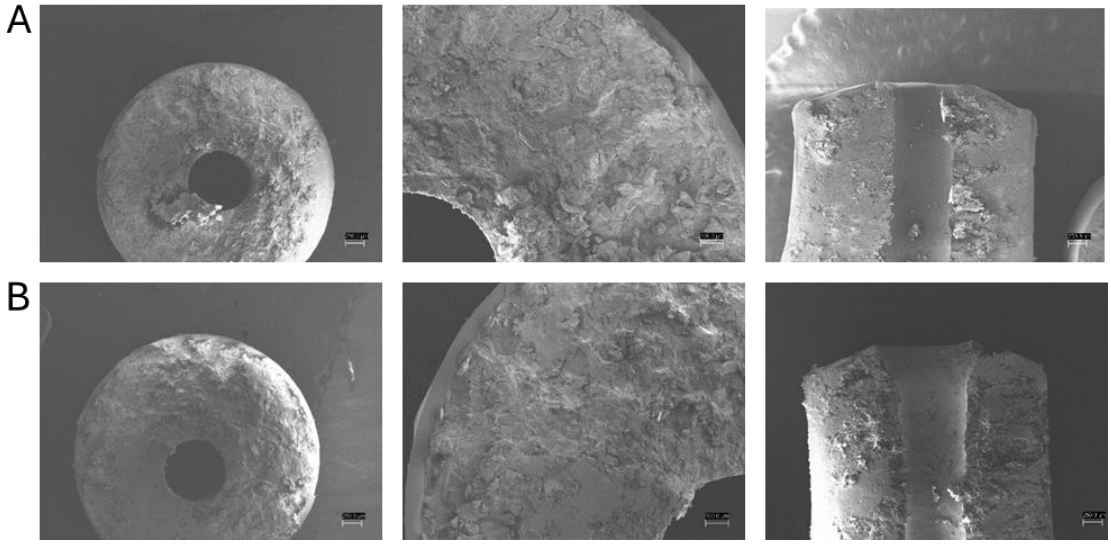

Fig. 6. SEM photographs of ethylcellulose-coated tablets in horizontal and vertical section related to tablets perforated before (A) and after coating process (B).

Moreover, tablets were characterized for weight, dimensions, crushing strength and thickness of the applied coating. The results are reported in Table 6.

Table 6. Shows ethylcellulose coated tablets' characterization results

	Mass (mg ± sd)	Heigh (mm ± sd)	Diameter (mm ± sd)	Crushing Strength (N ± sd)	Thickness (μm ± sd)	Weight gain (%)
LV45-P-EC	38.04 ± 0.73	4.62 ± 0.01	3.22 ± 0.00	113.0 ± 8.5	94 ± 2	9.5
LV30-P-EC	37.89 ± 0.88	4.38 ± 0.09	3.23 ± 0.01	102.0 ± 7.9	100 ± 5	9.6
M45-P-EC	37.79 ± 1.09	4.59 ± 0.06	3.24 ± 0.01	92.0 ± 4.4	96 ± 6	10
M30-P-EC	37.70 ± 1.46	4.23 ± 0.11	3.22 ± 0.01	98.8 ± 4.3	99 ± 4	10.3

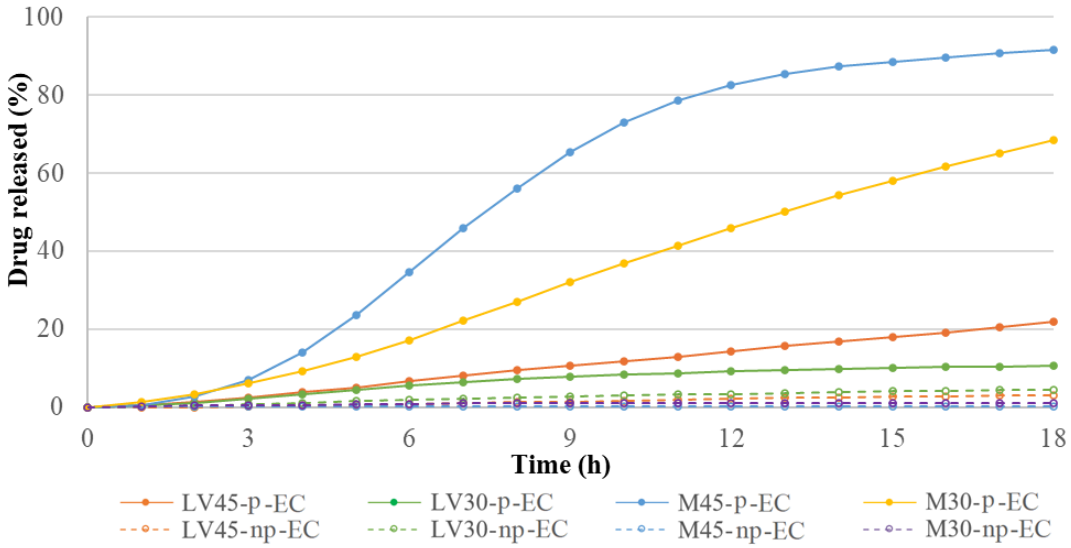

Fig. 3 Average drug release profiles from perforated (F) and non-perforated (NF) matrices coated with Surelease.

The type and amount of hydrophilic polymer in the cores affected release profiles reported in Fig. 3. Contrary to what was expected, tablets prepared with the lower viscosity hydrophilic polymer (Methocel™ 100LV) showed slower release profiles than those obtained from tablets containing the high viscosity polymer (Methocel™ K100M). For tablets prepared with a higher amount of polymer, the release rate was higher than those containing less polymer, both for high-viscosity and low-viscosity polymer. The coated tablets LV45-P-EC released approximately 20% of the active ingredient in 18 h, while the LV30-P-EC tablets released approximately 15%. The M45-P-EC tablets released approximately 90% of the active ingredient in 18 h, while the M30-P-EC tablets released approximately 70%. It has been hypothesized that the higher amount of polymer might have led to a greater quantity of gel, which caused a higher pressure on the coating and therefore caused a greater breakage compared to the lower percentage of polymer. It was also hypothesized that, thanks to the higher viscosity, the gel was more tenacious and therefore, by swelling, it had the ability to partially tear the insoluble coating, which is less susceptible when tablets contained low viscosity (LV) HPMC.

The non-perforated tablets for all compositions released a very small amount of drug in 18 h. For the perforated tablets, an initial lag phase of about 1.5 h was observed. The difference in the release between the perforated and non-perforated tablets lay in the presence of a surface without the controlling film, which allowed interaction with the aqueous fluids and therefore, a faster drug release.

It was assumed that the tablets prepared with the low viscosity HPMC released the active ingredient exclusively through the surface of the internal opening according to the control mechanism exerted by the hydrophilic polymer. The release speed of the active ingredient appeared to be very slow, probably due to the reduced surface area available for the diffusion of water and drug. Instead, the tablets prepared with the high viscosity polymer released the active ingredient both through the surface of the internal opening and through the film fractures that increased the interaction surface with the fluids and a faster drug release.

To increase the release rate of the active ingredient and to reduce the initial latency phase, HPMC at a very low viscosity (soluble polymer) was added to ethylcellulose-based film (5% based on the total amount of polymers) as a pore former. Tablets characteristics were measured and are showed in Table 7.

Table 7 shows ethylcellulose and HPMC coated tablets' characterization results

	Mass (mg ± sd)	Height (mm ± sd)	Diameter (mm ± sd)	Crushing Strength (N ± sd)	Thickness (µm ± sd)	Weight gain (%)
LV45-P-EC-H	37.98 ± 1.01	4.69 ± 0.01	3.24 ± 0.01	99.8 ± 14.8	105 ± 6	9.7
LV30-P-EC-H	37.94 ± 0.96	4.48 ± 0.06	3.23 ± 0.01	91.6 ± 5.3	102 ± 6	9.6
M45-P-EC-H	37.76 ± 0.89	4.65 ± 0.08	3.24 ± 0.02	92.8 ± 3.6	100 ± 9	10
M30-P-EC-H	37.82 ± 0.83	4.28 ± 0.06	3.22 ± 0.01	98.8 ± 7.3	98 ± 3	10.6

In Fig. 4 drug release profiles obtained from matrices coated with ethylcellulose and HPMC as a pore former is reported.

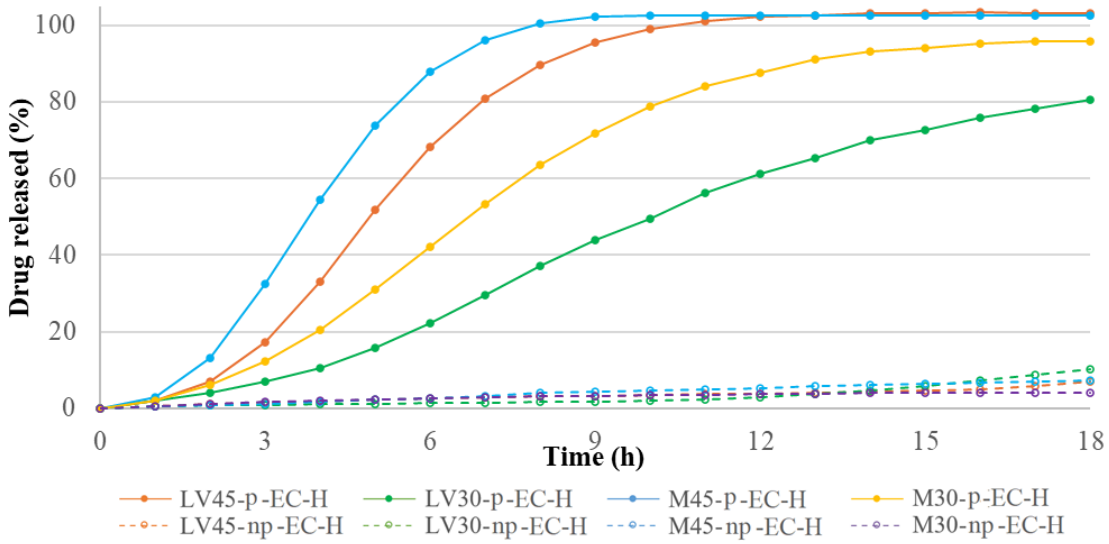

Fig. 4 Drug release profiles related to perforated (F) and non-perforated (NF) matrices coated with ethylcellulose and HPMC as a pore former.

Analogously to what observed with previous samples, the release profiles from these coated tablets showed an initial lag phase of about 1 hour, probably attributable to the time needed for the matrix to hydrate, followed by a constant rate phase where the release is modulated by the matrix and the coating. Being the coating film permeable, it allowed the release of the drug at a lower release rate compared to uncoated systems and higher compared to analogous systems coated without pore former. The LV45-P-EC-H tablets released 100% of the drug in 15 h, while the LV30-P-EC-H tablets released approximately 80% in 18 h. The M45-P-EC-H tablets released 100% of the drug in approximately 9 h, while the M30-P-EC-H tablets release approximately 100% of the drug in 18 h. As already seen for the tablets coated with ethylcellulose (Fig. 3), the amount and viscosity of the polymer used for the formulation of the tablets affected the release. Also in this case, the higher the amount and viscosity of the polymer employed, the faster the drug release. Non-perforated tablets of each of the four types of prepared mixtures release a reduced quantity of drug, approximately 10% in 18 h.

Coated tablets were also prepared by using polymethacrylates (formulation C) as the coating materials. These polymers are typically used as permeable coating materials in combination, to obtain a prolonged release of the active ingredient when applied to crystals, pellets and tablets (Akhgari et al., 2016).

Table 8 shows characterization results of coated tablets, which, also in this case, pointed out that coated tablets exhibit a higher crushing force than the non-coated ones.

Table 8 shows polymethacrylates coated tablets' characterization results

	Mass (mg ± sd)	Height (mm ± sd)	Diameter (mm ± sd)	Crushing Strength (N ± sd)	Thickness (μm ± sd)	Weight gain (%)
LV45-P-PM	38.91 ± 0.75	4.64 ± 0.09	3.24 ± 0.02	101 ± 10	103 ± 8	12
LV30-P-PM	38.87 ± 0.78	4.42 ± 0.11	3.23 ± 0.05	96 ± 3	101 ± 2	12.4
M45-P-PM	38.61 ± 0.71	4.66 ± 0.08	3.25 ± 0.05	94 ± 9	103 ± 3	12.4
M30-P-PM	38.55 ± 0.62	4.27 ± 0.04	3.24 ± 0.03	86 ± 3	109 ± 15	12.3

Drug release profiles from matrices coated with Eudragit RS and RL 1:1 are showed in Fig. 5.

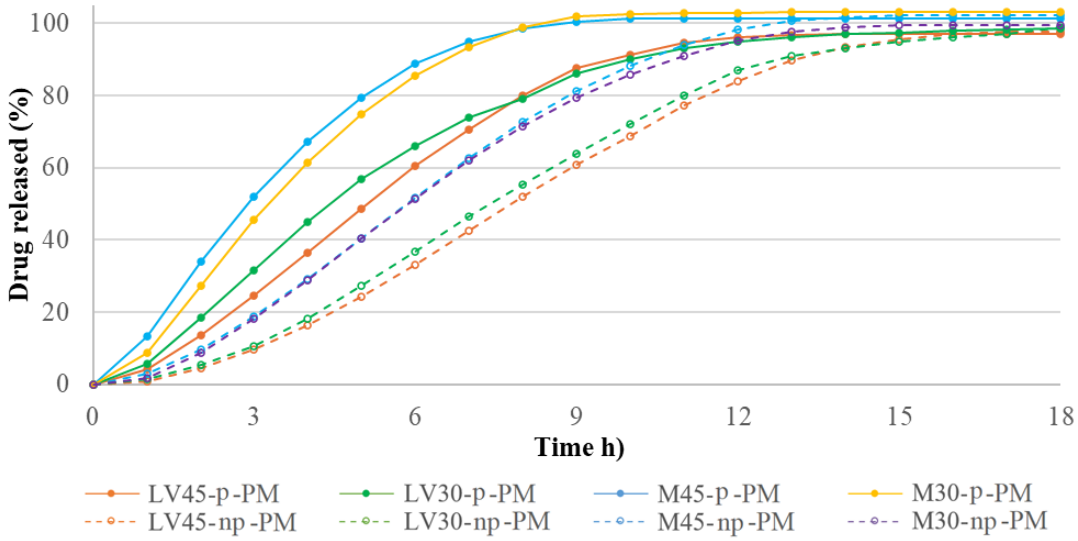

Fig. 5 Drug release profiles related to perforated (F) and non-perforated (NF) matrices coated with polymethacrylates.

The main control mechanism of the matrices coated with these polymers is exerted by the permeable membrane. Even if the tablets are not perforated, the release profile is fast compared to the matrices coated with ethylcellulose-based systems.

The two perforated tablets made of low viscosity HPMC, LV45-P-PM and LV30-P-PM, showed a comparable release profile and the complete release of the active ingredient occurred in approximately 12 hours. For what concerns the two perforated tablets made of high viscosity hypromellose, M45-P-PM and M30-P-PM, drug release profile is practically superimposable. Also the non-perforated tablets appeared to have a comparable behavior, releasing 100% of paracetamol in approximately 15 hours. For the non-perforated tablets, an initial lag phase is observed, probably linked to the time needed for the water to permeate the membrane and for the swelling hydrophilic polymer to hydrate. A shorter time is needed for this to occur in the case of the perforated tablets, which expose an uncoated surface. Even though, also in this case, different release profiles were detected, depending on HPMC type and on the fact that the tablets were

perforated or not, curves appeared to be more comparable between each other than those obtained for matrices coated with ethylcellulose or ethylcellulose plus HPMC. That evidence suggested that release rate control, in this case, is more controlled by the coating than by the presence of and hole and HPMC viscosity.

3.3 Prototypes of bladder-retentive systems

Expandable bladder-retentive systems were assembled using tablets joined by a biodegradable suture thread (Ethicon®, Vicryl Rapide™). A ring-shaped system consisting of twenty coated perforated tablets connected with a resorbable suture thread (Ethicon®, Vicryl Rapide™) knotted in a ring was proposed as a bladder-retentive system. In its expanded configuration, the system had a diameter of approximately 30 mm, a size sufficient to prevent its passage through the urethral sphincter and consequently its prolonged permanence inside the organ of interest. As already mentioned, all the coated tablets exhibited a good mechanical resistance, useful also considering the pressure necessary to push the system inside a catheter for administration. For the development of the system described, perforated tablets prepared with the low viscosity hydroxypropyl methylcellulose and coated with ethylcellulose (LV45-P-EC) were used, which showed the lowest drug release rate. The system described can be administered into the urinary bladder by using a urethral catheter when in a compact configuration.

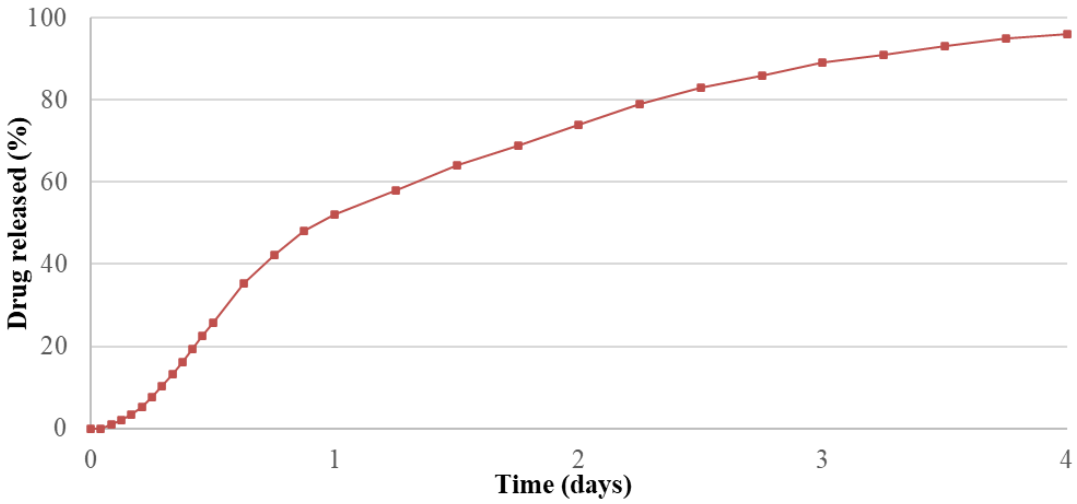

Fig. 7 Drug release profiles from ring-shaped system prepared by coating with ethylcellulose hydrophilic matrices prepared with low viscosity HPMC (LV45-P-EC)

The graph highlights that the release rate of the active ingredient was very slow, with approximately 100% of the drug released in 4 days. There was an initial latency phase comparable to that observed in for perforated and coated tablets with ethylcellulose, although it show a faster release of the drug maybe due to the presence of the thread that keeps the hole opened, maintaining the contact surface between the non-coated area of the tablets and the aqueous medium, while without the thread the hole might close, reducing the interaction surface, as a consequence of HPMC swelling.

The system could be eventually physiologically eliminated once the matrices and the string dissolve/erode. For what concerns the thread, it appeared to slowly dissolve after 15 days in deionized water at 37°C.

4. CONCLUSIONS

The aim of this work was to develop a system consisting of subunits connected by a biodegradable thread that could be administered using a urethral catheter inside the urinary bladder and that could expand its size once inside the organ in order to prevent its passage through the urethral sphincter.

Starting from tablets formulation and production, matrices made of low viscosity or high viscosity HPMC were produced, perforated and coated with three different formulations: ethylcellulose, ethylcellulose and HPMC as a pore former, and a methacrylic mixture. Prolonged drug release profiles were obtained with all of the formulations and the influence of the HPMC viscosity and the presence of perforation in the matrices were assessed.

Finally, to obtain a drug delivery system able to be retained in the urinary bladder for a few days, 20 perforated tablets made of low viscosity HPMC and coated with ethylcellulose, were produced and connected each other by means of and absorbable suture thread. Drug release profile of the full system exhibited a 4 days lasting release. After this time the matrices were completely dissolved, except for the thin insoluble coating layer and the suture thread was flexible inconsistent. Thanks to these characteristics, the system could eventually be retained in the organ releasing the drug in a prolonged manner, and be physiologically eliminated by the organ through urination since only very soft and small parts of the system remain undissolved.

REFERENCES

Akhgari, A., & Tavakol, A. (2016). Prediction of optimum combination of Eudragit RS/Eudragit RL/ethyl cellulose polymeric free films based on experimental design for using as a coating system for sustained release theophylline pellets. *Advanced Pharmaceutical Bulletin*, *6*(2), 219. https://doi.org/10.15171/apb.2016.030

Colaco, M. A., & Evans, R. J. (2013). Current recommendations for bladder instillation therapy in the treatment of interstitial cystitis/bladder pain syndrome. *Current urology reports*, *14*, 442-447. https://doi.org/10.1007/s11934-013-0369-y

Crouzet, J., Bertrand, X., Venier, A. G., Badoz, M., Husson, C., & Talon, D. (2007). Control of the duration of urinary catheterization: impact on catheter-associated urinary tract infection. *Journal of Hospital Infection*, *67*(3), 253-257. https://doi.org/10.1016/j.jhin.2007.08.014

Dmochowski, R. R., & Staskin, D. R. (2002). Advances in drug delivery: improved bioavailability and drug effect. *Current urology reports*, *3*, 439-444. https://doi.org/10.1007/s11934-002-0094-4

GuhaSarkar, S., & Banerjee, R. (2010). Intravesical drug delivery: challenges, current status, opportunities and novel strategies. *Journal of Controlled Release*, *148*(2), 147-159. https://doi.org/10.1016/j.jconrel.2010.08.031

Jang, E. B., Hong, S. H., Kim, K. S., Park, S. Y., Kim, Y. T., Yoon, Y. E., & Moon, H. S. (2020). Catheter-related bladder discomfort: how can we manage it?. *International neurourology journal*, *24*(4), 324. https://doi.org/10.5213/inj.2040108.054

Kolawole, O. M., Lau, W. M., Mostafid, H., & Khutoryanskiy, V. V. (2017). Advances in intravesical drug delivery systems to treat bladder cancer. *International journal of pharmaceutics*, *532*(1), 105-117. https://doi.org/10.1016/j.ijpharm.2017.08.120

Krause, P., Fuhr, U., Schnitker, J., Albrecht, U., Stein, R., & Rubenwolf, P. (2013). Pharmacokinetics of intravesical versus oral oxybutynin in healthy adults: results of an open label, randomized, prospective clinical study. *The Journal of urology*, *190*(5), 1791-1797. https://doi.org/10.1016/j.juro.2013.05.011

Krhut, J., Navratilova, M., Sykora, R., Jurakova, M., Gärtner, M., Mika, D., ... & Zvara, P. (2016). Intravesical instillation of onabotulinum toxin A embedded in inert hydrogel in the treatment of idiopathic overactive bladder: A double-blind randomized pilot study. *Scandinavian journal of urology*, *50*(3), 200-205. https://doi.org/10.3109/21681805.2015.1121406

Lin, T., Wu, J., Zhao, X., Lian, H., Yuan, A., Tang, X., ... & Hu, Y. (2014). In situ floating hydrogel for intravesical delivery of adriamycin without blocking urinary tract. Journal of pharmaceutical sciences, 103(3), 927-936. https://doi.org/10.1002/jps.23854

Liu, S., Zhang, C., Peng, L., Lu, Y., & Luo, D. (2021). Comparative effectiveness and safety of intravesical instillation treatment of interstitial cystitis/bladder pain syndrome: a systematic review and network meta-analysis of randomized controlled trials. *International Urogynecology Journal*, *32*, 1061-1071. https://doi.org/10.1007/s00192-020-04490-3

Maroni, A., Melocchi, A., Zema, L., Foppoli, A., & Gazzaniga, A. (2020). Retentive drug delivery systems based on shape memory materials. *Journal of Applied Polymer Science*, *137*(25), 48798. https://doi.org/10.1002/app.48798

Nicolle, L. E. (2012). Urinary catheter-associated infections. *Infectious Disease Clinics*, *26*(1), 13-27. https://doi.org/ 10.1016/j.idc.2011.09.009

Palugan, L., Cerea, M., Cirilli, M., Moutaharrik, S., Maroni, A., Zema, L., ... & Gazzaniga, A. (2021). Intravesical drug delivery approaches for improved therapy of urinary bladder diseases. *International Journal of Pharmaceutics: X*, *3*, 100100. https://doi.org/10.1016/j.ijpx.2021.100100

Reynolds, T. D., Mitchell, S. A., & Balwinski, K. M. (2002). Investigation of the effect of tablet surface area/volume on drug release from hydroxypropylmethylcellulose controlled-release matrix tablets. *Drug development and industrial pharmacy*, *28*(4), 457-466. https://doi.org/10.1081/DDC-120003007

Tyagi, P., Tyagi, S., Kaufman, J., Huang, L., & de Miguel, F. (2006). Local drug delivery to bladder using technology innovations. *Urologic Clinics*, *33*(4), 519-530. https://doi.org/10.1016/j.ucl.2006.06.012

Vigani, B., Rossi, S., Sandri, G., Bonferoni, M. C., Caramella, C. M., & Ferrari, F. (2020). Recent advances in the development of in situ gelling drug delivery systems for non-parenteral administration routes. *Pharmaceutics*, *12*(9), 859. https://doi.org/10.3390/pharmaceutics12090859

Yoon, H. Y., Yang, H. M., Kim, C. H., Goo, Y. T., Kang, M. J., Lee, S., & Choi, Y. W. (2020). Current status of the development of intravesical drug delivery systems for the treatment of bladder cancer. *Expert Opinion on Drug Delivery*, *17*(11), 1555-1572. https://doi.org/10.1080/17425247.2020.1810016

Zacchè, M. M., Srikrishna, S., & Cardozo, L. (2015). Novel targeted bladder drug-delivery systems: a review. *Research and reports in urology*, 169-178.

https://www.colorcon.com/markets/pharmaceuticals/film-coatings/sustained-release/surelease

https://healthcare.evonik.com/en/drugdelivery/oral-drug-delivery/oral-excipients/eudragit-portfolio

Chapter 4

Organ-retentive osmotically driven system (ORODS): a novel expandable platform for in situ drug delivery

Published as:

Micol Cirilli, Alessandra Maroni, Saliha Moutaharrik*, Anastasia Foppoli, Evelyn Ochoa, Luca Palugan, Andrea Gazzaniga, Matteo Cerea, International Journal of Pharmaceutics, 123295 (2023)

https://doi.org/10.1016/j.ijpharm.2023.123295

* Corresponding author

§ The contribution given by Micol Cirilli to the work associated with published article was conceptualization, methodology, formal analysis, validation, investigation, writing – original draft, writing – review & editing, visualization.

ABSTRACT

Drug delivery systems capable of being retained within hollow organs allow the entire drug dose to be delivered locally to the disease site or to absorption windows for improved systemic bioavailability. A novel Organ-Retentive Osmotically Driven System (ORODS) was here proposed, obtained by assembling drug-containing units having prolonged release kinetics with osmotic units used as increasing volume compartments. Particularly, prototypes having H-shape design were conceived, manufactured and evaluated. Such devices were assembled by manually inserting a tube made of regenerated cellulose (osmotic unit) into the holes of two perforated hydrophilic tableted matrices containing paracetamol as a tracer drug. The osmotic unit was obtained by folding and gluing a plain regenerated cellulose membrane and loading sodium chloride inside. When immersed in aqueous fluids, this compartment expanded to approximately 80% of its maximum volume within 30 min of testing, and a *plateau* was maintained for about 6 h. Subsequently, it slowly shrank to approximately 20% of the maximum volume in 24 h, which would allow for physiological emptying of the device from hollow organs. While expanding, the osmotic unit acquired stiffness. Drug release from H-shaped ORODSs conveyed in hard-gelatin capsules was shown to be prolonged for more than 24 h.

KEYWORDS

Gastro-retentive delivery systems

Intravesical delivery systems

Osmotic delivery systems

Prolonged release

3D printing

Hydrophilic matrix

1. INTRODUCTION

Great attention has been directed over the years to systems capable of being retained within hollow organs, such as the stomach and urinary bladder (Maroni et al., 2020, Uboldi et al., 2022). The goal is to improve local therapies by delivering the entire drug load to the target site. Moreover, in the case of gastro-retentive delivery systems, there is a strong interest in the possibility of improving the bioavailability of drugs having either an absorption window in the upper gastrointestinal tract or poor solubility/stability in the enteric environment. (Ibrahim et al., 2019, Kumar and Kaushik, 2018, Lopes et al., 2016, Pawar et al., 2012, Prinderre et al., 2011, Streubel et al., 2006, Supratim et al., 2021). In both instances, a sophisticated approach based on different formulation strategies and manufacturing technologies would be needed to combine a sufficiently long-lasting retention with the prolonged release of the bioactive compound regardless of the patho-physiological variables found *in situ* (pH, ionic strength, volume, composition and hydrodynamics of the medium, presence of enzymes, mucus, etc.) (Maroni et al., 2020). The time course of release of the active ingredient and of residence of the delivery system within the target compartment should approximately overlap and be as long as possible when it comes to chronic treatments. (Cima et al., 2014, Hoffman et al., 2004).

This approach would not only improve the therapeutic outcome but also the patient compliance, which is well known to strongly be affected by the dosing regimen (Stockwell Morris and Schulz, 1992, Vrettos et al., 2021). Particularly, the administration of bioactive compounds that, when given as immediate-release dosage forms, require frequent dosing throughout the day would have a high impact on the living habits of patients and ultimately impair their adherence to the therapy. In this respect, it has been reported that reducing the complexity of the dosing schedule to once- or twice-a-day administrations results in major benefits (Paquin et al., 2013). These would even be more relevant in the case of invasive routes of administration, such as intravesical instillations, involving pain and discomfort that are leading causes of dropouts. Interestingly, “Ultra-long-acting oral formulations” that are not subject to the influence of gastrointestinal

transit, have been included in the FDA Emerging Technology Program and allowed infradian release time spans to be achieved (Altreuter et al., 2018).

While more consolidated strategies are available to slow down drug release, reliable organ retention is still a challenging goal. Different systems for extended residence time have been proposed so far, which are mainly based on bioadhesion, buoyancy and size enlargement. The latter approach requires an original small-sized configuration, to allow for administration, and a spatial encumbrance large enough to prevent early emptying from the organ. (Palugan et al., 2021a, Tripathi et al., 2019).

The size enlargement can be based on various mechanisms that exploit physical phenomena, such as swelling associated with glass-rubber transition, elastic recovery or intrinsic shape memory properties of the materials employed (Gazzaniga et al., 2023). Retentive systems, when taking on the bulky configuration, are also expected to have: i) sufficient stiffness to withstand mechanical forces possibly exerted by the organ wall and ii) dissolution, biodegradation or disassembling to decrease in size and spontaneously empty from the organ without external intervention when exhausted (Altreuter et al., 2018, Cima et al., 2014, Farokhzad et al., 2006, Klausner et al., 2003, Zacchè et al., 2015).

According to the current need for more effective, tolerable and acceptable drug therapies, this paper reports on the design of a novel organ-retentive drug delivery platform, which would expand *in situ* based on osmotically driven increase in size. The Organ-Retentive Osmotically Driven Systems (ORODSs) are intended for prolonged retention and release mainly in the stomach or urinary bladder. Fabrication and preliminary data on the *in vitro* performance of a gastro-retentive system having H-shaped configuration are also reported and discussed as a proof of concept.

2. EXPERIMENTAL

2.1. Materials

Dialysis membrane made of regenerated cellulose having a cutoff of 12–14000 Dalton (Spectrum Labs™ Repligen, Spectra/Por™ 2, CA, USA); sodium chloride (NaCl, water solubility 360 mg/mL at 37 °C), potassium chloride (KCl), hydrochloric acid 37% (HCl) (VWR International S.r.l., IT); paracetamol (Compap™, Mallinckrodt, IE); microcrystalline cellulose (MCC, Avicel® PH 200, FMC, BE); hypromellose (Methocel® K4M, Colorcon, UK); hard-gelatin capsules (Capsugel® ConiSnap® Size 00, Lonza, BE); acrylic glue (Loctite, DE).

2.2. Methods

2.2.1. ORODS fabrication

The prototypes were fabricated by manually inserting and gluing a tube made of regenerated cellulose (osmotic unit) into the through holes of 2 perforated hydrophilic matrices (500 mg) obtained by tableting (tablet press FA/8, Officine Ronchi, IT), using 20x8 mm concave punches and a compaction force (F_a) of approximately 10 kN, from a 50% paracetamol, 40% hypromellose and 10% microcrystalline cellulose powder mixture. The matrices (4 mm in thickness) were perforated (elliptical opening of 5.0x1.5 mm) by a precision driller (Proxxon, DE). The osmotic unit (average diameter and flat width of 3.7 mm and 4.8 mm, respectively) was obtained by folding a plain dry membrane of defined area and layout (20x55 mm flat size) and gluing the edges together. Particularly, the membrane was bent along its main axis and sealed at two edges by gluing to give an open tube. After loading 50 mg of sodium chloride as an osmotic agent, the tube was also sealed at its open end. The assembled devices were gently folded by hand and inserted into hard-gelatin capsules.

2.2.2. Evaluation of fluid inflow into isolated osmotic unit

Fluid inflow was evaluated by placing isolated osmotic units in deionized water (800 mL, 37.0 ± 0.5 °C) and USP 44 hydrochloric acid buffer pH 1.2 (HCl 37%

7.07 mL/L, KCl 3.727 g/L), measuring their diameter (n = 3, 5 different positions) at established time points using a digital caliper (Absolute Digimatic CD-15CP, Mitutoyo, UK) and calculating the corresponding volume of the tubes. Samples were gently blotted with a paper tissue before measurement.

2.2.3. Mechanical testing of isolated osmotic units

Mechanical testing of isolated osmotic units was performed adapting the standard test method for flexural properties of unreinforced and reinforced plastics and electrical insulating materials American Standard Testing Material (ASTM) D790 (Venkata Pavan et al., 2022, ASTM D790. Annual Book of ASTM Standards, 1997). The test was carried out using a TA-XT2 analyzer (Texture Technologies, Hamilton, MA, USA) equipped with a three-point bend fixture (support span of 22 mm, support cylindrical rods and nose of 2 mm in diameter, 50 N load cell) and software for analyzing displacement and load (Fig. 1). Tester probes were designed by AutoCAD 2022 and fabricated by FDM 3D printing (Mod. A10pro, Geeetech, Shenzhen, CN) using a commercial PLA filament (Geeetech PLA Black, 1.75 mm in diameter). Printing parameters were: printing speed 60 mm/s, nozzle diameter 0.4 mm, environment temperature 25 °C, slicing software Cura file, printing bed temperature 40 °C, nozzle temperature 180 °C. Operational parameters of the test were 7 mm maximum displacement at 2 mm/min rate of displacement. Force-displacement and strain–stress profiles were acquired after immersion of the isolated osmotic units in 800 mL distilled water and USP 44 hydrochloric acid buffer pH 1.2 at 37 °C for 120 min (n = 3). Samples were gently blotted with a paper tissue before measurement.

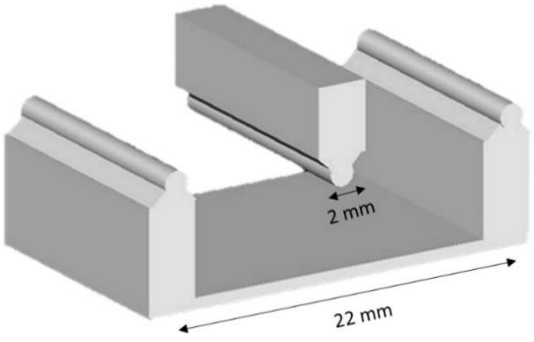

Fig. 1. CAD design of tester probes for mechanical testing of isolated osmotic units.

2.2.4. Residual sodium chloride assay

Osmotic units (n = 3) containing 50 mg of sodium chloride were placed in deionized water and in USP 44 hydrochloric acid buffer pH 1.2 (800 mL, 37.0 ± 0.5 °C). At pre-established timepoints the osmotic units were removed from the fluid and dried for 24 h in a static oven at 40 °C. The residual amount of salt was calculated according to the following equation:

Residual sodium chloride at t_x (%) = [50 mg – (osmotic unit mass at t_0 - osmotic unit mass at t_x)] /50 mg × 100.

2.2.5. Drug release testing

ORODS-containing capsules were evaluated for drug release in a USP 40 paddle dissolution apparatus (At7 Smart, Sotax, Basel, CH; 100 rpm, 900 mL deionized water or USP 44 hydrochloric acid buffer pH 1.2, 37.0 ± 0.5 °C). Paracetamol was quantified spectrophotometrically (Lambda 35, Perkin Elmer Italia, IT; 248 nm, 1 mm cuvette) in fluid samples withdrawn at successive time points.

3. RESULTS AND DISCUSSION

3.1. ORODS design

The new Organ-Retentive Osmotically-Driven Systems (ORODSs) intended for retention in the stomach or urinary bladder, are obtained by assembling one or more drug-containing units (prolonged drug release compartments) with one or more osmotic units (increasing volume compartments). The latter are in the form of closed tubes of various shapes, with walls made up of semipermeable polymeric membranes. The tubes are filled with substances that promote the inflow of aqueous fluids. Depending on the physical characteristics of the semipermeable membrane, water or aqueous solutions may enter the osmotic compartment, which would expand and acquire stiffness, causing an overall enlargement (larger encumbrance) of the assembled device. Meanwhile, the drug-containing units, which are tightly linked to the osmotic unit, slowly release the bioactive compound and eventually dissolve or erode.

The concentration of the loaded osmotic agents decreases over time and, finally, the osmotic compartment returns to its collapsed form, allowing physiological emptying of the entire device from the organ without any invasive interventions.

The drug-containing units made of soluble and/or biodegradable polymers can be obtained by tableting, injection-molding, hot melt extrusion (HME) or 3D printing. They have through or blind openings, into which the tubes are inserted and firmly attached.

Tube-shaped semipermeable membranes are available on the market. Tubes of specific diameters can also be obtained by folding and sealing together the edges of plain semipermeable membrane samples of defined area and layout.

In the case of gastro-retentive systems, the assembled devices in the initial configuration would conveniently be administered in hard-gelatin capsules. The bulky configuration of the devices should be larger than the wide-open pylorus by at least 2 dimensions. The maximum average inner diameter of the pylorus is reported in the literature to be around 20 mm (Bellinger et al., 2016). After operation, the drug-containing units would dissolve and/or erode, while the semipermeable tubes detach and shrink thus making passage through the pylorus possible.

The devices intended for retention within the urinary bladder would be inserted into the organ using a catheter. Therefore, the retentive device in its original configuration should not exceed 7 mm in width considering the internal diameter of commonly used urinary catheters (Andreessen et al., 2012). On the other hand, there are no particular restrictions in terms of length. When exhausted, the drug-containing units would dissolve and/or erode, eventually allowing for elimination of small hydrated matrix fragments or dissolved polymer in the urine. Once shrunk and detached from the matrices, the osmotic unit would be reduced in size and modified in shape so as to easily pass through the urethra and be physiologically emptied, with no need for external intervention.

Either for gastric or urinary bladder retention, ORODSs should take on their bulky configuration promptly after administration, so as to limit the risk of early discharge form the organ, maintain it over the entire time course of drug release and finally resume a less cumbersome configuration, following erosion/biodegradation and disassembly, to allow for spontaneous emptying.

The rate of fluid inflow into the osmotic unit, leading to the bulky configuration of the assembled device, as well as the rate of shrinking of the same unit after it has reached its maximum expansion, can be modulated through the use of semipermeable membranes having different composition (*e.g.* regenerated cellulose, cellulose acetate), permeability, cutoff, surface area and/or thickness, as well as through the selection of differing types and amounts of osmotic agent loaded. Even though a small amount of sodium chloride was here employed, considering that most guidelines suggest a low salt intake (<5.75 g of sodium chloride), the expansion of the system could be pursued for instance by the use of potassium chloride, mannitol, sucrose or mixtures thereof (Williams et al., 2018).

The drug-containing units should be able to slowly release the active ingredient over 12 h or more. Hydrophilic matrices based on soluble polymers, such as hydrophilic cellulose derivatives, polyvinyl alcohol (PVA) or polyethylene oxide (PEO), would especially be suited as drug-containing units of the retentive device. Their dissolution/erosion rate could also be fine-tuned by incorporating specific enzymes (*e.g.* cellulase) or soluble/insoluble fillers. (Cerea et al., 2018, Cerea et al., 2020a, Cerea et al., 2020b, Foppoli et al., 2020, Palugan et al., 2021b).

ORODSs having diverse architecture, intended for either stomach or urinary bladder retention, were conceived according to the above-described design concept. Even in the expanded form, the system maintained a soft surface texture, respectful of the mucous membrane of the organs in which it can be used. The main prototypes devised so far, H-, ring- and T-shaped, are depicted in Fig. 2.

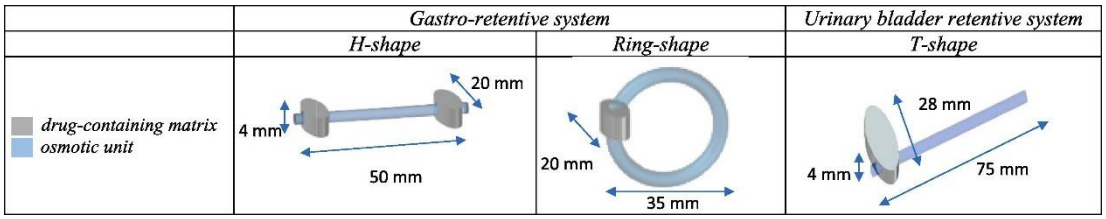

Fig. 2. Schematics of ORODSs having different shapes in their bulky configuration for retention.

3.2. H-shaped gastro-retentive ORODS

The fabrication and evaluation of a particular ORODS system for gastric retention, having H-shape, are here described. Fig. 3 shows the system assembled and folded for insertion into a hard-gelatin capsule, so as to enable oral administration. When in contact with aqueous media, the gelatin capsule dissolves quickly, and the ORODS is set free (Fig. 3A, 3B). Thus, the fluid starts entering, causing the H-shaped ORODS to unfold and achieve the bulky configuration required for retention (Fig. 3C, 3D).

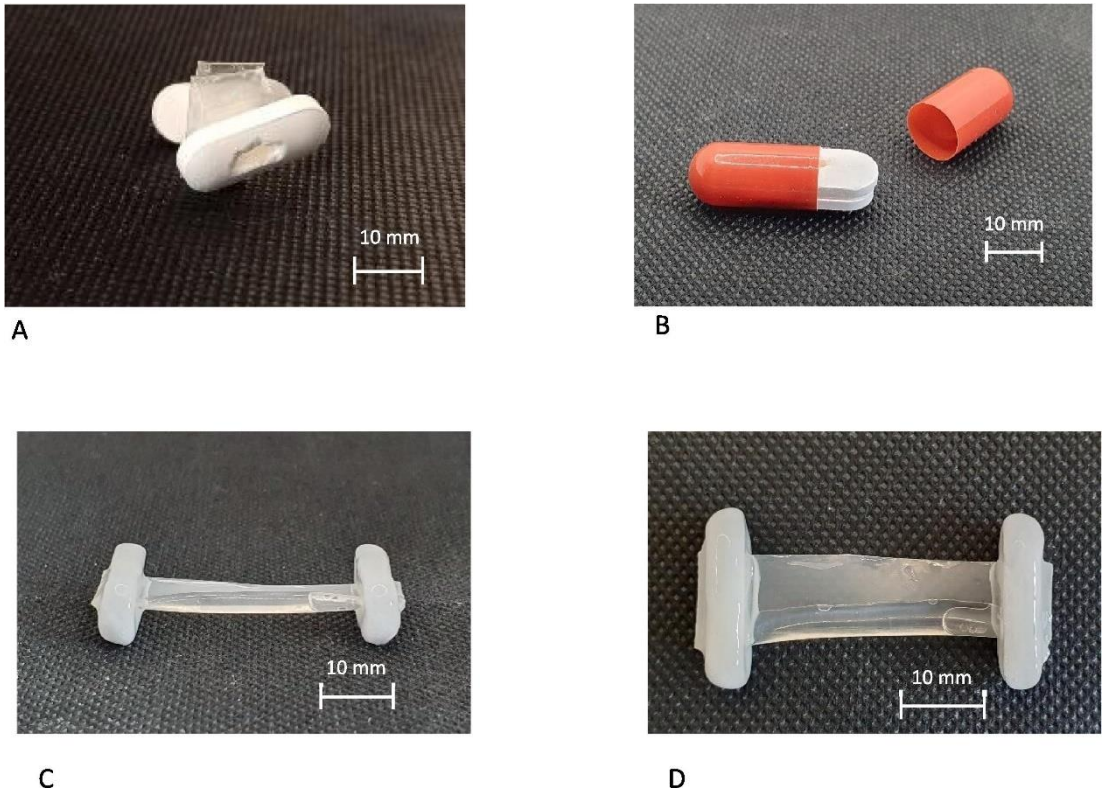

Fig. 3. H-shaped ORODS in its initial configuration for administration, before (A) and after (B) insertion into a hard-gelatin capsule, and with water-filled osmotic unit (C-side view; D-top view).

The average profile of increase in volume over time of isolated osmotic units loaded with 50 mg of sodium chloride is shown Fig. 4. Due to fluid inflow, the units immediately started to enlarge, reaching about 80% of the maximum volume achieved within the first 30 min of testing. A *plateau* was maintained for about 6 h. Afterwards, the volume slowly decreased, and at 24 h the osmotic unit was shrunk to approximately 20% of the maximum volume. Notably, a relatively limited variability of data was observed, indicating a robust performance under the investigated conditions.

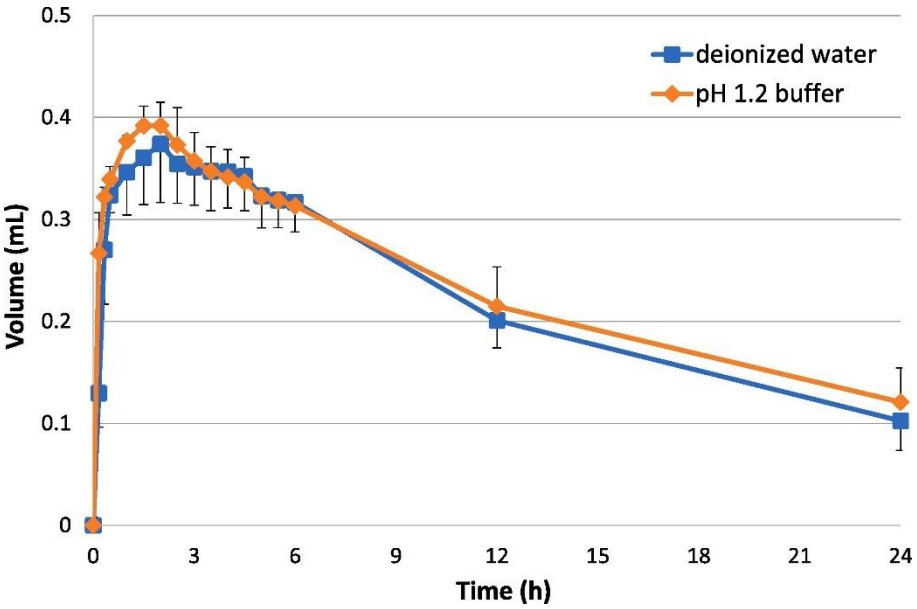

Fig. 4. Mean volume *vs.* time profiles for isolated osmotic units of H-shaped ORODSs immersed in deionized water and hydrochloric acid buffer pH 1.2 (n = 3, vertical bars represent standard deviation, positive and negative values for pH 1.2 buffer and water, respectively).

As the volume increased, the osmotic unit acquired stiffness. The mechanical strength of a single isolated osmotic unit was assessed after 2 h of immersion in deionized water or in hydrochloric acid buffer pH 1.2, *i.e.* approximately at the time when the maximum volume was achieved, applying the three-point bend method adapted from ASTM D790 standard, which is usually employed for quality control and specification purposes in different fields (Fig. 5). The support and nose components of the assembled equipment were purposely designed for this test and fabricated via FDM 3D printing using commercially available PLA filament. The nose had a rounded tip with a curvature radius of

1 mm that, at the maximum displacement (7 mm), corresponded to a contact surface area of approximately 10 mm^2 with the cellulosic membrane.

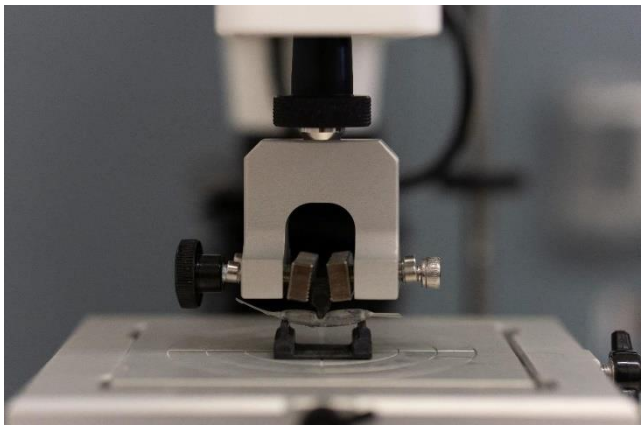

Fig. 5. Setup for evaluation of mechanical strength of isolated osmotic units of H-shaped ORODS.

The displacement of the nose of the three-point bend fixture moving downward caused an increase in the force opposed by the filled osmotic unit (Fig. 6). When the load was removed, the force did not immediately drop to zero, suggesting a possible elastic recovery of the sample. The experiment was repeated, and the average maximum value for 3 replicates overall was 136 g ± 8 sd in deionized water and 142 g ± 12 sd in the hydrochloric acid buffer. Such results pointed out the ability of the system to develop and retain spatial encumbrance following fluid entry and, in addition, the effectiveness of the tube sealing. Neither the glue used nor the regenerated cellulose membrane was affected by the acidic medium. The resistance as measured by this testing procedure was in line with that reported in the literature with reference to gastric peristalsis, *i.e.* 100 g (Laulicht et al., 2010, Bellinger et al., 2016). However, extensive *in vitro* and *in vivo* studies will be required for proper evaluation of mechanical behavior inside hollow organs. (Neumann et al., 2017, Neumann et al., 2021, Schneider et al., 2017, Schneider et al., 2018, Schneider et al., 2019).

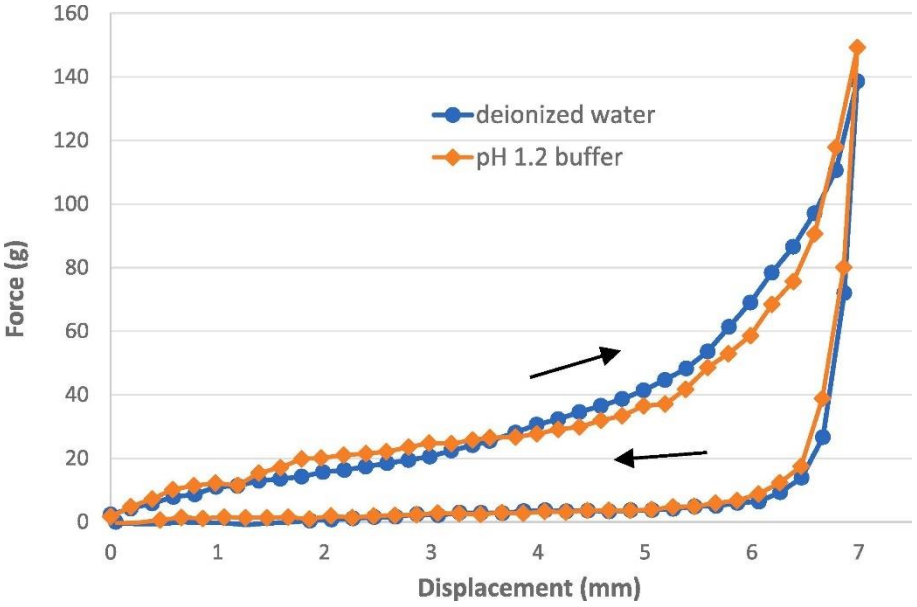

Fig. 6. Force *vs.* displacement profiles for isolated osmotic units of H-shaped ORODSs at their maximum volume (2 h immersion in deionized water or hydrochloric acid buffer pH 1.2).

The loss of sodium chloride from the osmotic unit was also evaluated by measuring the salt concentration in deionized water and hydrochloric acid buffer pH 1.2 via gravimetric assay. As shown in Fig. 7, the residual amount of sodium chloride in the osmotic unit decreased rapidly when evaluated in both fluids. Within 0.5 h, approximately 70% and 90% of osmotic agent leached out in hydrochloric acid buffer and deionized water, respectively. The process was slower in the acidic medium likely due to the inherent salt content of the buffer medium. The time course of salt loss from the tube was not aligned with the volume *vs.* time profiles acquired (Fig. 3). Further studies will be needed to investigate these aspects in depth. Particularly, the use of dialysis membranes having different cutoff sizes and/or diverse types and loads of osmotic agent will be explored. However, as demonstrated by the mechanical test, the residual sodium chloride concentration gradient was sufficient to allow for sustained maintenance of stiffness of the unit over time.

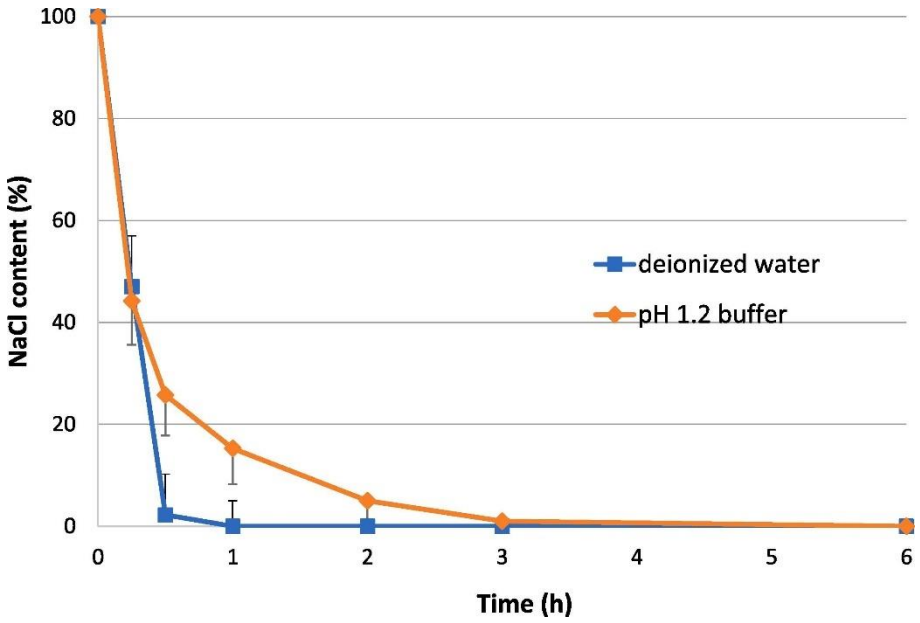

Fig. 7. Mean residual amount of sodium chloride in isolated osmotic units of H-shaped ORODS immersed in deionized water or hydrochloric acid buffer pH 1.2 (n = 3, vertical bars represent standard deviation).

H-shaped ORODSs conveyed in hard-gelatin capsules were evaluated for release of paracetamol, used as a tracer drug (Fig. 8). The HPMC matrices of the device, coupled through the osmotic unit, were proved to prolong, under the applied test conditions, the release of the drug for more than 24 h, according to the typical kinetics of hydrophilic matrix systems. As expected based on the pH-independent nature of both the matrix-forming polymer and tracer drug, the release profiles in deionized water and hydrochloric buffer pH 1.2 turned out practically superimposed.

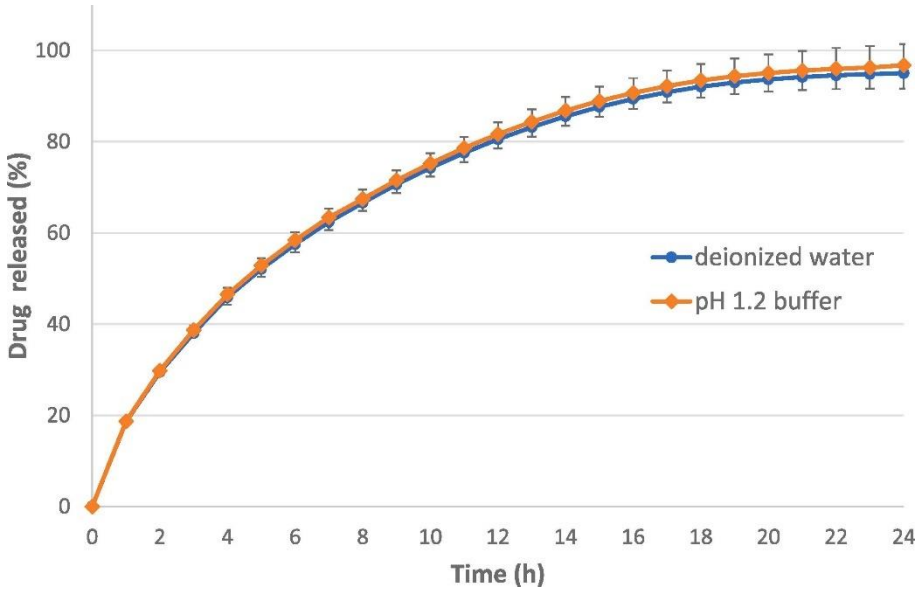

Fig. 8. Mean release profile of paracetamol from H-shaped ORODSs conveyed in hard-gelatin capsules immersed in deionized water and hydrochloric acid buffer pH 1.2 (n = 3, vertical bars represent standard deviation, positive and negative values for pH 1.2 buffer and water, respectively).

4. CONCLUSIONS

Novel Organ-Retentive Osmotically-Driven Systems (ORODSs) devices were proposed that, thanks to the inherent design, can considerably increase their spatial encumbrance based on osmotic inflow of water or biological fluids, slowly release the loaded drug and finally shrink for physiological emptying. Thus, after administration in the folded space-saving configuration, the systems would be retained for a relatively long period of time in hollow muscular organs due to the bulky conformation acquired. Then, the operational configuration would be reversed, enabling spontaneous removal of the exhausted system. Such devices consisted in assembled drug-containing units for prolonged release and osmotic compartments responsible for size enlargement of the final system.

In this preliminary study, feasibility and proof of principle of the ORODS platform were assessed. Particularly, prototypes having different design were conceived, and an H-shaped system was manufactured and evaluated for behavior in deionized water and hydrochloric acid buffer pH 1.2. The results obtained in terms of changes in volume and stiffness undergone by the isolated osmotic

compartment turned out potentially suitable for the pursued *in vivo* performance. Moreover, the expected release of the tracer drug from the assembled device was obtained. Further studies are needed in order to refine the design and behavior of ORODS, assess the role of the type and amount of osmotic agent and the effect of the thickness as well as composition of different dialysis membranes.

REFERENCES

Altreuter, David H., Ameya R. Kirtane, Tyler Grant, Cecilia Kruger, Giovanni Traverso, and Andrew M. Bellinger. 2018. "Changing the Pill: Developments toward the Promise of an Ultra-Long-Acting Gastroretentive Dosage Form." Expert Opinion on Drug Delivery 15 (12): 1189–98. https://doi.org/https://doi.org/10.1080/17425247.2018.1544615.

Andreessen, Linda, Mary H. Wilde, and Pam Herendeen. 2012. "Preventing Catheter-Associated Urinary Tract Infections in Acute Care: The Bundle Approach." Journal of Nursing Care Quality 27 (3): 209–17. https://doi.org/10.1097/NCQ.0b013e318248b0b1.

Bellinger, Andrew M, Mousa Jafari, Tyler M Grant, Shiyi Zhang, † Hannah, C Slater, Edward A Wenger, et al. 2016. "Oral, Ultra-Long-Lasting Drug Delivery: Application toward Malaria Elimination Goals." Science Translational Medicine 8. https://www.science.org.

Cerea, Matteo, Anastasia Foppoli, Luca Palugan, Alice Melocchi, Lucia Zema, Alessandra Maroni, and Andrea Gazzaniga. 2020. "Non-Uniform Drug Distribution Matrix System (NUDDMat) for Zero-Order Release of Drug with Different Solubility." International Journal of Pharmaceutics 581. https://doi.org/10.1016/j.ijpharm.2020.119217.

Cerea, Matteo, Alessandra Maroni, Luca Palugan, Marco Bellini, Anastasia Foppoli, Alice Melocchi, Lucia Zema, and Andrea Gazzaniga. 2018. "Novel Hydrophylic Matrix System with Non-Uniform Drug Distribution for Zero-Order

Release Kinetics." Journal of Controlled Release 287: 247–56. https://doi.org/10.1016/j.jconnrel.2018.08.027.

Cerea, Matteo, Alessandra Maroni, Luca Palugan, Saliha Moutaharrik, Alice Melocchi, Lucia Zema, Anastasia Foppoli, and Andrea Gazzaniga. 2020. "Oral Hydrophilic Matrices Having Non Uniform Drug Distribution for Zero-Order Release: A Literature Review." Journal of Controlled Release 325: 72–83. https://doi.org/http://doi.org/10.1016/j.jconrel.2020.06.033.

Cima, Michael J., Heejin Lee, Karen Daniel, Laura M. Tanenbaum, Aikaterini Mantzavinou, Kevin C. Spencer, Qunya Ong, et al. 2014. "Single Compartment Drug Delivery." Journal of Controlled Release 190: 157–71. https://doi.org/10.1016/j.jconrel.2014.04.049.

Farokhzad, Omid C., Jordan D. Dimitrakov, Jeffrey M. Karp, Ali Khademhosseini, Michael R. Freeman, and Robert Langer. 2006. "Drug Delivery Systems in Urology - Getting 'Smarter.'" Urology 68: 463–69. https://doi.org/10.1016/j.urology.2006.03.069.

Foppoli, Anastasia, Alessandra Maroni, Luca Palugan, Lucia Zema, Saliha Moutaharrik, Alice Melocchi, Matteo Cerea, and Andrea Gazzaniga. 2020. "Erodible Coatings Based on HPMC and Cellulase for Oral Time-Controlled Release of Drugs." International Journal of Pharmaceutics 585. https://doi.org/10.1016/j.ijpharm.2020.119425.

Gazzaniga, Andrea, Anastasia Foppoli, Matteo Cerea, Luca Palugan, Micol Cirilli, Moutaharrik Saliha, Alice Melocchi, and Alessandra Maroni. 2023. "Towards 4D Printing in Pharmaceutics." International Journal of Pharmaceutics: X 5. https://doi.org/10.1016/j.ijpx.2023.100171.

Hoffman, Amnon, David Stepensky, Eran Lavy, Sara Eyal, Eytan Klausner, and Michael Friedman. 2004. "Pharmacokinetic and Pharmacodynamic Aspects of Gastroretentive Dosage Forms." International Journal of Pharmaceutics 277 (1–2): 141–53. https://doi.org/10.1016/J.IJPHARM.2003.09.047.

Ibrahim, Mohamed, Youssef W Naguib, Hatem A. Sarhan, and Hamdy Abdelkader. 2019. “Gastro-Retentive Oral Drug Delivery Systems: A Promising Approach for Narrow Absorption Window Drugs.” Journal of Advanced Biomedical and Pharmaceutical Sciences 2: 98–110. https://doi.org/10.21608/jabps.2019.11357.1042.

Klausner, Eytan A., Eran Lavy, Michael Friedman, and Amnon Hoffman. 2003. “Expandable Gastroretentive Dosage Forms.” Journal of Controlled Release 90: 143–62. https://doi.org/10.1016/S0168-3659(03)00203-7.

Kumar, Manoj, and Deepak Kaushik. 2018. “An Overview on Various Approaches and Recent Patents on Gastroretentive Drug Delivery Systems.” Recent Patents on Drug Delivery & Formulation 12 (2): 84–92. https://doi.org/10.2174/1872211312666180308150218.

Laulicht, Bryan, Anubhav Tripathi, Vincent Schlageter, Pavel Kucera, and Edith Mathiowitz. 2010. “Understanding Gastric Forces Calculatedfrom High-Resolution Pill Tracking.” Proceedings of the National Academy of Sciences 107 (18). https://doi.org/www.pnas.org/cgi/doi/10.1073/pnas.1002292107.

Lopes, Carla M., Catarina Bettencourt, Alessandra Rossi, Francesca Buttini, and Pedro Barata. 2016. “Overview on Gastroretentive Drug Delivery Systems for Improving Drug Bioavailability.” International Journal of Pharmaceutics 510 (1): 144–58. https://doi.org/10.1016/j.ijpharm.2016.05.016.

Maroni, Alessandra, Alice Melocchi, Lucia Zema, Anastasia Foppoli, and Andrea Gazzaniga. 2020a. “Retentive Drug Delivery Systems Based on Shape Memory Materials.” Journal of Applied Polymer Science 137 (25): 1–10. https://doi.org/10.1002/app.48798.

Neumann, Marco, Claudia Heimhardt, Knut Seidlitz, Mirko Koziolek, Felix Schneider, Christiane Schiller, Ulrike Hanke, et al. 2021. “Development of a Furosemide-Containing Expandable System for Gastric Retention.” Journal of

Controlled Release 338 (October): 105–18. https://doi.org/10.1016/j.jconrel.2021.08.026.

Neumann, Marco, Felix Schneider, Mirko Koziolek, Grzegorz Garbacz, and Werner Weitschies. 2017. “A Novel Mechanical Antrum Model for the Prediction of the Gastroretentive Potential of Dosage Forms.” International Journal of Pharmaceutics 530 (1–2): 63–70. https://doi.org/10.1016/j.ijpharm.2017.07.067.

Palugan, Luca, Matteo Cerea, Micol Cirilli, Saliha Moutaharrik, Alessandra Maroni, Lucia Zema, Alice Melocchi, et al. 2021. “Intravesical Drug Delivery Approaches for Improved Therapy of Urinary Bladder Diseases.” International Journal of Pharmaceutics: X 3.

Palugan, Luca, Ilaria Filippin, Micol Cirilli, Saliha Moutaharrik, Lucia Zema, Matteo Cerea, Alessandra Maroni, Anastasia Foppoli, and Andrea Gazzaniga. 2021. “Cellulase as an ‘Active’ Excipient in Prolonged-Release HPMC Matrices: A Novel Strategy towards Zero-Order Release Kinetics.” International Journal of Pharmaceutics. https://doi.org/10.1016/j.ijpharm.2021.121005.

Palugan, Luca, Ilaria Filippin, Micol Cirilli, Moutaharrik Saliha, Lucia Zema, Matteo Cerea, Alessandra Maroni, Anastasia Foppoli, and Andrea Gazzaniga. 2021. “Cellulase as an ‘Active’ Excipient in Prolonged-Release HPMC Matrices: A Novel Strategy towards Zero-Order Release Kinetics.” International Journal of Pharmaceutics 607. https://doi.org/10.1016/j.ijpharm.2021.121005.

Paquin, Allison M., Kristin M. Zimmerman, Tia R. Kostas, L. Pelletier, Angela Hwang, Mark Simone, Lara M. Skarf, and James L. Rudolph. 2013. “Complexity Perplexity: A Systematic Review to Describe the Measurement of Medication Regimen Complexity.” Expert Opinion Drug Safety 12 (6): 829–40. https://doi.org/10.1517/14740338.2013.823944.

Pawar, Vivek K, Shaswat Kansal, Shalini Asthana, and Manish K Chourasia. 2012. “Industrial Perspective of Gastroretentive Drug Delivery Systems: Physicochemical, Biopharmaceutical, Technological and Regulatory

Consideration." Expert Opinion on Drug Delivery 9 (5): 551–65. https://doi.org/10.1517/17425247.2012.677431.

Prinderre, Pascal, Christophe Sauzet, and Claus Fuxen. 2011. "Advances in Gastro Retentive Drug-Delivery Systems." Expert Opinion on Drug Delivery 8 (9): 1189–1203. https://doi.org/10.1517/17425247.2011.592828.

Schneider, Felix, Regine Beeck, Melanie Hoppe, Mirko Koziolek, and Werner Weitschies. 2017. "In Vitro Simulation of Realistic Gastric Pressure Profiles." European Journal of Pharmaceutical Sciences 107 (September): 71–77. https://doi.org/10.1016/j.ejps.2017.06.037.

Schneider, Felix, Melanie Hoppe, Mirko Koziolek, and Werner Weitschies. 2018. "Influence of Postprandial Intragastric Pressures on Drug Release from Gastroretentive Dosage Forms." AAPS PharmSciTech 19 (7): 2843–50. https://doi.org/10.1208/s12249-018-1022-3.

Schneider, Koziolek, and Weitschies. 2019. "In Vitro and In Vivo Test Methods for the Evaluation of Gastroretentive Dosage Forms." Pharmaceutics 11 (8): 416. https://doi.org/10.3390/pharmaceutics11080416.

Standard Test Methods for Flexural Properties of Unreinforced and Reinforced Plastics and Electrical Insulating Materials. ASTM D790. Annual Book of ASTM Standards. 1997. Vol. ASTM, S. Book. https://www.astm.org/standards/d790.

Stockwell Morris, L., and R. M. Schulz. 1992. "Patient Compliance - an Overview." Journal of Clinical Pharmacy and Therapeutics 17: 283–95. https://doi.org/10.1111/j.1365-2710.1992.tb01306.x.

Streubel, Alexander, Juergen Siepmann, and Roland Bodmeier. 2006. "Gastroretentive Drug Delivery Systems." Expert Opinion on Drug Delivery 3 (2): 217–33. https://doi.org/10.1517/17425247.3.2.217.

Supratim, Das, Kaur Sukhbir, and Kumar Rai Vineet. 2021. "Gastroretentive Drug Delivery Systems: A Recent Update on Clinical Pertinence and Drug Delivery."

Drug Delivery and Translational Research 11: 1849–77. https://doi.org/http://doi.org/10.1007/s13346-020-00875-5.

Tripathi, Julu, Prakash Thapa, Ravi Maharjan, and Seong Hoon Jeong. 2019. “Current State and Future Perspectives on Gastroretentive Drug Delivery Systems.” Pharmaceutics 11 (4). https://doi.org/10.3390/pharmaceutics11040193.

Uboldi, Marco, Alice Melocchi, Saliha Moutaharrik, Luca, Palugan, Matteo Cerea, Anastasia Foppoli, Alessandra Maroni, Andrea Gazzaniga, and Lucia Zema. 2022. “Administration Strategies and Smart Devices for Drug Release in Specific Sites of the Upper GI Tract.” Journal of Controlled Release 348: 537–52. https://doi.org/HTTPS://doi.org/10.1016/j.jconrel.2022.06.005.

Venkata Pavan, M., K. Balamurugan, and T.P. Latchoumi. 2021. “PLA-Cu Reinforced Composite Filament: Preparation and Flexural Property Printed at Different Machine Conditions.” Advanced Composite Materials. https://doi.org/10.1080/09243046.2021.1918608.

Vrettos, Napoleon Nikolaos, Clive J. Roberts, and Zheying Zhu. 2021. “Gastroretentive Technologies in Tandem with Controlled-Release Strategies: A Potent Answer to Oral Drug Bioavailability and Patient Compliance Implications.” Pharmaceutics. MDPI. https://doi.org/10.3390/pharmaceutics13101591.

Williams, Bryan, Giuseppe Mancia, Wilko Spiering, Enrico Agabiti Rosei, Michel Azizi, Michel Burnier, Denis L Clement, et al. 2018. “2018 ESC/ESH Guidelines for the Management of Arterial Hypertension.” European Heart Journal 39 (33): 3021–3104. https://doi.org/10.1093/eurheartj/ehy339.

Zacchè, Martino Maria, Sushma Srikrishna, and Linda Cardozo. 2015. “Novel Targeted Bladder Drug-Delivery Systems: A Review.” Research and Reports in Urology 7: 169–78. https://doi.org/10.2147/RRU.S56168.

Chapter 5

Gastroretentive systems for prolonged release of metformin based on osmotically driven expansion

To be submitted for publication

§ The contribution given by Micol Cirilli to the work associated with published article was conceptualization, methodology, formal analysis, validation, investigation, writing – original draft, visualization.

ABSTRACT

Metformin is a relatively old drug used mainly to treat type 2 and gestational diabetes, which needs to be administered two or three times a day in high doses, having high solubility and poor absorption in distal intestine. Aiming at preparing a gastroretentive formulation for prolonged release of metformin, an expandable device based on osmotically-driven mechanism was developed. The system is composed of an expandable compartment obtained from tubular dialysis membranes filled with an osmotic agent linked to hydrophilic matrices containing metformin. Different expanding devices were prepared using dialysis membranes having different cut-off (3.5-5 and 12-14 kD) and by filling sodium chloride or mannitol. Prolonged drug release was obtained using metformin granulated with ethylcellulose and tableted with hypromellose K15M in multilayered matrices with drug-free external layers. The assembled devices were loaded into a hard-gelatine capsules suitable for oral ingestion and when in contact with aqueous fluids rapidly expanded thanks to the osmotic influx leading to an overall enlargement that might prevent transit through the pylorus when administered in vivo. Since the device was prepared with hydrophilic polymers, metformin-containing units dissolved and/or eroded, while the semipermeable tubes detached and shrank allowing for physiological expulsion of the device.

KEYWORDS

Gastro-retentive delivery systems

Osmotic delivery systems

Prolonged release

Hydrophilic matrix

Metformin

1. INTRODUCTION

Type 1 diabetes mellitus (T1DM), also known as autoimmune diabetes, is a chronic disease characterized by insulin deficiency due to pancreatic β-cell loss and leads to hyperglycemia [Katsarou, 2017]. 5% to 10% of the world population is affected by T1DM while Type 2 diabetes mellitus (T2DM) accounts for around 90% of all cases of diabetes. People affected by T2DM develop a condition defined as insulin resistance. During this state, insulin is ineffective and initially its secretion increases to maintain glucose homeostasis and overcome the reduced response to insulin, but over time decreases resulting in T2DM [Goyal, 2018].

Due to the increasing prevalence of T2DM, the development of many new approaches to safely treat hyperglycemia is of great interest. Especially, treatment of T2DM has focused on increasing insulin levels, either by direct insulin administration or oral agents that can promote insulin secretion), on improving tissue sensitivity, such as with insulin sensitizer biguanide metformin or thiazolidinediones, or on reducing the rate of carbohydrate absorption from the gastrointestinal tract by the use of a-glucosidase inhibitors or agents that decrease gastric motility [Israili,2011].

Focusing on T2DM, metformin is one of the most popular oral glucose-lowering medications, and it is widely considered to be the optimal initial therapy [Sanchez-Rangel,2017]. This drug, also indicated for polycystic ovary syndrome, is mostly administered orally with an immediate-release profile, which leads to an absorbance of approximately 60-70% of the dose from the small intestine, due to narrow absorption window confined to the small intestine with negligible absorption in the stomach or large intestine. Metformin is excreted in urine unchanged, with no metabolites reported [Rena, 2017, Kumar, 2012]. Metformin's efficacy is dose-dependent with the minimal efficacious dose being 500 mg daily and maximal efficacy being 2000 mg daily [Sanchez-Range, 2017, Garber, 1997]. Metformin uptake is saturable and dose-dependent, consistent with the theory that it is mostly transporter-dependent McCreight, 2016, Bonnet, 2017].

Orally administered immediate release dosage forms of metformin have shown to frequently cause GI adverse events (AEs) including diarrhea, nausea, flatulence, indigestion, vomiting, and abdominal discomfort. Those metformin-induced collateral effects clearly have a bad impact on quality of life and compliance to the therapy in patients with T2DM [Bonnet, 2017]. Side effects mainly occur when high doses of the drug are administered in a conventional mode, leading to local high concentrations and appeared to be less severe and better tolerated when patients were administered with sustained drug release compositions (Feher, 2007]. The delivery of metformin by systems capable of remaining in the stomach for a long time are expected to introduce great advantages in combination with a prolonged release mode of the drug. (Corti, 2008], Zhao, 2012, Wadher, 2011]. To date various products containing metformin for prolonged release are available on the market. Among these, Glocophage® XR and Glumetza® are based on hydrophilic matrix system [FDA1] and Fortamet® uses a more traditional osmotic technology [FDA3, Guo 2021, Sun 2022].

Different approaches have been proposed in the literature for obtaining gastroretentive systems such as bioadhesion, buoyancy and size enlargement [Palugan 2021, Tripathi 2019]. In particular, the latter approach consists of a small-sized dosage form able to increase its dimension after oral administration in order to prevent early emptying from the stomach [Streubel 2006, Lopes 2016, Uboldi 2022, Altereuter 2018]. Dimensions need to reduce after the drug is completely released so that the system can be physiologically expelled from the organ [Maroni 2020, Gazzaniga 2023]. Many strategies and mechanisms of size enlargement have been proposed and, among them, an osmotically driven expansion was recently presented [Cirilli 2023]. The Organ-Retentive Osmotically Driven Systems (ORODSs) were previously described as device intended for stomach and urinary bladder retention, having the required characteristics of dimensions, stiffness and biodegradability. Moreover, thanks to ORODS design, this approach appeared able to increase its spatial encumbrance once in contact with fluids, eventually reducing its dimensions after having released the drug. In this work, according to the need of improved therapies for diabetes, ORODSs

have been further evaluated in terms of mechanism of expansion, types of dialysis membrane and osmotic agent type and amount, for prolonged release of metformin.

2. EXPERIMENTALS

2.1 Materials

Dialysis tubular membrane made of regenerated cellulose having a cut-off of 3.5-5.0 and 12–14 kD (Spectrum Labs™ Repligen, Spectra/Por™ 2, CA, USA); sodium chloride (NaCl, water solubility 360 mg/mL at 37 °C), mannitol (Mannogem XL®, SPI Pharma, USA) potassium chloride (KCl), hydrochloric acid 37% (HCl) (VWR International S.r.l., IT); hydrochloride metformin (Metapharmaceutical, ES); microcrystalline cellulose (MCC, Avicel® PH 200, FMC, BE); hypromellose (Methocel® K15M, Colorcon, UK); ethylcellulose (Ethocel®, Colorcon, UK); ethanol 96% (VWR Chemicals). Hard gelatin capsules (Capsugel® ConiSnap® Size 00, Lonza, BE); acrylic glue (Loctite, DE).

2.2 Methods

2.2.1 Osmotic unit preparation

The osmotic units (average diameter and flat width of 6.4 mm and 10 mm, respectively, and length of 45 mm) were obtained by loading 75, 150 or 300 mg of sodium chloride or mannitol as the osmotic agent. The units were sealed with methacrylic glue.

2.2.2 Evaluation of fluid inflow into isolated osmotic unit

Fluid inflow was evaluated by placing isolated osmotic units in deionized water (800 mL, 37.0 ± 0.5 °C) and USP 44 hydrochloric acid buffer pH 1.2 (HCl 37% 7.07 mL/L, KCl 3.727 g/L), measuring their diameter (n = 3, 5 different positions) at established time points using a digital caliper (Absolute Digimatic CD-15CP, Mitutoyo, UK) and calculating the corresponding volume of the tubes. Samples were gently blotted with a paper tissue before measurement.

$V = \text{height} \times \pi \times ab$ eq. 1

2.2.3 Residual osmotic agent content evaluation

Osmotic units (n = 3) containing 50 mg of sodium chloride or mannitol were placed in deionized water and in USP 44 hydrochloric acid buffer pH 1.2 (800 mL, 37.0 ± 0.5 °C). At pre-established timepoints the osmotic units were removed from the fluid and dried for 24 h in a static oven at 40 °C. The percentage of residual amount of osmotic agent was calculated according to equation eq. 2.

$Rt\ (\%) = [50\ mg - (M_0 - M_t)]\ /50\ mg \times 100$ eq. 2

R_t: Percentage of residual osmotic agent at time t

Mo: initial mass of osmotic agent

Mt: mass of osmotic agent at time t

2.2.4 Mechanical testing of isolated osmotic units

Mechanical testing of isolated osmotic units was performed adapting the standard test method for flexural properties of unreinforced and reinforced plastics and electrical insulating materials American Standard Testing Material (ASTM) D790 (Venkata Pavan et al., 2022, ASTM D790. Annual Book of ASTM Standards, 1997). The test was carried out using a TA-XT2 analyzer (Texture Technologies, Hamilton, MA,USA) equipped with a three-point bend fixture (support span of 22 mm, support cylindrical rods and nose of 2 mm in diameter, 50 N load cell) and software for analyzing displacement and load (Fig. 1). Operational parameters of the test were 7 mm maximum displacement at 2 mm/min rate of displacement. Force-displacement and strain–stress profiles were acquired after immersion of the isolated osmotic units in 800 mL distilled water and USP 44 hydrochloric acid buffer pH 1.2 at 37 °C for 24 h (n = 3). Samples were gently blotted with a paper tissue before measurement.

2.2.5 Metformin hydrophilic matrices preparation

Hydrophilic matrices were obtained by tableting (Tablet press FA/8, Officine Ronchi, IT) at compaction force of approximately 10-15 kN, using 20x8 mm punches, being one concave and one flat for tablets delivering 250 mg drug (Met250), and both concave punches for tablets with 500 mg drug (Met500). Metformin was granulated with ethylcellulose solution in acetone (10% w/w) in mortar. 10 mL of solution were used for wetting 100 g drug powder for the preparation of Met250/GR and Met500/GR matrices. The wet mass was forced through a sieve having 0.750 mm opening mesh and the granules were dried in a static oven at 40°C for 12 hours. The composition of the granulate is reported in Tab.1.

Tab. 1 Composition of metformin granules used for obtaining Met250/GR and Met500/GR matrices.

Component	% (w/w)
Metformin	71,5
Ethylcellulose	28,5
Total	100,0

Tablets were prepared using powder mixtures described in Tab. 2. The tableted matrices were perforated (elliptical opening of 5.0x1.5 mm) by a precision driller (Proxxon, DE). Schematic diagrams of tablets prepared with different set of tableting punches for obtaining flat faced tablets (Met250) and double convex tablets (Met500), and corresponding multilayered tablets presenting one or two external drug-free layers are reported in Fig.1. External drug-free layers were prepared with 60, 80 or 100 mg of HPMC K15M or ethylcellulose by multiple compressions.

Tab. 2. Compositions of hydrophilic matrices prepared by tableting single or multiple layers.

Code	Metformin layer	External drug free layer 1	External drug free layer 2
Met250 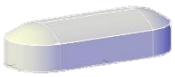	Metformin 50% HPMC K15M 30% Dicalcium phosphate 19% MgSt 1%	x	x
Met250/GR 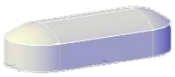	Metformin 49,5% HPMC K15M 29,7% Ethylcellulose 19,8% MgSt 1.0%	x	x
Met250-80H 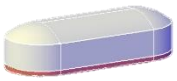	Metformin 50% HPMC K15M 30% Dicalcium phosphate 19% MgSt 1%	HPMC K15M 80 mg	x
Met250/GR-80H 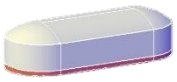	Metformin 49,5 % Ethylcellulose 19,8 % HPMC K15M 29.7% MgSt 1%	HPMC K15M 80 mg	x
Met250-80H-80H 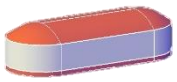	Metformin 50% HPMC K15M 30% Dicalcium phosphate 19% MgSt 1%	HPMC K15M 80 mg	HPMC K15M 80 mg
Met250/GR-80H-80H 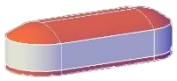	Metformin 49,5 % Ethylcellulose 19,8 % HPMC K15M 29,7% MgSt 1%	HPMC K15M 80 mg	HPMC K15M 80 mg
Met500 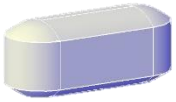	Metformin 50% HPMC K15M 30% dicalcium phosphate 19,8% MgSt 1%	x	x
Met500/GR 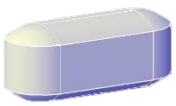	Metformin 49,5 % Ethylcellulose 19,8 % HPMC K15M 29,7% MgSt 1%	x	x

Met500-80H 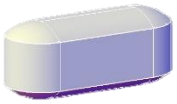	Metformin 50% HPMC K15M 30% dicalcium phosphate 19,8% MgSt 1%	HPMC K15M 80 mg	x
Met500/GR-80H 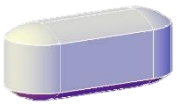	Metformin 49,5 % Ethylcellulose 19,8 % HPMC K15M 29,7% MgSt 1%	HPMC K15M 80 mg	x
Met500-80H-80H 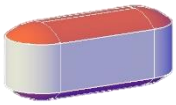	Metformin 50% HPMC K15M 30% dicalcium phosphate 19,8% MgSt 1%	HPMC K15M 80 mg	HPMC K15M 80 mg
Met500/GR-80H-80H 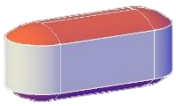	Metformin 49,5 % Ethylcellulose 19,8 % HPMC K15M 29,7% MgSt 1%	HPMC K15M 80 mg	HPMC K15M 80 mg

2.2.6 Drug release testing

ORODS-containing capsules were evaluated for drug release in a USP 40 paddle dissolution apparatus (At7 Smart, Sotax, Basel, CH; 100 rpm, 900 mL deionized water or USP 44 hydrochloric acid buffer pH 1.2, 37.0 ± 0.5 °C). Metformin was quantified spectrophotometrically (Lambda 35, Perkin Elmer Italia, IT; 234 nm, 1 mm cuvette) in fluid samples withdrawn at successive time points.

2.2.7 Gastric-retentive system preparation

The prototypes were fabricated by manually inserting and gluing a tube made of regenerated cellulose (osmotic unit) in circular shape into the through holes of 2 perforated hydrophilic matrices (Met250) or one hydrophilic matrix tablet (Met500) for obtaining ring-shaped ORODS type A or typeB, respectively (Fig. 2). The assembled devices were gently folded by hand and inserted into hard-gelatin capsules size 00.

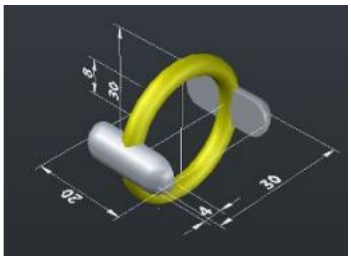

Ring-shaped ORODS Type A

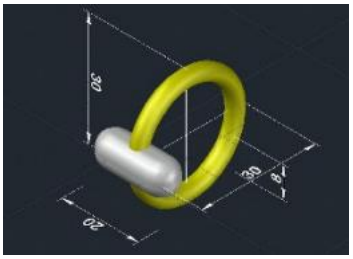

Ring-shaped ORODS Type B

Fig. 1. Schematic diagrams of ring-shaped ORODS and two (type A, left) or with one (type B, right) hydrophilic matrices.

2.2.8 Gastric-retentive system opening test

The prototypes, inserted into hard-gelatin capsules, were placed into vessels of a dissolution apparatus (At7 Smart, Sotax, Basel, CH) containing 900 ml of deionized water at 37°C with a stirring of 100 rpm. Time was measured until the capsule was dissolved and until the system reached his final dimensions. DDS were measured by a digital caliper before immersion, in space saving configuration (i.e. capsule dimensions) and when reaching their maximum expansion.

3. RESULTS AND DISCUSSION

ORODSs were prepared with the purpose of having a gastro retentive system having a sustained release of metformin, therefore, osmotically driven expansion from osmotic units and drug release rate from drug containing hydrophilic matrices, were studied before the system was assembled.

Two materials exhibiting high osmotic pressure when in solution and different physical-chemical properties were chosen to assess their behavior when loaded into the osmotic units: sodium chloride being electrolyte and having a Mw = 58,44 g/mol with a solubility of 36 g/100 ml in water, and mannitol not being electrolyte and with a Mw = 182,17 g/mol, solubility of 21,6 g/100 ml in water, were considered. 75, 150 and 300 mg of osmotic agent were filled into the osmotic units in order to evaluate the water influx rate and mechanical properties of

expanding compartments when immersed in deionized water or acidic buffer. Also, two different dialysis membrane types having 3.5-5 kD and 12-14 kD cut-off, respectively were tested to consider the influence of the membrane on the osmotic unit behavior.

3.1 Evaluation of leakage of osmotic agent from the osmotic unit .

Leakage of osmotic agent from osmotic units was calculated by the residual amount of solid remained in the tubes over time after immersion in water and pH 1.2 buffer for 3 hours. Results demonstrated that mannitol was retained in the osmotic units for longer time than sodium chloride. In the graphs reported in Fig. 3 almost the total amount of sodium chloride left the osmotic unit in approximately one hour after the immersion in the fluids, while for mannitol the outflow appears to be slower, especially in the case of osmotic units made of cellulosic membrane having a cut-off of 12-14 kD. For these membranes, a considerable amount of mannitol was still present in the tubes after more than 3 h of immersion, while residual sodium chloride in the osmotic units was less than 20%. A higher leaching rate of osmotic agent was observed for units made with the membrane having a smaller cut-off (3.5-5 kD), probably because porosity was not a limiting factor for the outflow of such small molecules, and probably the thickness of the membrane, higher for the 12-14 kD membrane, lead to a slower leakage of the osmotic agents.

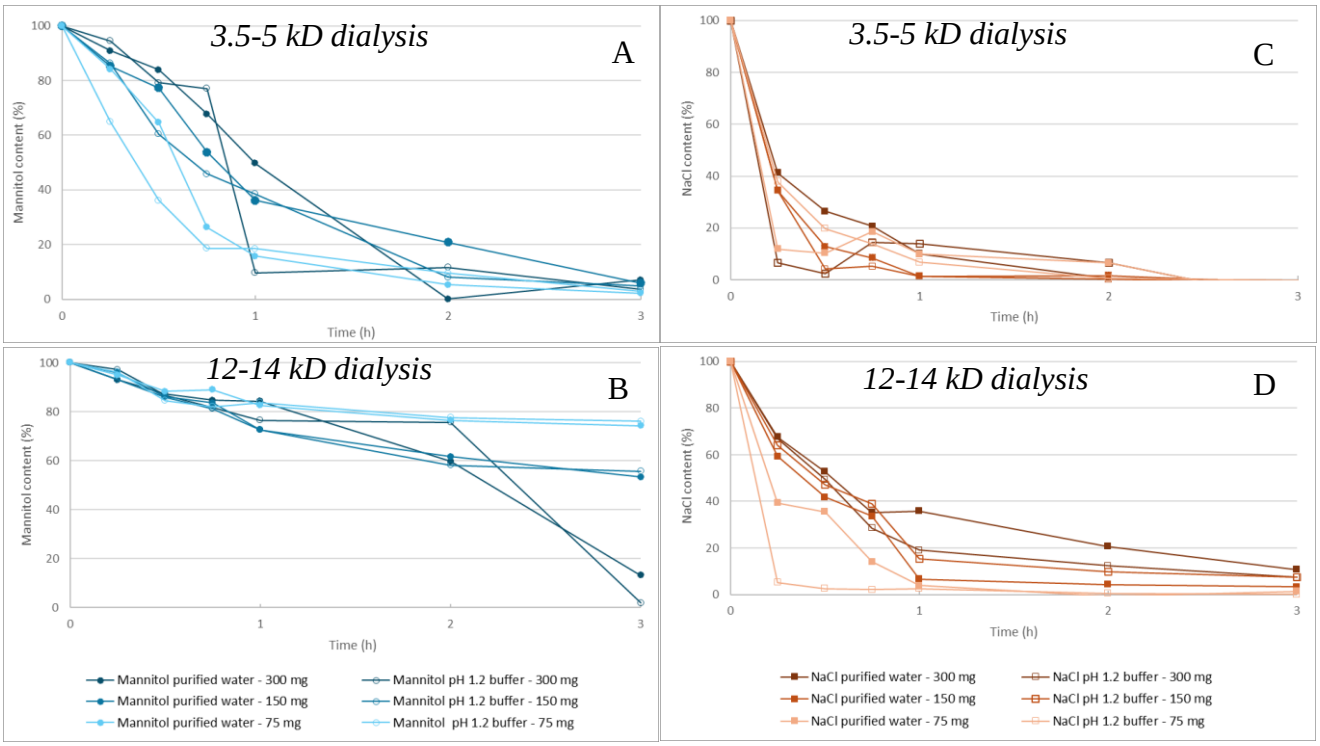

Fig. 3 Mean residual amount of sodium chloride and mannitol in isolated osmotic units immersed in deionized water or hydrochloric acid buffer pH 1.2. Graphs A and B are related to mannitol where A concerns osmotic units made of dialysis membrane having a cut-off of 3.5-5 kD and B made of dialysis membrane with a cut-off of 12-14 kD. Graphs C and D are related to units containing sodium chloride and made of dialysis membranes having cut-off of 3.5-5 kD in case of C and 12-14 kD in case of D.

3.2 Volume increase of osmotic units

Volume increase of osmotic units caused by fluids inflow into the isolated tubular membrane was evaluated by measuring the expansion in diameter after immersion in aqueous fluids. Depending on the type and amount of osmotic agent loaded and cut-off of the membrane, the expansion was expressed as percentage of the maximum volume. Results showed that, independently from osmotic agent, volume increase reached the highest values in approximately 1 h either when using 3.5-5 kD cut off membrane or the one with 12-14 kD cut off. The expansion of the tube was proportional to the amount of sodium chloride or mannitol used, both in water and in pH 1.2 buffer. Note that the initial measurements were influenced by the volume occupied by the loaded osmotic agent. From the graphs it is possible to observe that 300 mg osmotic agent allowed the unit to be filled to

almost 100% of the volume, while 150 mg and 75 of material led to a lower volume increase. The maximum expansion values reached for lower amounts of sodium chloride (75 and 150 mg) when using 12-14 kD cut-off membranes resulted smaller than those observed for mannitol. The lower solubility of mannitol might help in maintaining a higher amount of osmotic agent in the tube for longer time and to reach a bigger volume compared to the salt, which tended to diffuse out in a faster mode. These results are in accordance with residual amount of osmotic agent data. In general, it can be observed that the volume of tubes loaded with highest amount of osmotic agent tended to slowly decrease over time reducing the sized of approximately 20% over 24 h, with faster reduction rates for sodium chloride. All of the graphs show that no important difference was detected in the behavior of the osmotic units when tested in purified water and in pH 1.2 buffer. It also need to be noted that, since mannitol has a lower density it occupied a bigger volume when loaded inside the dry units compared to sodium chloride. Therefore if considering volume increase of the unit with respect to the time zero, sodium chloride expressed a higher ability to increase osmotic unit volume. For instance, considering units containing 300 mg of osmotic agent, those containing mannitol approximately doubled their volume to reach the maximum, while those loaded with sodium chloride tripled their volume from almost 30% of the maximum volume up to 100%.

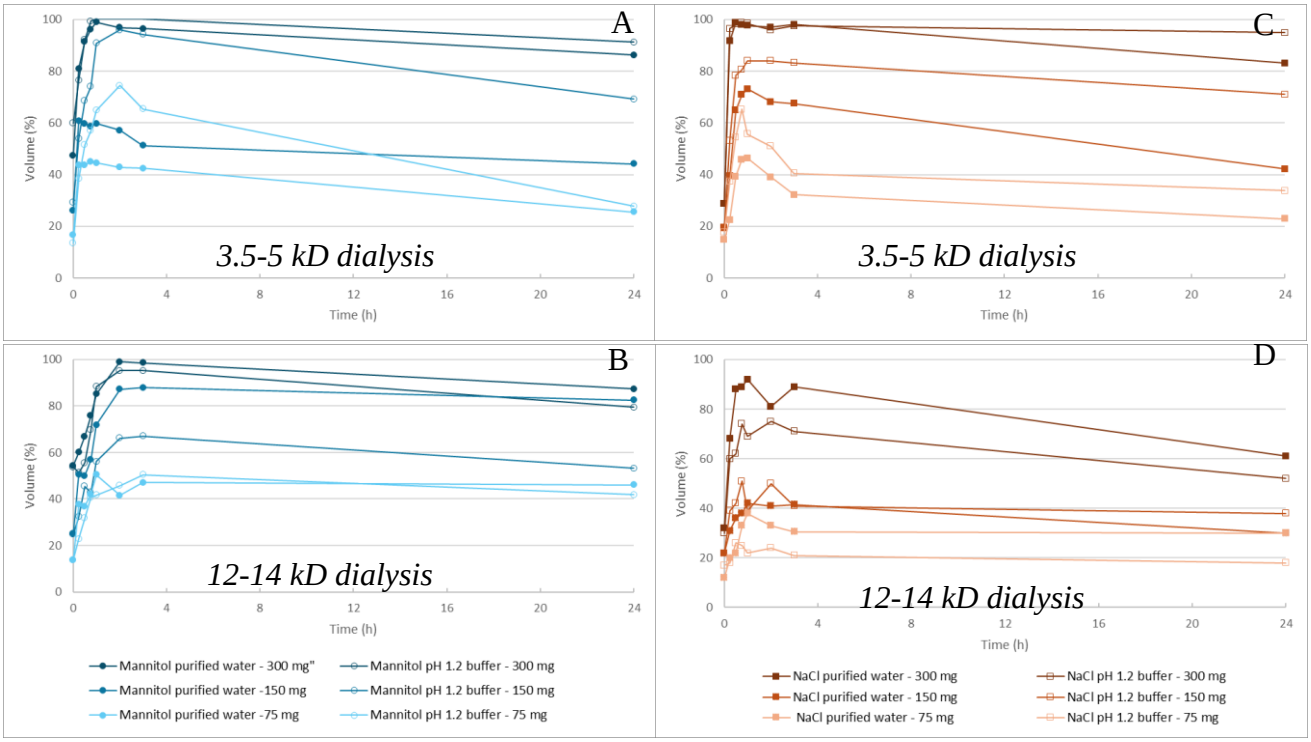

Fig. 4 Mean volume vs. time profiles for isolated osmotic units of H-shaped ORODSs immersed in deionized water and hydrochloric acid buffer pH 1.2 (n = 3). A and B show profiles of units containing mannitol, A shows results of units made of dialysis membrane having a cut-off of 3.5-5 kD while B having a cut-off of 12-14 kD. Graphs C and D are related to units loaded with sodium chloride with C having units made of dialysis membranes having a cut-off of 3.5-5 kD while D having a cut-off of 12-14 kD.

.

3.3 Mechanical resistance of osmotic units

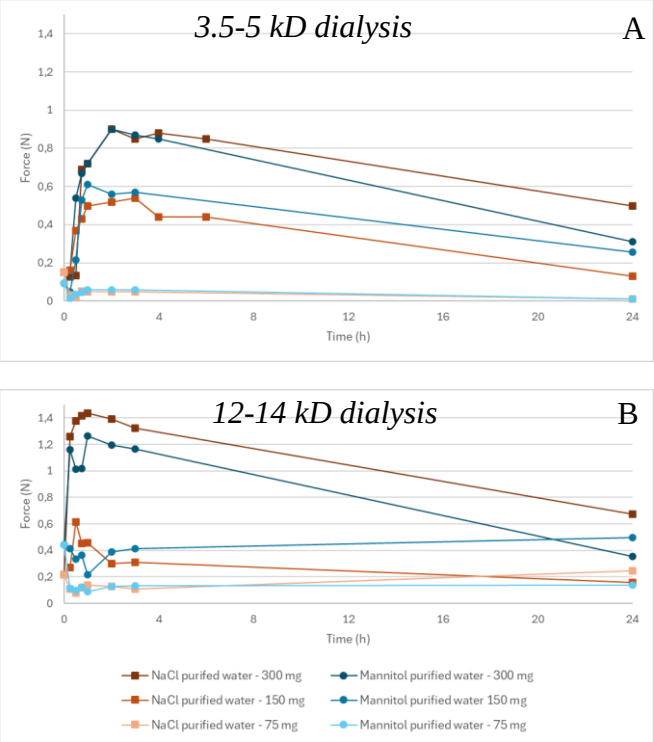

Fig. 5 Force vs time profiles for isolated osmotic units immersed in deionized water (or hydrochloric acid buffer) with a displacement of 7 mm at 2 mm/min rate of displacement. Graph A shows results obtained by testing osmotic units made of dialysis membrane having cut off 3.5-5 kD while graph B is about osmotic units made of the membrane having cut off of 12-14 kD.

To assess whether the volume increase of the osmotic unit was followed by a different mechanical strength, the isolated tubes loaded with different amounts of mannitol or sodium chloride were tested for flexural resistance after incubation in water/HCl over time. The mechanical properties of isolated osmotic units were evaluated after immersion in water for different times. The graphs depicted in Fig. 5, show that osmotic units prepared with the cellulosic membrane having a cut-off of 3.5-5 kD were weaker than those having a cut-off of 12-14 kD. Regardless the permeability of the dialysis tubes, this behavior can be attributed to the thinner thickness of the membrane having smaller cuf-off. The membrane with a 3.5-5 kD cut-off presented an average thickness of 0.08 mm when dry and 0.1 mm when hydrated, while the membrane with 12-14 kD cut-off has an average thickness of 0.2 mm when dry and 0.3 mm when hydrated. The different thickness of the two membranes causes a different resistance the thicker one showing a

force of 0,44 N and the thinner one of 0,15 N, measured before hydration. Since membrane texture can have an impact on the mechanical resistance/behavior of the osmotic unit, this can possibly lead to the possibility to modulate unit strength not only by loading different amounts and types of osmotic agents but also by selecting different kind of commercial membranes or by producing tailor made ones.

3.4 Prolonged release tablets containing metformin.

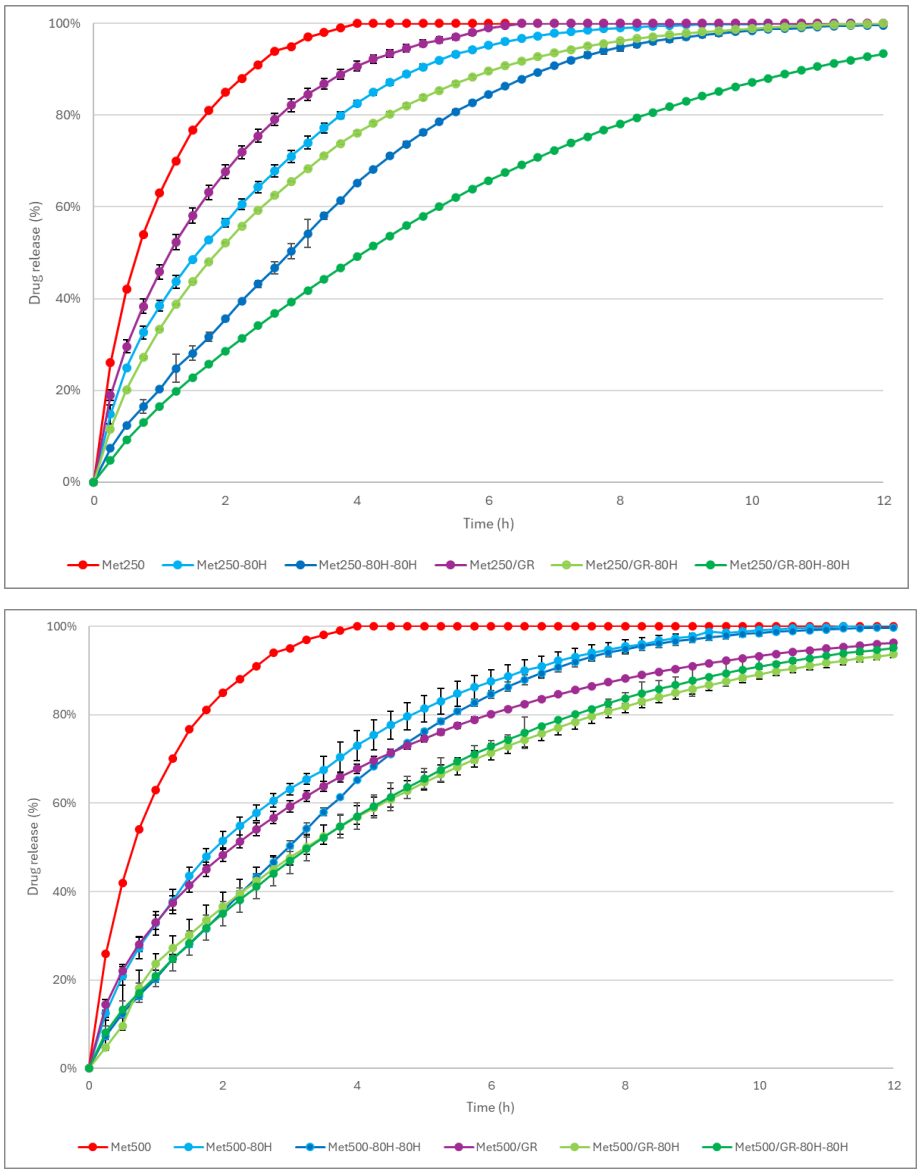

Fig. 6. Mean release profiles of metformin from hydrophilic matrices without and with drug-free layers tested in hydrochloric acid buffer pH 1.2 (n = 3, vertical bars represent standard deviation)

Matrices with different punches-sets were prepared to design the final system with one tablet delivering the full dose of 500 mg metformin (Met500) or two “half tablets” containing each half of the dose (Met250). Hydrophilic matrices are a robust and flexible dosage forms for controlling drug release. Being soluble and erodible, hydrophilic matrices have the great advantage of being able to be emptied form the stomach physiologically and without any external intervention. Hypromellose type K15M was chosen among the other hydrophilic polymers since it offers adequate tableting properties, acceptable flowability, pH independent behavior and good modulation of drug release. Tablets were prepared by tableting the mixture of the drug with , a diluent, calcium phosphate dibasic and a lubricant magnesium stearate.

Aiming at obtaining a prolonged drug release of metformin for at least 6 h, multi-layer tablets were prepared having one or two external drug-free layers that could further reduce the interaction area of the hydrophilic matrix with the solvent. Multi-layer tablets were prepared both for the 250 and 500 mg dose of metformin. The drug-free layer was prepared with ethylcellulose or with hypromellose. The minimum amount of material necessary to prepare complete tableted layers was selected by preparing multi-layered tablets using increasing amounts of powders mixtures (60-80-100 mg) added with red dye. The amount of 60 mg of drug-free layer was discarded for being uncapable of covering homogeneously the entire top or bottom surface of the tablets, and 80 mg of material was selected.

In order to further reduce the release rate of metformin from the hydrophilic matrices, a wet granulation process of the drug with ethylcellulose, an insoluble film forming polymer, was carried out with the intention of partially coating the drug surface and thus reducing the dissolution area (Met250/GR and Met500/GR). Compared to matrices prepared with metformin powder, for those prepared with granulated drug the release rate resulted slowed, and in particular with 500 mg dose tablets. Based on the showed results, for the purpose of a prolonged drug release formulation, matrices having the two inert layers, both for the Met250/GR and for the Met500/GR s, appear to be to most promising ones. Release profiles reported in Fig. 5 showed that matrices prepared with granulated

metformin when loaed with 250 or 500 mg dose resulted in comparable release rates considering the same configuration in terms of number of drug-free layers or type of materials used. Matrices having two external drug-free layers made of 80 mg hypromellose K15M were selected since a not-significant difference was detected between the two amounts 80 and 100 mg in slowing down the drug release rate, both for matrices having Met250/GR and Met500/GR as a central layer, (for Met250/GR tablets: f2 = 81,86 for hypromellose and f2 = 96,61 for ethylcellulose, for Met500/GR tablets: f2 = 59,23 for Hypromellose and f2 = 63,12 for ethylcellulose). Since the central layer was mainly prepared with hypromellose, the same material was chosen for obtaining the external layers and thus creating a fully dissolvable matrix. Based on the showed results, for the purpose of a prolonged drug release formulation, matrices having the two inert layers, both for the Met250/GR and for the Met500/GR s, appear to be to most promising ones.

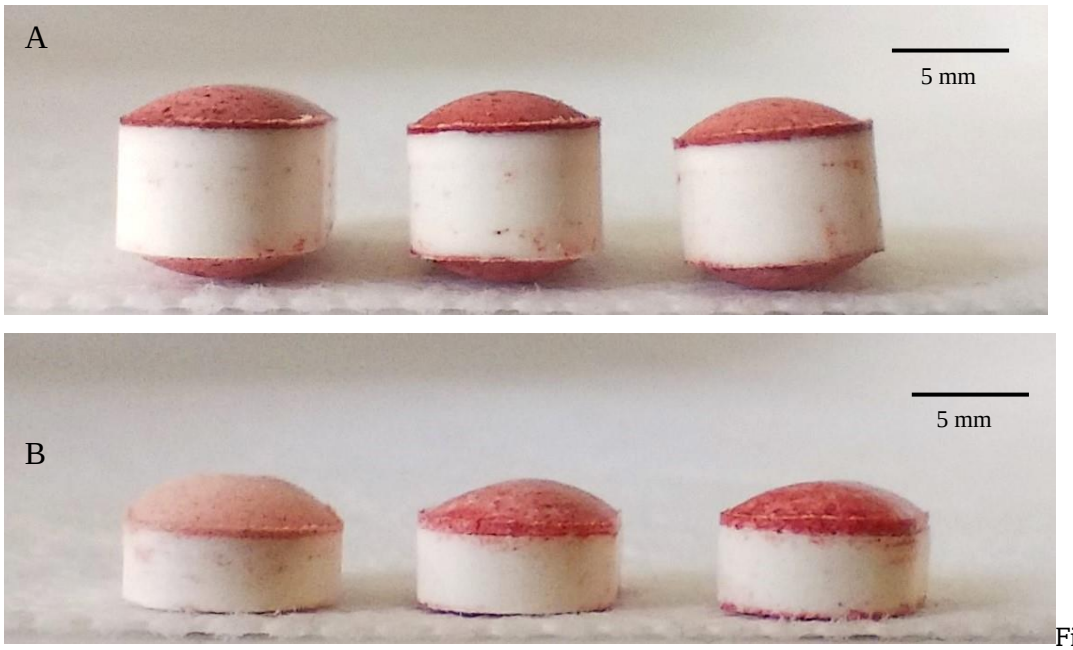

Fig. 7. Tablets with two external drug-free layers. Picture A: Met250/GR-60H-60H, Met250/GR-80H-80H and Met250/GR-100H-100H; picture B: Met500/GR-60H-60H, Met500/GR-80H-80H and Met500/GR-100H-100H

3.5 Assembled gastro-retentive systems.

The prototypes of ORODS gastro-retentive systems prepared for prolonged release of metformin and osmotic-controlled expansion were assembled with ring configurations using two matrices Met250/GR-80H-80H for type A and one matrix Met500/BR-80H-80H for type B (Fig. 8). For what concerns the osmotic units, the most promising types based on the results of mechanical test have been employed were dialysis tubes filled with 300 mg sodium chloride, which could resist 1.4 N compression force were selected. This mechanical resistance is in accordance with values reported by Bellinger et al. for withstanding gastric-peristaltic force during housekeeper waves.

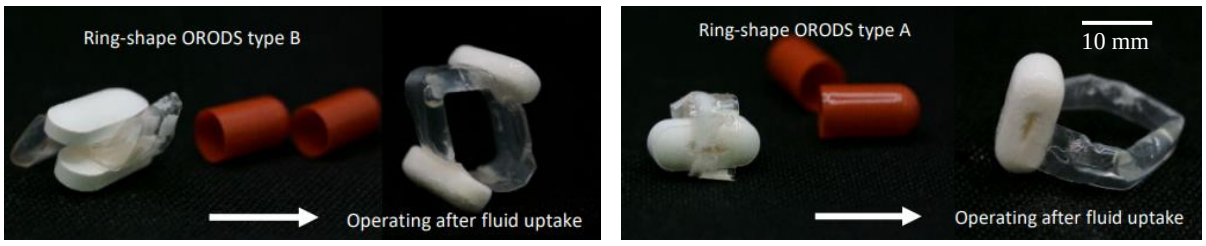

Fig. 8 Ring-shaped ORODS type A and type B prepared with Met250/GR-80H-80H and Met500/GR-80H-80H, respectively, and osmotic units prepared with dialysis membrane 12-14 kD filled with 300 mg sodium chloride in compacted (left) and in expanded configuration (right).

The system appeared to be able to open in approximately 4 min, when the capsule dissolved, and to reach after 20 min the maximum expansion configuration (Fig. 9). Dimensions reached, 30 mm length, 30 mm height and 20 mm depth are theoretically compatible with the gastric-retention, being bigger for at least two dimensions than the than the pylorus opening size (20 mm) (reference). After 24 h the systems appeared shrunk and smaller than 20 mm

4. CONCLUSIONS

In this work, ORODS components were studied and, particularly, osmotic units made of dialysis membrane having two different cut-off and containing sodium chloride or mannitol as osmotic agents were considered and impact in fluids inflow of the membrane and the agent was assessed also depending on the amount loaded into the units. Units were evaluated in water and in pH 1.2 (mimic of the gastric pH) in terms of volume increase, residual osmotic agent over time

and mechanical resistance over time. Based on the results of the mentioned parameters, it has been confirmed that no big difference between the two osmotic agents has been detected but a great impact has been attributed to the loaded quantities. Units containing the bigger amount, among the tested ones, resulted in having a stiffness of more than 1 N especially for membranes having the bigger cut-off which appeared to be also thicker before hydration. The resulting value a promising one thinking about gastric contraction pressure. Moreover, those units appeared to undergo a small deflation which, after 24 hours showed to lead to a weaker mechanical resistance that, possibly, could represent result in a physiological ejection of the system form the organ. For what concerns drug containing unit, hydrophilic matrices made of HPMC containing 250 mg or 500 mg of metformin have been produced and tested and, since the drug has a relatively high solubility, drug release rate appeared to be too fast in the first basic formulations prepared by simple mixture with hydrophilic polymer (hypromellose K15M). For these reason a wet granulation process of the metformin with ethylcellulose was performed and matrices containing obtained granules appeared to be able to have a slower drug release profile. In order to prolong more the drug release, one or two drug free layers made of hypromellose or ethylcellulose were prepared on the external surfaces of the tablet. This strategy allowed to reach the complete release of the drug in approximately 12 h. Finally ORODS devices in a circular shape were prepared with different configuration and opening time and dimensions of the system have been acquired by immersing the system into deionized water at 37°C with a stirring of 100 rpm. The system appeared to be able to open in approximately 4 min, when the capsule dissolved, and to reach the maximum expansion configuration which is bigger than the opened pylorus after 20 min .

REFERENCES

Altreuter, D. H., Kirtane, A. R., Grant, T., Kruger, C., Traverso, G., & Bellinger, A. M. (2018). Changing the pill: developments toward the promise of an ultra-long-acting gastroretentive dosage form. Expert opinion on drug delivery, 15(12), 1189-1198. https://doi.org/10.1080/17425247.2018.1544615

ASTM. (1990). Annual Book of ASTM Standards, 1990: Subject Index; Alphanumeric List. American Society for Testing & Materials.

Bonnet, F., & Scheen, A. (2017). Understanding and overcoming metformin gastrointestinal intoler-ance. Diabetes, Obesity and Metabolism, 19(4), 473-481. https://doi.org/10.1111/dom.12854

Cirilli, M., Maroni, A., Moutaharrik, S., Foppoli, A., Ochoa, E., Palugan, L., ... & Cerea, M. (2023). Organ-Retentive Osmotically Driven System (ORODS): A Novel Expandable Platform for in Situ Drug Deliv-ery. International Journal of Pharmaceutics, 644, 123295. https://doi.org/10.1016/j.ijpharm.2023.123295

Corti, G., Cirri, M., Maestrelli, F., Mennini, N., & Mura, P. (2008). Sustained-release matrix tablets of met-formin hydrochloride in combination with triacetyl-β-cyclodextrin. European Journal of Pharmaceutics and Biopharmaceutics, 68(2), 303-309. https://doi.org/10.1016/j.ejpb.2007.06.004

Feher, M. D., Al-Mrayat, M. E., Brake, J., & Leong, K. S. (2007). Tolerability of prolonged-release metformin (Glucophage® SR) in individuals intolerant to standard metformin—results from four UK centres. The Brit-ish Journal of Diabetes & Vascular Disease, 7(5), 225-228. https://doi.org/10.1177/14746514070070050501

Garber, A. J., Duncan, T. G., Goodman, A. M., Mills, D. J., & Rohlf, J. L. (1997). Efficacy of metformin in type II diabetes: results of a double-blind, placebo-controlled, dose-response trial. The American journal of medi-cine, 103(6), 491-497. https://doi.org/10.1016/S0002-9343(97)00254-4

Gazzaniga, A., Foppoli, A., Cerea, M., Palugan, L., Cirilli, M., Moutaharrik, S., ... & Maroni, A. (2023). To-wards 4D printing in pharmaceutics. International Journal of Pharmaceutics: X, 5, 100171. https://doi.org/10.1016/j.ijpx.2023.100171

Goyal, R., & Jialal, I. (2018). Diabetes mellitus type 2.

Guo, L. X., Liu, G. E., Chen, L., Wang, H. F., Guo, J., Zheng, X. L., ... & Lei, M. X. (2021). Comparison of clinical efficacy and safety of metformin sustained-release tablet (II)(Dulening) and metformin tablet (Glucophage) in treatment of type 2 diabetes mellitus. Frontiers in Endocrinology, 12, 712200. https://doi.org/10.3389/fendo.2021.712200

Israili, Z. H. (2011). Advances in the treatment of type 2 diabetes mellitus. American journal of therapeu-tics, 18(2), 117-152. https://doi.orf/10.1097/MJT.0b013e3181afbf51

Katsarou, A., Gudbjörnsdottir, S., Rawshani, A., Dabelea, D., Bonifacio, E., Anderson, B. J., ... & Lernmark, Å. (2017). Type 1 diabetes mellitus. Nature reviews Disease primers, 3(1), 1-17 https://doi.org/10.1038/nrdp.2017.16

Kumar, R., Chandra, A., & Garg, S. (2012). Formulation and in vitro evaluation of sustained release gas-troretentive tablets of metformin hydrochloride. Int J Ther App, 7, 13-7.

Lopes, C. M., Bettencourt, C., Rossi, A., Buttini, F., & Barata, P. (2016). Overview on gastroretentive drug de-livery systems for improving drug bioavailability. International journal of pharmaceutics, 510(1), 144-158. https://doi.org/10.1016/j.ijpharm.2016.05.016

Maroni, A., Melocchi, A., Zema, L., Foppoli, A., & Gazzaniga, A. (2020). Retentive drug delivery systems based on shape memory materials. Journal of Applied Polymer Science, 137(25), 48798. https://doi.org/10.1002/app.48798

McCreight, L. J., Bailey, C. J., & Pearson, E. R. (2016). Metformin and the gastrointestinal tract. Diabetology, 59(3), 426-435. https://doi.org/10.1007/s00125-015-3844-9

Palugan, L., Cerea, M., Cirilli, M., Moutaharrik, S., Maroni, A., Zema, L., ... & Gazzaniga, A. (2021). Intravesi-cal drug delivery approaches for improved therapy of urinary bladder diseases. International Journal of Pharmaceutics: X, 3, 100100. https://doi.org/10.1016/j.ijpx.2021.100100

Pavan, M. V., Balamurugan, K., & Latchoumi, T. P. (2022). PLA-Cu reinforced composite filament: Preparation and flexural property printed at different machining conditions. Advances in Computational Mathematics, 31(1), 102-117. https//doi.org/10.1080/09243046.2021.1918608

Rena, G., Hardie, D. G., & Pearson, E. R. (2017). The mechanisms of action of metfor-min. Diabetologia, 60(9), 1577-1585. https://doi.org/10.1007/s00125-017-4342-z

Sanchez-Rangel, E., & Inzucchi, S. E. (2017). Metformin: clinical use in type 2 diabetes. Diabetologia, 60, 1586-1593. https://doi.org/10.1007/s00125-017-4336-x

Streubel, A., Siepmann, J., & Bodmeier, R. (2006). Gastroretentive drug delivery systems. Expert opinion on drug delivery, 3(2), 217-233. https://doi.org/10.1517/17425247.3.2.217

Sun, M. L., Liu, C., Bai, H. H., Wei, Y. L., Zhang, W., Liu, H. J., ... & Wang, X. (2022). Bioequivalence and safety evaluation of two preparations of metformin hydrochloride sustained-release tablets (Boke® and Glucophage®-XR) in healthy Chinese volunteers: a randomized phase I clinical trial. Annals of Medicine, 54(1), 2626-2635. https://doi.org/10.1080/07853890.2022.2125574

Tripathi, J., Thapa, P., Maharjan, R., & Jeong, S. H. (2019). Current state and future perspectives on gastroretentive drug delivery systems. Pharmaceutics, 11(4), 193. https://doi.org/10.3390/pharmaceutics11040193

Uboldi, M., Melocchi, A., Moutaharrik, S., Palugan, L., Cerea, M., Foppoli, A., ... & Zema, L. (2022). Admin-istration strategies and smart devices for drug release in specific sites of the upper GI tract. Journal of Con-trolled Release, 348, 537-552. https://doi.org/10.1016/j.jconrel.2022.06.005

Wadher, K. J., Kakde, R. B., & Umekar, M. J. (2011). Study on sustained-release metformin hydrochloride from matrix tablet: Influence of hydrophilic polymers and in vitro evaluation. International journal of phar-maceutical investigation, 1(3), 157. https//doi.org/ 10.4103/2230-973X.85966

Zhao, L., Wei, Y., Mei, Y., Yang, L., You, Y., Yang, X., & Jiang, Y. (2012). Preparation and in vitro drug release evaluation of once-daily metformin hydrochloride sustained-release tablets. Pharmacology & Pharmacy, 3(04), 468. http://dx.doi.org/10.4236/pp.2012.34064

Chapter 6

Development of novel oral delivery systems using additive manufacturing technologies to overcome biopharmaceutical challenges for future targeted drug delivery

To be submitted for publication

§ The contribution given by Micol Cirilli to the work associated with published article was conceptualization, methodology, formal analysis, investigation, writing – original draft, visualization.

ABSTRACT

The development of robust and cost-effective systems for the drug delivery of complex active compounds, particularly those in BCS classes III and IV, presents major challenge. These drugs, including large molecules, peptides and proteins, are often poorly permeable and stability sensitive, and have traditionally required parenteral delivery. Recent advances in additive manufacturing have made it possible to create novel and complex structures tailored to specific delivery requirements without prohibitive costs. Although Spritam remains the only 3D printed tablet on the market, this work aims to utilize additive manufacturing technology to develop a prototype for a novel drug spring-based delivery platform. This paper outlines the design and in vitro characterization of this new delivery device, addresses biopharmaceutical challenges and provides an outlook for future development.

KEYWORDS

Retentive delivery systems

Intestinal delivery systems

3D printing

Fused deposition modelling

Stereolithography

Hydrophilic matrix

1. INTRODUCTION

The oral route of administration has always been the most common way for both conventional and non-conventional dosage forms. [Homayun et al., 2019] [Hua, 2020] However, there are several challenges associated with this dosage form, such as the limited or highly variable bioavailability of an increasing number of active ingredients. The reasons for this are many and varied and lie both in the gastrointestinal tract itself, such as the high variability in the transit behavior of the dosage form caused by the physiology of the GIT in conjunction with the specific absorption windows of the active ingredients, and in the solubility and permeability requirements of the drugs themselves. [Ibrahim et al., 2019] [Lopes et al., 2016] [Davis, 2005] However, the solubility and permeability requirements of the drugs themselves, especially the increasing number of BCS Class III and IV drugs currently in development, are also a challenge [Ghadi et al., 2017], as is the stability of the drugs, especially the novel peptide or protein-based drugs. [Craik et al., 2013] As a result of these challenges, many compounds are currently only parenterally bioavailable, which affects both patient compliance and the regulatory requirements for these dosage forms, as well as their manufacture and cost. A major pharmaceutical and biopharmaceutical challenge is therefore to develop novel, robust and cost-effective oral systems that meet these requirements. [Vrettos et al., 2021] The small intestine is the most important organ for the absorption of orally administered drugs due to its villi and microvilli, the resulting very large absorption surface and the particularly pronounced blood circulation. [Helander et al., 2014] [Hurr, 2023] The muscular structures enable the transport of food within the small intestine, the pH in the small intestine is neutral and the mucosal surface is permanently moist, with fluid distribution not being homogeneous but in the form of so-called water pockets. [Schiller et al., 2005]

In recent years, a variety of capsule- or tablet-based delivery technologies have been developed for targeted drug delivery in the small intestine, including some very creative approaches such as drug-loaded stents, various mucoadhesive

delivery concepts or even oral mini-melt extruders. [Chun et al., 2010] [Bektaş et al., 2017] [Rump et al., 2023]

With the impressive development of different additive manufacturing technologies, for example, completely new technological possibilities and in some cases materials are now available for the development of novel dosage concepts, allowing a new design based on the white paper method of oral dosage forms completely detached from the classic capsules and tablets. [Maroni et al., 2020] [Gazzaniga et al., 2023]

The ability to design and manufacture systems with specific shapes, configurations and complex geometries that interact with the physiology of the gastrointestinal tract in a way that can lead to targeted application in a specific area of the gastrointestinal tract can be made possible through the use of novel technologies such as 3D printing, where the construction of solid objects of any shape is achieved by adding materials layer-by-layer based on a digital model. [Norman et al., 2017] [Chen et al., 2020] [Englezos et al., 2023]

3D-printing includes many techniques that differ from each other in the nature of the substrate, mechanism of layer formation/deposition mode, printer used and, of course, characteristics of the final product. [Großmann et al., 2022] Thanks to the possibility of producing small batches, this technology is also very interesting for personalized and on-demand production, which keeps costs down despite sometimes extremely complex structures. [Cui et al., 2021]

Based on this, the aim of the present work was to design and develop a prototype of a novel drug delivery platform that can control drug release in the upper gastrointestinal tract, especially in the small intestine, and to enable targeted drug release at the small intestinal mucosa. The novel application technology shown in Figure 1 should contain two matrices loaded with a drug component, such as mucoadhesive films or mini-tablets, connected by a spring-based release mechanism. The spring should press the matrices with the drug components onto the small intestinal mucosa with a defined pressure over a defined length after the previous protective film or thread has dissolved, triggered by a trigger

mechanism. The components should preferably be combined with a component that erodes or dissolves under physiological conditions to allow degradation after a defined time and thus safe emptying of the prototype.

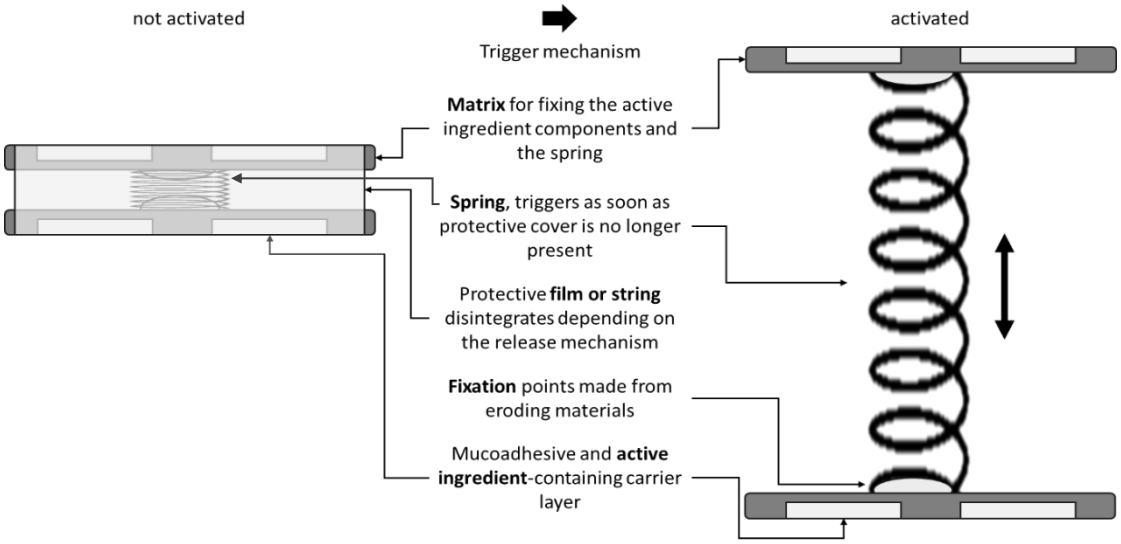

Figure 1: Concept sketch of the spring-like delivery device and initial CAD interpretation of the same.

The aim of the this work was to prepare the conceptually described application device and to characterize and discuss biorelevant key components such as the spring and trigger mechanism.

2. EXPERIMENTALS

2.1 Materials

Placebo matrices/Supports have been designed by using Free-Cad (V 0.20.2), an open-source parametric 3D software, and sliced with the Ultimaker Cura program (V 5.3.1, Ultimaker, The Netherlands) for the setting of printing parameters. Objects made of PLA were printed with the Ultimaker 3D fused deposition modeling (FDM) printer (Ultimaker, Netherlands). Nozzle size used for the printing was AA 0.4 mm, printing temperature 215°C. Infill was 100% and the printing speed 25 mm/s. Objects made of HPMC K15M were printed with the

same FDM 3D printer equipped with a AA nozzle having diameter 0.4mm, setting building plate at 60°C and extrusion temperature 185°C; fan was disabled and no infill geometry was set but the matrices were entirely made by concentric walls (12 walls). Matrices prepared have dimensions of 22 mm * 7.8 mm * 3 mm. Objects having circular concavities with a diameter of 4 mm, made to host inside small tablets, where also prepared.

2.2 Methods

2.2.1 3D printing of the matrices

Placebo matrices/Supports have been designed by using Free-Cad (V 0.20.2), an open-source parametric 3D software, and sliced with the Ultimaker Cura program (V 5.3.1, Ultimaker, The Netherlands) for the setting of printing parameters. Objects made of PLA were printed with the Ultimaker 3D fused deposition modeling (FDM) printer (Ultimaker, Netherlands). Nozzle size used for the printing was AA 0.4 mm, printing temperature 215°C. Infill was 100% and the printing speed 25 mm/s. Objects made of HPMC K15M were printed with the same FDM 3D printer equipped with a AA nozzle having diameter 0.4 mm, setting building plate at 60°C and extrusion temperature 185 °C; fan was disabled and no infill geometry was set but the matrices were entirely made by concentric walls (12 walls). Matrices prepared have dimensions of 22 mm x 7.8 mm x 3 mm. Objects having circular concavities with a diameter of 4 mm, made to host inside small tablets, where also prepared.

2.2.2. Tablet preparation

Drug-free tablets were prepared from a powder mixture (calcium dihydrogen phosphate 96%, sodium crosscarmellose 1.0%, magnesium stearate 2.0%, fumed silica 1.0%) using a single-stamp tablet press (KP2, VEB Kombinat NAGEMA) with a flat die, diameter: 3.00 mm.

2.2.3 Spring design

Springs having different dimensions were designed by using Free-Cad (V 0.20.2), an open-source parametric 3D modeler. Various geometries were tested to assess the influence of the springs: the coil diameter, the spring diameter, the number of working coils and the coil geometry (rectangular and circular section) were varied as shown in Figure 2.

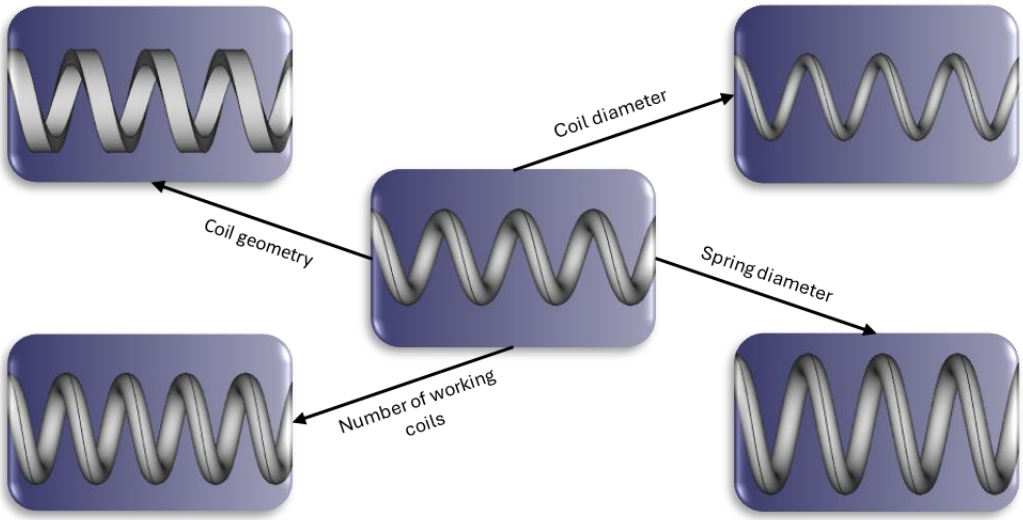

Figure 2: Schematic illustration of the different design alternatives considered for modifying the mechanical properties of the springs used.

A total of thirteen different springs were investigated, which can be categorized into five groups (Table 1). Both circular and rectangular coil geometries were analysed. The coil diameter varied between 1.0 and 1.5 mm, and the rectangular profile was 1 x 1.5 mm as standard. The springs were analysed with either four or five coils. The spring diameter varied between 5 and 8 mm.

Table 1: Design properties and dimensions of springs prepared

Code	Coil section geometry	Coil diameter (mm)	Coils number	Spring diameter (mm)
C.CS1.0.C4.D5	Circular	d = 1.0	4	5
C.CS1.5.C4.D5	Circular	d = 1.5	4	5
C.CS1.5.C4.D6				6
C.CS1.5.C4.D7				7
C.CS1.5.C4.D8				8
C.CS1.5.C5.D6	Circular	d = 1.5	5	6
C.CS1.5.C5.D7				7
C.CS1.5.C5.D8				8
R.CS1*1.5.C4.D5	Rectangular	1 x 1.5	4	5
R.CS1*1.5.C4.D6				6
R.CS1*1.5.C4.D7				7
R.CS1*1.5.C5.D6	Rectangular	1 x 1.5	5	6
R.CS1*1.5.C5.D7				7

2.2.4 FDM 3D printing of the springs

For preliminary tests springs 3D models were sliced using the Ultimaker Cura (V 5.3.1) and printed with FDM 3D printer equipped with two nozzle (Mod. 3, Ultimaker (UK). For 3D printing with PVA supports, the following settings was used: for TPU, printing temperature 225°C, infill 15%, printing speed 10 mm/s and nozzle AA 0.4 mm were used; for PVA: printing temperature 220°C, infill 5%, printing speed 10 mm/s and nozzle BB 0.4 were used. For 3D printing without supports, the following settings was used: TPU printing temperature 225°C, infill 25%, printing speed 15 mm/s and nozzle AA 0.4 mm.

2.2.5 SLA 3D printing of the springs

The Formlabs PreForm (V 3.30.0) program was used to set printing parameters for the stereolithography printer as here reported: support density 1.00, contact point dimension 0.20 mm without internal supports. The springs were printed in

Clear Resin V4 by FormLabs 3 SLA printer (Formlabs, USA) and afterwards washed in isopropanol and cured for 30 min at 375-405 nm.

2.2.6 Mucoadhesive film preparation and gastric resistant string and glue preparation

All films were produced using the solvent casting technique. All the solvent used was pre-filled into a laboratory glass bottle. Plasticizers and other polymers were then added. The prepared formulation is shown in Table 2.

Table 2: Polymeric blends to produce of mucoadhesive films

POLYMER	***PLASTICIZER***	*Solvent*
PVA 18-88	Anhydrous glycerol	Demineralized water
18.0 g	2.0 g	80.0 g

The dispersion was then stirred on a stirring plate (IKA® RCT basic, IKA®-Werke GmbH & CO. KG, Staufen, Germany) at 150 rpm for 1 h until a clear solution was obtained. If air bubbles were still visible, the polymer mass was centrifuged at 4400 rpm for 15 minutes (Centrifuge 5702 R, Eppendorf SE, Hamburg, Germany). The bubble-free solution 1 was then applied to a specially coated paper, the so-called release liner, using a doctor blade (mtv messtechnik oHG, Erftstadt, Germany) with a width of 500 µm and a motorized vacuum coating bench at 12.0 mm/s (Automatic Precision Film Applicator CX4, mtv messtechnik oHG, Erftstadt, Germany). The coated laminates were then dried in a fume cupboard at room temperature.

The following formulation (Table 3) was instead used to produce the gastric resistant strings (formulation 1) and as the glue to fix system components (formulation 2).

Table 3: Polymer blends to produce of gastric resistant string preparation and gastric resistance glue

Formulation	*Polymer*		*Plasticizer*	*Solvent*
1	Eudragit L100-55 20.0 g	Eudragit L100	Triethylcitrat 4.0 g	Aceton 76.0 g
2		20.0 g		

The dispersions were stirred in a glass bottle on a stirring plate (IKA® RCT basic, IKA®-Werke GmbH & CO. KG, Staufen, Germany) at 150 rpm for 24 hours until a clear solution was obtained.

Commercially available 40 cm long multifilament polyvinyl alcohol fishing lines were coated by a simple dipping process. The acetone used evaporated at room temperature.

2.2.7 Assembly of the novel application device

Enteric-retentive systems were prepared by manually assembling and gluing a spring with two PLA units by using the acetonic Eudragit L solution 2 (Table 2). The device was hold in the space-saving configuration by wrapping a gastric-resistant string around system with compressed spring. Prototypes made with the matrices having the concavities where prepared by pushing two small tablets inside so that they were framed into the matrix. With respect to prototypes having a mucoadhesive film surrounding the system, the foil was put on the system and closed around it by slightly moisten one edge of the film to make it adhesive and capable to be sealed to the other edge.

2.2.8 Spring strength test

Elastic strength of the springs was tested with a texture analyzer (LLOYD, TA plus Ametek, UK), and the associated software, Nextgen Plus, version 3.0 (Ametek, Berwyn, PA, USA), with the following settings: displacement speed at

10 mm/min, load cell of 10 N (upper limit). The test was run by selecting a maximum load of 1.4 N.

2.2.9 Evaluation of opening time of enteric-retentive systems

Systems, maintained in their space-saving configuration by the gastro-resistant string wrapped around the device, were placed in 800 mL pH 1.2 buffer at 37°C and under magnetic stirring (130 rpm) for 120 min. After this time, fluid was change with 800 mL pH 6.8 phosphate buffer. To protect the system from the magnetic stirrer, a distance mesh insert designed and 3D-printed by Großmann, L et a. was used. Evaluation of opening time of the systems was performed in triplicate for each spring configuration.

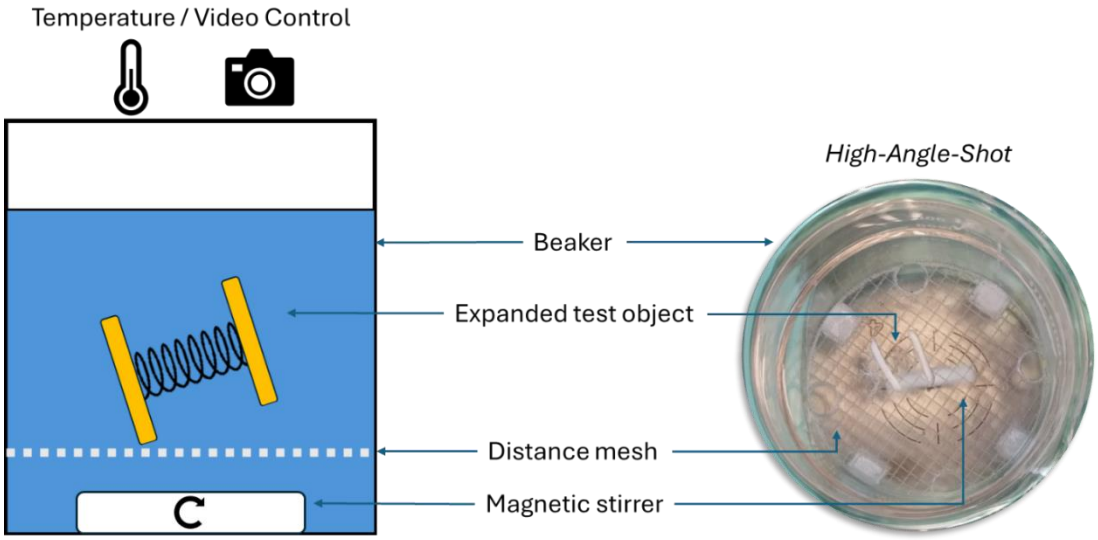

Figure 3: Sketch of the test set-up to investigate the trigger mechanism of the novel, additively manufactured, spring-based application system.

3. RESULTS AND DISCUSSION

Different geometries of the expanding device were designed according to the purpose of the system and the desired drug release time. As a result, different drug containing units such as films, minitablets and hydrophilic matrices were considered. In addition, springs of different lengths, shapes and strengths were manufactured to meet specific requirements. The matrices were designed in a classic oblong shape with a convex top and a flat bottom with a small concavity

for the spring. Alternatively, 22 mm x 7.8 mm x 3 mm PLA matrices (carriers) were printed in the same shape but with two concavities on the top to hold two drug-containing minitablets (Figure 4). Depending on the purpose of the device, various modifications and characteristics of its components can be adjusted, such as springs of different sizes and strengths. The system must reach the organ, expand and withstand contractions. Accordingly, different drug-containing units or delivery devices can be tailored depending on the absorption site and drug dose. Figure 8 shows prototypes of devices equipped with drug-containing matrices or units designed to deliver small tablets or films. These tablets and films are made of polymeric materials that form gels with mucoadhesive properties that enhance adhesion to the internal surface of the organ.

3.1 FDM Printing realization of the matrices

Matrices were produced in different configurations and materials to have the possibility to vary depending on the purpose of the whole system. Objects made of PLA and having a concavity in the flat part to permit the positioning of a spring were designed and printed and their possible utilization would be to be supports for a drug loaded film that can be applied to the external surface of such objects. Similar objects were printed in HPMC so that hydrophilic matrices were obtained with the idea of producing drug containing mucoadhesive matrices. Finally another design was made and printed having two housings on the upper surface especially made to be able to contain two small mucoadhesive tablets. Work was focused on the design and printability of such shapes, therefore no drug was loaded into such prototypes.

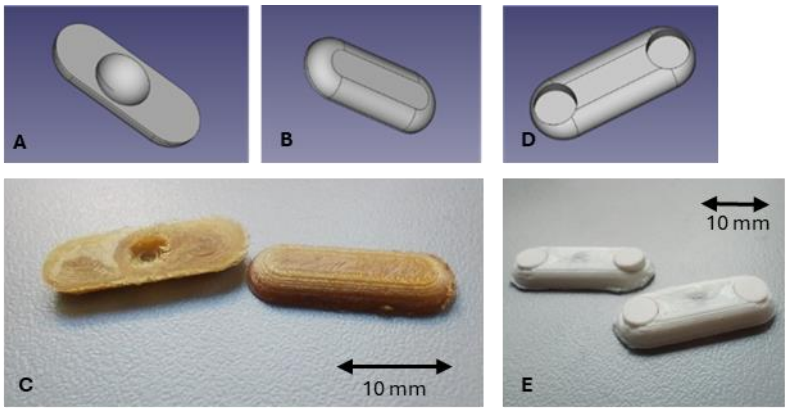

Figure 4: Designs and pictures of prototypes prepared by 3D printing of matrices (C) and supports for minitablets (E).

3.2 Spring printing and evaluation

Springs having a conical shape a small space-saving geometry when compressed were designed. However, this shape did not allow the production of springs having the desired high and diameter (Figure 5C/D). Springs with cylindrical geometry were therefore designed in different shapes and dimensions of the section, number of coils and diameter (Table 1) to evaluate their relationship between those parameters and their strength and flexibility. Preliminary trials were performed by printing springs by means of FDM 3D printer and by using filament of TPU 95A as an elastic polymer (data not presented) (Figure 5 C and D) resulted in prototypes with poor definition and low mechanical resistance. To obtain objects with a good reproducibility and a good resolution, SLA 3D printer was selected using V4 Clear resin as printing material (Figure 5 A and B). Results with this technique have been satisfying in terms of precision and resolution, and suitable for the printing of springs and units. Springs having different characteristics in terms of cross section geometry, cross section dimensions, number of coils and their diameter, have been designed and produced for evaluating their mechanical properties.

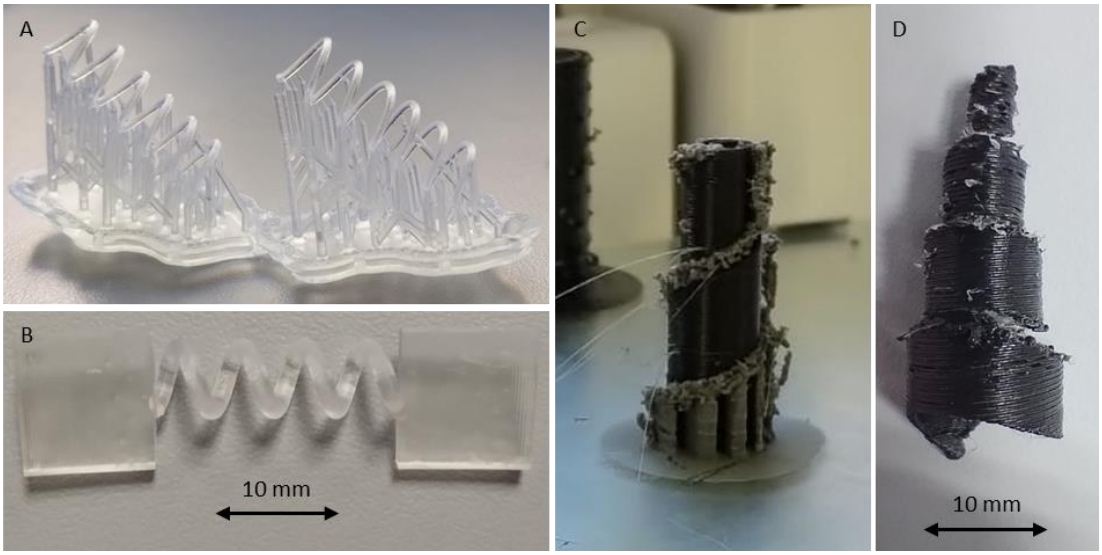

Figure 5: A: SLA 3D printed spring. B: SLA printed spring with support for mechanical testing. C: FDM printed spring with a two component printing system using water soluble PVA as a support. D: Cleaned FDM printed TPU spring.

To evaluate the mechanical properties, springs with clamps were designed (Figure 5 A). As there is no data on how much force a spring can apply to the support without causing pain to the patient, the spring was tested in the Texture Analyser. The maximum force was set at 1.4 N based on Smart Pill data from studies with healthy volunteers. In these studies, a maximum force of 1.4 N was transferred from the small intestine to the SmartPill without any discomfort reported by the volunteers [Schneider et al., 2016]. The resulting graphs are reported in Figure 6 and 7.

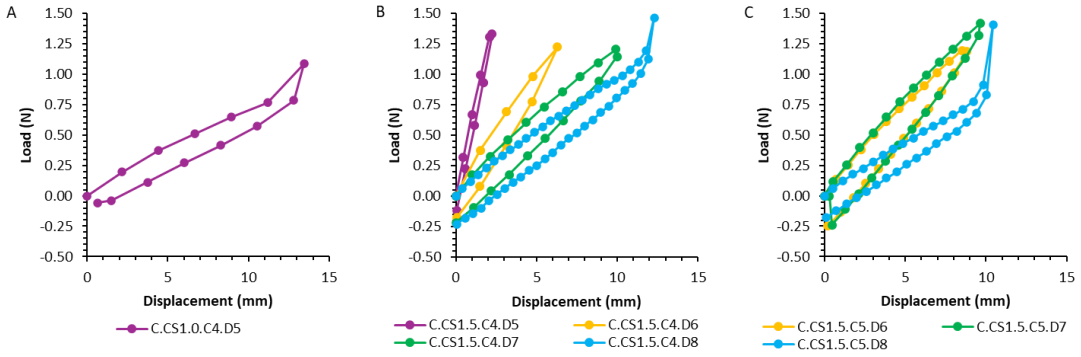

Figure 6: Force-displacement diagrams for cylindrical springs: A: Small coil diameter of 1 mm. B: Variation of the spring diameter from 5 to 8 mm. C: Increasing the number of working coils and varying the coil diameter.

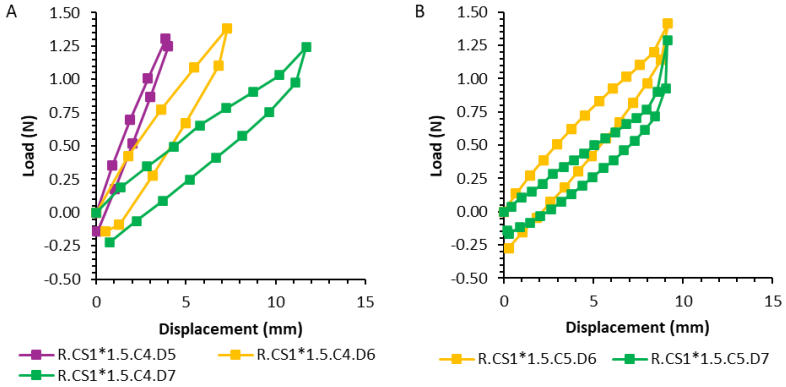

Figure 7: Force-displacement diagrams for cylindrical springs with rectangular cross-section: A: Variation of the spring diameter. B: Variation of the spring diameter with an increased number of working coils.

The recorded force-displacement diagrams show slight deviations in the resulting force for compression and return journeys. As expected, springs having a smaller diameter, less coils and bigger cross section dimension appear to be harder, while those having a bigger diameter, more coils and a smaller cross section diameter result weaker/softer. Springs having a rectangular section of 1 x 1.5 mm showed a behavior like the spring having the same characteristics but a circular section cross section of 1.5 mm, meaning that section shape (circular or rectangular) leads to no difference in terms of spring's strength. Spring C.CS1.C4.C5, having the smaller cross section, was not able to generate the maximum value of 1.4 N event when reached the maximum compression displacement at 13.5 mm. In particular, the spring with a diameter of 8 mm showed a strong increase in force after 10 mm of compression, which can be attributed to the contact between coils and thus to the maximum deflection of the spring (Figure 6C). The rectangular profile springs behaved in the same way as the round springs (Figure 7). Elasticity modulus for resin V4 employed in the 3D printing of the spring was reported to be 2,8 GPa ($2{,}8 \times 10^9$ N/m^2) [https://formlabs-media.formlabs.com/datasheets/1801089-TDS-IT-0P.pdf]. Mechanical properties of the springs are then given also by diameter, cross section geometry and diameter, length of the spring and number of coils, as described by Hooke's law equation.

3.3 Assembly and Evaluation novel dosage form

For enteric-retentive systems an additional holding filament having gastric-resistant properties was wrapped around the device in the space-saving configuration before placing the systems inside the body of a hard gelatine capsule. The gastric-resistant filament maintains the device in the space-saving configuration. The dissolution of the holding filament occurs in the intestinal lumen where pH turns relatively less acid, and the device is expected to expand immediately and gain a dimension that is compatible with the internal lumen

diameter of small intestine, eventually allowing the drug containing units to adhere to intestinal walls.

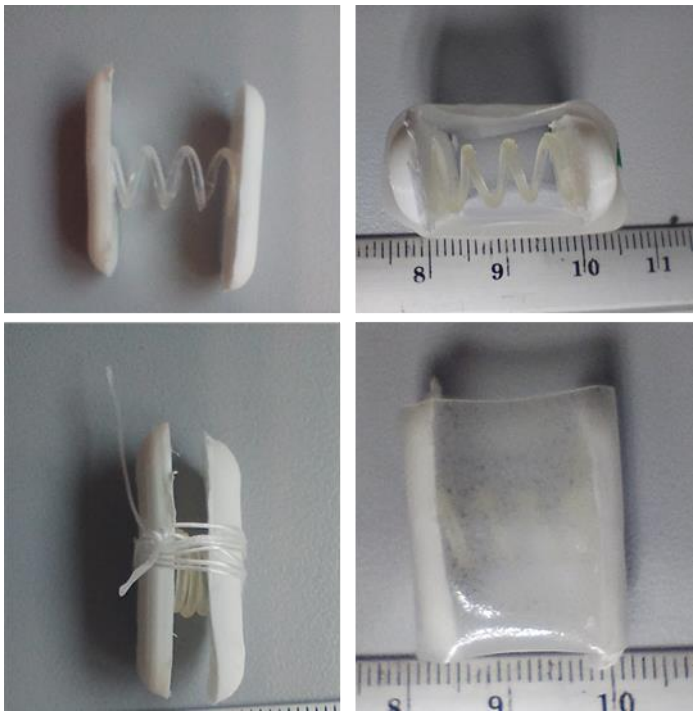

Figure 8: Overview of the different construction states and compositions of the application device. A: PLA matrix with spring with thin coil diameter. B: PLA matrix with spring with thin coil diameter with a gastric juice-resistant thread as trigger mechanism in central formation. C: PLA matrix with enteric film as protection so that the trigger mechanism can trigger in a pH-controlled manner. D: Side view of C.

Based on the results obtained with the measurements of spring strength, systems consisting of a spring and two drug-delivering units has been assembled by gluing the components (spring and two units/supports) using an adhesive acetonic solution prepared dissolving a polymer having pH-dependent solubility (Eudragit L100), soluble at pH above 5. Systems based on springs having 5 coils with circular section with 1 mm or 1.5 mm diameter and coil diameter 5 mm or 7 mm (C.CS1.C4.D5 or C.CS1,5.C4.D7, respectively) have been chosen for testing. The springs have been selected based minimum strength observed on the string having strength comparable to values of pressure exerted in the intestinal tract.

Since the enteric-retentive system is not meant to remain assembled in the intestine for a long period, but only for approximately 15 min, it is important that

the device is able to withstand the dominant contraction frequency of approximately 12 cycles per minute and a slow-wave propagation velocity of 15 cm/min [Shames, 2019]. However, the systems also need to be removed promptly from the space-saving configuration compatible with the oral administration to the expanded form, able to maintain the device in place and allow the release of the drug. For enteric-retentive systems the space-saving configuration was obtained by wrapping the device with a gastric resistant string prepared by coating a water soluble PVA string with a gastric-resistant polymer, Eudragit L100-55, a polymer having pH-dependent solubility, soluble at pH above 5.5.

To assess of the opening time of the enteric-retentive devices, systems forced in their space-saving configuration by the gastro-resistant string were placed pH 1.2 buffer for 120 min; after this time, aqueous media was changed for pH 6.8 phosphate buffer to mimic gastrointestinal transit.

Results showed that the gastro-resistant strings were able to resist with no detectable modifications for two hours in acidic conditions and to maintain the system in a space saving configuration. Opening times after pH change resulted 5.5 ± 1.2 min for systems prepared with springs having diameter 5 mm and section 1 mm and 2.5 ± 0.3 min for those prepared with springs having 7 mm diameter and 1.5 mm section. As expected, the system prepared with springs having smaller diameter section resulted significantly slower ($p<0.01$) than those with thicker springs. The pressure was clearly related to the strength of the spring previously evaluated with the texture analyzer. In both cases, systems were disassembled in less than 60 min ± 10 thanks to the dissolution of the glue made of Eudragit L100 used to attach the springs to the supports. The dimensions of the system before being forced in the space saving configuration were recovered after opening as demonstrated by measures reported in Table 4. Springs, and consequently the whole systems, were able to return to their original shape after being maintained in aqueous fluids and compressed in the space saving configuration for two hours.

Table 4 Measures of enteric-retentive systems in the expanded and space-saving configuration before and after opening in pH 1.2 buffer for 120 min and pH 6.8 buffer for remaining duration of the test.

	Expanded before test	Closed before test	Expanded after test	Opening time at pH 6.8
Diameter 7 mm, section 1.5 mm	24.1 ± 0.1 mm	11.2 ± 0.3 mm	24.1 ± 0.2 mm	2.5 ± 0.3 min
Diameter 5 mm, section 1 mm	22.0 ± 0.2 mm	9.1 ± 0.1 mm	22 ± 0.2 mm	5.5 ± 1.2 min

However, it should be noted that the device was not subjected to mechanical stress in our in vitro test, as is often the case with oral dosage forms in the gastrointestinal tract. The mechanical stability of the device, which may swell during gastric passage, needs to be investigated in further studies. It is also of great interest to simulate further studies on the residence time of the device, e.g. after postprandial ingestion, in a biorelevant way, to assess the behavior of the dosage form, which in such a case is likely to have already been released in the stomach and may disintegrate into its components due to the postprandial environment. Suitable dosage forms, such as films or mini-tablets loaded with bio-relevant active ingredients, will also be produced to test their functionality in a simulation model adapted to the human gastrointestinal tract, e.g. the dog.

4. CONCLUSIONS

A new concept for a 3D printed expandable drug delivery system was proposed to administer active ingredients having narrow absorption window exactly to the anatomical site in which they are absorbed. 3D printed systems intended for organ retention have been designed, size expansion strategy has been employed and springs have been selected as expandable unit. Different springs in terms of diameter, number of coils and cross section have been produced and tested to evaluate their behavior when a strength comparable to the organ contractions was exerted on them by a texture analyzer. As expected, different configurations

of the spring led to different strength and, therefore, hypothetical different purposes of the systems depending on the exhibited resistance. The results obtained, showing that the system can remain in space-saving configuration for two hours into acidic conditions, thanks to a gastro-resistant string enveloping the system, and then expand in pH 6.8 when the string dissolves due to pH change. Since the work was focused on small intestine deliver of the drug, the results obtained in terms of ability of resisting the acidic environment and regaining the expanded configuration afterwords are promising and make this prototype interesting for upper intestine targeted drug delivery.

REFERENCES

Bektaş, H., Gürbulak, B., Düzköylü, Y., Çolak, Ş., Gürbulak, E. K., Cakar, E., & Bayrak, S. (2017). Clinical outcomes of upper gastrointestinal stents and review of current literature. *JSLS: Journal of the Society of Laparoendoscopic Surgeons*, *21*(4). https://doi.org/10.4293/JSLS.2017.00058

Chen, G., Xu, Y., Kwok, P. C. L., & Kang, L. (2020). Pharmaceutical applications of 3D printing. *Additive Manufacturing*, *34*, 101209. https://doi.org/10.1016/j.addma.2020.101209

Chun, H. J., Kim, E. S., Hyun, J. J., Kwon, Y. D., Keum, B., & Kim, C. D. (2010). Gastrointestinal and biliary stents. *Journal of gastroenterology and hepatology*, *25*(2), 234-243. https://doi.org/10.1111/j.1440-1746.2009.06152.x

Craik, D. J., Fairlie, D. P., Liras, S., & Price, D. (2013). The future of peptide-based drugs. *Chemical biology & drug design*, *81*(1), 136-147. https://doi.org/10.1111/cbdd.12055

Cui, M., Pan, H., Su, Y., Fang, D., Qiao, S., Ding, P., & Pan, W. (2021). Opportunities and challenges of three-dimensional printing technology in pharmaceutical formulation development. *Acta Pharmaceutica Sinica B*, *11*(8), 2488-2504. https://doi.org/10.1016/j.apsb.2021.03.015

Davis, S. S. (2005). Formulation strategies for absorption windows. *Drug discovery today*, *10*(4), 249-257. https://doi.org/10.1016/S1359-6446(04)03351-3

Englezos, K., Wang, L., Tan, E. C., & Kang, L. (2023). 3D printing for personalised medicines: implications for policy and practice. *International Journal of Pharmaceutics*, *635*, 122785. https://doi.org/10.1016/j.ijpharm.2023.122785

Gazzaniga, A., Foppoli, A., Cerea, M., Palugan, L., Cirilli, M., Moutaharrik, S., ... & Maroni, A. (2023). Towards 4D printing in pharmaceutics. *International Journal of Pharmaceutics: X*, *5*, 100171. https://doi.org/10.1016/j.ijpx.2023.100171

Ghadi, R., & Dand, N. (2017). BCS class IV drugs: Highly notorious candidates for formulation development. *Journal of Controlled Release*, *248*, 71-95. https://doi.org/10.1016/j.jconrel.2017.01.014

Großmann, L., Kieckhöfer, M., Weitschies, W., & Krause, J. (2022). 4D prints of flexible dosage forms using thermoplastic polyurethane with hybrid shape memory effect. *European Journal of Pharmaceutics and Biopharmaceutics*, *181*, 227-238. https://doi.org/10.1016/j.ejpb.2022.11.009

Helander, H. F., & Fändriks, L. (2014). Surface area of the digestive tract–revisited. *Scandinavian journal of gastroenterology*, *49*(6), 681-689. https://doi.org/10.3109/00365521.2014.898326

Homayun, B., Lin, X., & Choi, H. J. (2019). Challenges and recent progress in oral drug delivery systems for biopharmaceuticals. *Pharmaceutics*, *11*(3), 129. https://doi.org/10.3390/pharmaceutics11030129

Hua, S. (2020). Advances in oral drug delivery for regional targeting in the gastrointestinal tract-influence of physiological, pathophysiological and pharmaceutical factors. *Frontiers in pharmacology*, *11*, 524. https://doi.org/10.3389/fphar.2020.00524

Hurr, T. (2023). Surface area values for the human stomach including changes in length and diameter or width with meal volume. *Qeios*. https://doi.org/10.32388/9QEQS1.2

Ibrahim, M., Naguib, Y. W., Sarhan, H. A., & Abdelkader, H. (2019). Gastro-retentive oral drug delivery systems: A promising approach for narrow absorption window drugs. *Journal of advanced Biomedical and Pharmaceutical Sciences*, *2*(3), 98-110. https://doi.org/10.21608/jabps.2019.11357.1042

Lopes, C. M., Bettencourt, C., Rossi, A., Buttini, F., & Barata, P. (2016). Overview on gastroretentive drug delivery systems for improving drug bioavailability. *International journal of pharmaceutics*, *510*(1), 144-158. https://doi.org/10.1016/j.ijpharm.2016.05.016

Maroni, A., Melocchi, A., Zema, L., Foppoli, A., & Gazzaniga, A. (2020). Retentive drug delivery systems based on shape memory materials. *Journal of Applied Polymer Science*, *137*(25), 48798. https://doi.org/10.1002/app.48798

Norman, J., Madurawe, R. D., Moore, C. M., Khan, M. A., & Khairuzzaman, A. (2017). A new chapter in pharmaceutical manufacturing: 3D-printed drug products. *Advanced drug delivery reviews*, *108*, 39-50. https://doi.org/10.1016/j.addr.2016.03.001

Rump, A., Tetyczka, C., Littringer, E., Kromrey, M. L., Bülow, R., Roblegg, E., ... & Grimm, M. (2023). In vitro and in vivo evaluation of carbopol 71G NF-based mucoadhesive minitablets as a gastroretentive dosage form. *Molecular Pharmaceutics*, *20*(3), 1624-1630. https://doi.org/10.1021/acs.molpharmaceut.2c00835

Shames, B. (2019). Anatomy and physiology of the duodenum. In *Shackelford's Surgery of the Alimentary Tract, 2 Volume Set* (pp. 786-803). Elsevier. https://doi.org/10.1016/B978-0-323-40232-3.00068-6

Schiller, C., Fröhlich, C. P., Giessmann, T., Siegmund, W., Mönnikes, H., Hosten, N., & Weitschies, W. (2005). Intestinal fluid volumes and transit of dosage forms

as assessed by magnetic resonance imaging. *Alimentary pharmacology & therapeutics*, *22*(10), 971-979. https://doi.org/10.1111/j.1365-2036.2005.02683.x

Schneider, F., Grimm, M., Koziolek, M., Modeß, C., Dokter, A., Roustom, T., ... & Weitschies, W. (2016). Resolving the physiological conditions in bioavailability and bioequivalence studies: Comparison of fasted and fed state. *European Journal of Pharmaceutics and Biopharmaceutics*, *108*, 214-219. https://doi.org/10.1016/j.ejpb.2016.09.009

Vrettos, N. N., Roberts, C. J., & Zhu, Z. (2021). Gastroretentive technologies in tandem with controlled-release strategies: A potent answer to oral drug bioavailability and patient compliance implications. *Pharmaceutics*, *13*(10), 1591. https://doi.org/10.3390/pharmaceutics13101591

https://formlabs-media.formlabs.com/datasheets/1801089-TDS-IT-0P.pdf

Concluding remarks

The focus of the research work was to study, design and develop retentive systems for prolonged drug delivery in hollow organs. Attention has been addressed specifically to three anatomic districts: urinary bladder, stomach and small intestine. During the last two decades, interest in drug delivery systems capable of being retained in these organs has been constantly growing. These kinds of delivery systems gained attention especially to overcome compliance problems related to chronic illnesses treatment, associated to frequent drug administration of high doses, or to overcome solubility/stability issues of active ingredients or, in case of drugs that may also exhibit a narrow absorption window in the gastrointestinal tract.

Given the fact that urinary bladder pathologies need high doses when treated by systemic administration and that frequent catheterizations are required when pharmacological therapies are given by local instillation, urinary bladder retentive systems can be of great advantage. The development of a ring-shape device for prolonged drug release in urinary bladder, prepared by connecting ethylcellulose-coated hydrophilic matrices with a biodegradable suture thread, was here proposed. Such a prototype presented a compact configuration sufficiently small to be inserted in an urinary catheter for administration, resulted able to release the drug up to four days while being retained inside the organ thanks to dimensions greater than the urethra, and, since it was prepared mainly with soluble materials, the system disassembled and dissolved after releasing the drug, thus not requiring any external intervention for its removal.

Drugs presenting solubility issues or specifically absorbed in the stomach or upper small intestine could find great benefit when delivered in prolonged manner by retentive systems specifically designed increase the transit time in these organs. With respect to the stomach, among all of the strategies proposed up to date to achieve retention, such as floating or bio-adhesion, size expansion is the most promising and implies that the system acquires an adequate encumbrance not to pass through the open pylorus but being able to solubilize/disassemble once the drug is completely released, allowing for physiological elimination. A size-enlarging system intended for gastric-retention was designed using an

osmotically driven expandable unit in order to obtain expansion, capable of increasing the size to more than 20 x 20 mm after administration, and hydrophilic matrices as drug containing unit. Expansion was achieved by means of units made of tubular dialysis membranes containing an osmotic agent able to promote fluids inflow thus leading to size increase, and the final system consisted of the described expandable unit connected to one or two drug containing hydrophilic matrices. Mechanical resistance of the expandable units was evaluated and resulted able to resist peristaltic contractions detected in the stomach. Hydrophilic matrices containing metformin were formulated and prolonged drug release up to 12 h was achieved.

With respect to systems for attaining retention in the upper small intestine, non-conventional techniques were employed to develop an expandable system consisting of two matrices/supports for drug containing units, connected by an elastic spring. 3D printing was used to print the supports by means of fused deposition modeling, while the springs were produced by using stereolithography since higher resolution and precision were required. The system proposed was meant to be expandable being administered with the spring in a compressed configuration, and to open after passing the pylorus, so that the system could push the drug containing supports/matrices against the intestinal lumen wall, allowing for a better contact between the drug containing units and the organ membrane. This could eventually enhance adhesion and drug absorption. Mechanical characteristics of the system, especially of the springs, were evaluated by using a texture analyzer and comparing the results to the forces detected in this anatomical site by *in vivo* studies conducted using a Smart pill®.

To conclude, considering the great need and benefits of systems capable of remaining *in situ* and delivering the drug in a prolonged manner, the development of different prototypes here proposed for the urinary bladder, stomach and upper small intestine can be an interesting starting point for further studies and progress in the field of retentive drug delivery systems.